ENGINEERING OF A COLLAGEN-GLYCOSAMINOGLYCAN COPOLYMER DERMAL REGENERATION MATRIX

Quenton Bester Wessels

Submitted to comply with the requirements for:

Master of Science (Human Cell Biology)

In the School of Medicine, Faculty of Health Sciences,
University of Pretoria, Pretoria, South Africa

2006-2007

Supervisor:
Prof. E Pretorius (University of Pretoria)

ACKNOWLEDGEMENTS

I thank the Lord Jesus Christ for His grace, blessing and inspiration in my life. He is the author of creation and in Him lies all the treasures of wisdom and knowledge.

I would also like to express my heartfelt appreciation to the following:

- The University of Pretoria with special reference to Prof. E Pretorius, Department Anatomy, section Histology and Cell Biology, for her guidance and encouragement.
- Southern Medical (Pty)Ltd – The Managing Director, Dr. M de Villiers, and colleagues.
- My family for their support and blessing when, in 2001, I informed them of my endeavour to pursue a new academic career at the University of Pretoria.
- My friends for all the interest shown as well as their inspiration.

May the information provided in this document touch the lives of those inflicted with severe burn wounds.

For the LORD giveth wisdom: out of his mouth cometh knowledge and understanding.

Proverbs 2:6

“Information is a source of learning. But unless it is organized, processed, and available to the right people in a format for decision making, it is a burden, not a benefit.”

William Pollard

ABSTRACT

ENGINEERING OF A COLLAGEN-GLYCOSAMINOGLYCAN COPOLYMER DERMAL REGENERATION MATRIX

QB Wessels

Supervisor: Prof. E. Pretorius

In the School of Medicine, Faculty of Health Sciences, University of Pretoria, Pretoria, South Africa

Background:

Tissue engineering and its contribution to regenerative medicine has advanced through the years. It has proven its efficacy especially in the treatment of advanced full thickness burn wounds. Tissue engineering is the synergy between biology and engineering. This fairly young science has one common goal and that is to regenerate new tissue. Various commercially available products have appeared on the market and this due to the ground-breaking work of many. One such well known product is Integra® which is the brain child of Yannas and Burke. This is a collagen-glycosaminoglycan copolymer which serves as a bioactive regeneration template or extracellular matrix analogue. Advanced wound healing is promoted along with the prevention of scar tissue formation and consequent contractures.

Aims:

This study provides an extensive review on the development of this dermal regeneration matrix and also aims to develop an equivalent product. Attention will be paid to: the biological building blocks and the motivation for their use; the essential production steps; and the final processing required in order to deliver a sterile product.

Materials and Methods:

A collagen and chondroitin 6-sulphate coprecipitate was prepared and subjected to either controlled or uncontrolled freezing. The frozen slurry was dried under vacuum for 17 hours after which each sample was coated with a thin silicone film. Glutaraldehyde crosslinking followed after which the product was thoroughly rinsed. The packaged products were then subjected to terminal sterilisation via gamma irradiation under various conditions. Various tests were conducted to evaluate the newly formed regeneration matrices and included scanning electron microscopy, enzymatic degradation by collagenase, and a cytotoxicity assay. Scanning electron microscopic analysis was done in order to reveal the adequacy of the scaffold architecture. Collagenase degradation of the scaffolds was used to project the rate of degradation of each template. Integra® served as the gold standard for each test. Quantifiable data was statistically analysed and any comparison made included the calculation of means, standard deviations and p-values (confidence interval of 95%).

Results:

Results indicated that highly porous bioactive tissue engineering matrices were obtained by either controlled freezing or uncontrolled freezing. The average pore diameter of the most homogenous scaffolds ranged between 52.47 and 136.44 μm with a mean of 87.34 μm. These templates were formed by using a 0.5% collagen concentration and a controlled freeze rate of 0.92 °C/min. Uncontrolled freezing (1.3 °C/min) of a 0.5% collagen concentration resulted in the formation of an irregular scaffold with an average pore diameter of 174.08 μm. It was found that the architecture of the most equivalent scaffold compared well with that of Integra® with $p = 0.424$. Scaffolds prepared using higher collagen concentrations (1.0%) and controlled freezing resulted in dense sponges with average pore diameters of 56.51 μm. Statistical analysis upon comparison indicated a significant difference $p = 0.000$ in the micro architecture. The rate of degradation of the most equivalent scaffold was 1.9 times that of Integra®. This implicates that the crosslinking was insufficient and due to one of the following: poor collagen

quality; method of crosslinking; and degradation due to terminal sterilization. The rate of scaffold degradation can be extended, either by additional crosslinking or the prevention of degradation induced by irradiation. Temperature vacuum dehydration crosslinking through esterification or amide formation can be used as an initial crosslinking method in further studies. This form of crosslinking will complete the conventional glutaraldehyde crosslinking that reacts with the free amine groups of lysine or hydroxylysine of the protein backbone of collagen. It should be stressed that the determination of an *in vivo* degradation rate, in the form of an animal study, will aid to confirm the efficacy of the biologically active regeneration matrix.

Keywords:

Tissue engineering; regenerative medicine; full thickness burn wounds; collagen; collagen-glycosaminoglycan copolymer; regeneration template; extracellular matrix analogue.

OPSOMMING

DIE INGENIEURSWESE VAN ‘N KOLLAGEEN-GLUKOSAMINOGLUKAAN KO-POLIMEER DERMALE REGENERASIE MATRIKS

QB Wessels
Studieleier: Prof. E. Pretorius

Skool van Geneeskunde, Fakulteit Gesondheidswetenskappe, Universiteit van Pretoria, Pretoria, Suid Afrika

Agtergrond:
Weefselingenieurswese se bydra to regeneratiewe geneeskunde het deur die jare ontwikkel en is vandag, veral in terme van gevorderde voldikte brandwonde, ongetwyfeld effekief. Hierdie gevorderde wetenskap is die sinergisme tussen biologiese wetenskappe en ingenieurswese. Die doel van weefselingenieurswese is die generasie van nuwe weefsel. Verskeie kommersiële weefselingenieurswese produkte het intussen, as gevolg van die baanbreker werk van menigte wetenskaplikes, die mark ingetree. By uitstek is Integra™ die bekenste hiervan. Hierdie kollageen-glukosaminoglukaan bioaktiewe matriks is die resultaat van die voortgesette werk van Yannas en Burke. Dit is ‘n ekstrasellulêre matriks eweknie wat dien as ‘n tydelike raamwerk vir dermale regenerasie. Sodoende word wondgenesing bevorder sowel as die bekamping van letsel formasie en geassosieerde wond konstraksie. Met die jare het die aanwending van Integra™ uitgebrei na ‘n regeneratiewe templaat vir plastiese en rekonstruktiewe chirurgie.

Doelwitte:
Hierdie studie verskaf nie net ‘n breedvoerige oorsig van die navorsing wat gedoen is vir die ontwikkeling van Integra® nie, maar poog ook om ‘n soortgelyke

produk ontwikkelling te dokumenteer. Daar word veral aandag gegee aan: die biologiese boustene en motivering van hul gebruik; die essensiële produksie stappe; asook die finale prosessering om ‘n steriele produk te lewer. ‘

Materiaal en Metodes:

‘n Kollageen chondroitin 6- sulfaat ko-presipitaat was gekontrolleerd en ongekontrolleerd gevries teen 0.92 °C/min en 1.3 °C/min respektiewelik. Hierna was die gevriesde oplossings onder vakuum gedroog vir ‘n minimum van 17 ure. Die resultaat was verskeie droë sponse wat later met ‘n dun laag silikoon rubber bekleed was. Kruisverbinding is gedoen met glutaraldehied en was gevolg met ‘n wasproses, verpakking en terminale sterilisasie het gevolg. Die finale produk was aan verskeie toetse onderwerp om beide die biover enigbaarheid en effektiwiteit te bepaal. Skanderings elektronmikroskopie was gebruik om die mikrostruktuur en integriteit van die regenerasie template te evalueer. Ensiematiese afbraak, deur van die proteolitiese ensiem kollagenase gebruik te maak, het ‘n aanduiding gegee van die tempo van afbraak. ‘n Vergelyking was getref tussen Integra® en die generiese kollageen-GAG matrikse. Kwantifiseerbare data was statisties geprosesseer en grafies voorgestel. Rekenkundige gemiddelde, standaardafwykings en p-waardes (met ‘n 95% sekerheids interval) was bereken.

Resultate:

Die resultate toon dat verskeie hoogs porieuse bioaktiewe template verkry is deur beide die gereguleerde vriestempo en die ongereguleerde vriestempo. Die gemiddelde porie grootte van die mees homogene template het gewissel tussen 52.47 en 136.44 µm met ‘n gemiddeld van 87.34 µm. Hierdie template was gevorm deur ‘n kollageen konsentrasie van 0.5% en ‘n gereguleerde vriestempo van 0.92°C/min. Ongereguleerde bevriessing van ‘n 0.5% kollageen oplossing, daarteenoor, het ‘n onreëlmatige templaat met ‘n gemiddelde porie diameter van 174.08 µm gelewer. Hierdie templaat het nie aan die voortgesette vereistes voldoen nie. Die eersgenoemde templaat was vergelyk met Integra® in terme van mikro-argitektuur. Die verskil was statisties nie beduidend nie met p = 0.424. ‘n

Hoër kollageen inhoud (1.0%) het digter templaat gelewer met ‘n gemiddelde porie diameter van 56.51 µm. Statistiese analise het ‘n beduidende verskil ($p = 0.000$) aangedui tussen hierdie template en Integra® in terme van argitektuur. Die tempo van afbraak van die mees geskikste template was 1.9 keer vinniger as die van Integra®. Dit implisseer dat die kruisverbinding oneffektief was. Moontlike redes hiervoor sluit ondermeer die kwaliteit van die kollageen, die metode van kruisverbinding, en terminale sterilisasie in. Ten spyte van hiervan moet in ag geneem word dat die matriks lank genoeg in die liggaam sal bly vir regenerasie om plaas te vind. Nie te min kan die kruisverbinding bevorder word deur aanvanklike fisiese kruisverbing deur hitte of addisionele chemiese kruisverbinding. ‘n Dierestudie sal bepaal of die matriks effektiewelik kan dien as ‘n regenerasie templaat sonder om letselvorming te weeg te bring.

Sleutelwoorde:

Weefselingenieurswese; regeneratiewe geneeskunde; gevorderde voldikte brandwonde; kollageen-glukosaminoglukaan bioaktiewe matriks; kollageen; regenerasie templaat; ekstrasellulêre matriks eweknie.

LIST OF ABBREVIATIONS

ABS	Acrylonitrile Butadiene Styrene
CEA	Cultured epithelial autografts
CGM	Collagen-glycosaminoglycan matrix
CV	Coefficient of variance
DHT	Dehydrothermal treatment
DMSO	Dimethyl sulfoxide
DNA	Deoxyribonucleic acid
DPBS	Dulbecco's phosphate buffered saline
EB	Electron beam
ECM	Extracellular matrix
EMEM	Eagle's minimum essential medium
EO	Ethylene oxide
EPDM	Ethylene-propylene dienne monomer
ETFE	Ethylene-tetrafluoroethylene
F	Fibre
FBM	Fibroblast basal medium
FEP	Fluorinated ethylene propylene
FGF	Fibroblast growth factor
GA	Glutaraldehyde
GAG	Glycosaminoglycan
HDPE	High density polyethylene
K-CGM	Keratinocyte seeded collagen-glycosaminoglycan matrix
KFG	Keratinocyte growth factor
LDPE	Low density polyethylene
LLDPE	Linear low density polyethylene
MTT	3-(4,5-Dimethylthiazol-2-yl)-2,5-diphenyltetrazolium bromide
P	Pore
PCTFE	Polyethylenechlorotrifluoroethylene
PDGF	Platelet derived growth factor

PDMS	Polydimethylsiloxane
PET	Polyethylene terephthalate
PETG	Polyethylene terephthalate copolyester
PTFE	Polytetrafluoroethylene
PVC	Polyvinyl chloride
PVDC	Polyvinylidene chloride
S	Sheet
SEM	Scanning electron microscope
TBSA	Total body surface area
TGF	Transforming growth factor
UHMWPE	Ultra high molecular weight polyethylene
VEGF	Vascular endothelial growth factor

INDEX

CHAPTER 1

INTRODUCTION AND PROBLEM STATEMENT **14**

1.1 INTRODUCTION 14
1.2 PROBLEM STATEMENT AND HYPOTHESIS 14
1.3 AIMS AND OBJECTIVES 16
1.4. SUMMARY 16

CHAPTER 2

LITERATURE REVIEW **17**

2.1 BACKGROUND 17
2.2 CLASSICAL INFLAMMATORY WOUND HEALING 20
2.3 COLLAGEN-GAG FACILITATION OF WOUND HEALING AND DERMAL REGENERATION 24
2.4 THE EFFICIENCY OF COLLAGEN BASED TISSUE ENGINEERING SCAFFOLDS 26
2.5 CGM FOR REGENERATION OF SKIN 31
2.5.1 Day 4 post-grafting 32
2.5.2 Day 8 post-grafting 33
2.5.3 Day 12 post-grafting 34
2.5.4 Day 15 post-grafting 35
2.5.5 Day 19 post-grafting 36
2.5.6 Day 35 post-grafting 36
2.6 ENGINEERING OF A DERMAL REGENERATION MATRIX 38
2.6.1 The components of an artificial skin 38
2.6.2 Collagen as biomaterial 40
2.6.3 Structure and distribution of collagen in tissue 41

2.6.4 Antigenicity of collagen 42
2.6.5 Collagen and wound healing 43
2.6.6 A review on silicones as biomaterials 43
2.7 SUMMARY 45

CHAPTER 3

ENGINEERING OF A DERMAL REGENERATION SCAFFOLD 47

3.1 INTRODUCTION 47
3.2 PREPARATION OF AN OPTIMAL COLLAGEN-GAG SUSPENSION 47
3.3 SCAFFOLD ARCHITECTURE 53
3.4 FORMATION OF AN ARTIFICIAL EPIDERMAL LAYER 60
3.5 CROSSLINKING 61
3.6 PACKAGING, TERMINAL STERILIZATION AND STORAGE 67
3.7 SUMMARY 72

CHAPTER 4

MATERIALS AND METHODS 73

4.1 INTRODUCTION 73
4.2 SCAFFOLD PREPARATION 74
4.2.1 Collagen-GAG coprecipitate formation and pouring 74
4.2.2 Controlled freezing 74
4.2.3 Lyophilization 77
4.2.4 Formation of an artificial epidermal layer 78
4.2.5 Optimal glutaraldehyde crosslinking 79
4.2.6 Removal of free aldehydes 79
4.2.7 Packaging, terminal sterilization and storage 80
4.3 ELECTRON MICROSCOPIC ANALYSIS 81
4.4 ENZYMATIC DEGRADATION ASSAY 83
4.5 CYTOTOXICITY ASSAY 84

CHAPTER 5

RESULTS AND DISCUSSION **86**

5.1 INTRODUCTION 86
5.2 COLLAGEN-GAG SCAFFOLD ARCHITECTURE 86
5.3 ENZYMATIC DEGRADATION ASSAY 93
5.4 CYTOTOXICITY ASSAY 96
5.5 SUMMARY 97

CHAPTER 6

CONCLUSION **99**

CHAPTER 7

REFERENCES **101**

CHAPTER 1

INTRODUCTION AND PROBLEM STATEMENT

1.1 INTRODUCTION

Advances in technology in the field of wound care have afforded practitioners solutions that are invaluable with regards to the management of their patients. Biological dressings have proven themselves to be useful in the management of burns and as an adjunct to advanced wound management in the treatment of hard to heal acute and chronic wounds. The origin and success and of these biological dressing is largely attributed to tissue engineering.

Tissue engineering is a fairly young science that focuses on the generation of new tissue through the synergy of both biology and engineering. The early 1970s prompted the pioneering work done by Dr. W.T. Green from the Boston Children's Hospital. His work focused on the regeneration cartilage through the seeding of chondrocytes onto bone. Although his attempts failed, Green foresaw the emergence of tissue engineering. He concluded that it will be possible to seed viable cells onto appropriate bioscaffolds. It was only a few years later that Greens' dream was materialized through the successful work by Burke and Yannas. This collaboration produced a collagen based artificial skin for the support of neodermis formation [1].

Collagen-based products such as sutures, allogenic and xenogenic skin, amnion, placenta and fascia have aided reparative medicine in soft tissue repair since the turn of the century. Several of these medical devices have been approved for medical use but only a few became commercially viable. Collagen has been motivated as the biomaterial of choice due to the following reasons [2]:

- Well defined methodology for extracting large qualities of medical grade collagen.

- Collagen-based devices have proved themselves through well known products.
- Collagen has a good safety record as biomaterial.
- This biomaterial in particular can be manipulated in various shapes for minimally invasive procedures.
- There has been an increase into the understanding of the biosynthesis and the role of collagen in wound healing.

Tissue engineers have focused on designing products with scaffolds or matrices that mainly contain collagen. This thesis therefore investigates the use of collagen as a biomaterial in the development of an engineered dermal regeneration matrix for reconstructive surgery and reparative medicine.

1.2 PROBLEM STATEMENT AND HYPOTHESIS

Adult dermal regeneration does not occur spontaneously [3-6]. Unassisted wound closure of deep dermal injuries result in excessive scarring and wound contraction. This in return impairs or inhibits the mobility of the affected area. A large full thickness wound that cannot close through contracture or re-epithelialization can be fatal. This is due to the loss of an intact physical barrier that leads to inflammation and enhanced catabolism [7,8].

The affordability of biological dressings is often questioned. Research in the field consequently led to the design and manufacture of affordable dermal regeneration matrices that will provide all the proven benefits to patients and wound care practitioners.

The physicochemical properties, microstructure and stability credit this engineered collagen-glycosaminoglycan (collagen-GAG) copolymer dermal regeneration matrix a reliable bioscaffold or substitute ECM that can serve as an artificial skin.

1.3 AIMS AND OBJECTIVES

The following will be addressed:

3.1 Collagen-GAG facilitation of dermal regeneration.

3.2 The efficiency of collagen based tissue engineering scaffolds.

3.3 The use of collagen in the engineering of a biocompatible artificial skin (dermal regeneration matrix) and paying special attention to:

A. Preparation of an optimal collagen-GAG suspension.

B. Scaffold architecture - The influence of freezing rate on the pore structure.

C. The influence of freezing container on the scaffold porosity.

D. Formation of an artificial epidermal layer.

E. Optimal procedure for crosslinking of the scaffold.

F. Procedures for removal of unbound aldehydes.

G. Optimal packaging, terminal sterilization and storage.

H. Cytotoxicity analysis to asses the effectiveness of free aldehyde removal.

I. Determination of the rate of degradation of the scaffold.

J. Electron microscopic analysis of the engineered scaffold.

1.4. SUMMARY

Tissue engineered skin substitutes, such as Integra®, have become an invaluable resource in reparative medicine. The representative epidermal and dermal components of such a dermal regeneration matrix are known to enhance wound healing and closure of deep dermal injuries. In so doing, skin substitutes not only saves lives as in the case of full-thickness burn wounds but also improves the quality of live of those affected.

.

CHAPTER 2

LITERATURE REVIEW

2.1 BACKGROUND

Reparative medicine employs current technology and various materials in its aim to replace, repair or enhance tissue and organs. The clinical need to address injuries, birth defects and degeneration beyond the scope of a singular scientific discipline has become the driving force behind reparative medicine. A number of strategies are employed in reparative medicine and include; substitution of one body part with another, the utilization of synthetic materials and devices, the use of allografts or xenografts, the use of an external device to augment or replace the non-functioning organ, and the employment of living cells. The latter strategy is known as tissue engineering and serves to repair, preserve, or improve the function of tissues and organs [9].

Intact skin has two functional and anatomical layers known as the epidermis and dermis. The epidermis serves as a physical barrier against infection and fluid loss. The deeper dermal layer provides a scaffold for blood vessels and nerves and also renders the epidermis elastic and mechanically sound. Accessory structures such as the follicles and sweat glands pass through both the dermis and epidermis. The epidermis is maintained through the diffusion of nutrients and oxygen from the dermal capillaries [10]. Injury to both the epidermis and dermis requires the employment of wound care to prevent infection and fluid loss. The following paragraphs provide a brief history of the progression of wound care and wound dressings through the ages.

Wound care over the ages advanced from the use of ointments and pastes, the meticulous surgery of Hippocrates and Celsus, to bioengineered skin substitutes [11]. A Sumerian clay tablet, dating back to 2100 B.C., testifies on the notion to

dress a wound. The ancient text describes the washing of wounds with beer and hot water as well as the coverage of these wounds with oils, herbs and ointments [12,13]. Egyptian physicians used a range of remedies to treat ailments and open wounds. Papyrus text, 1400 B.C., employed a combination of honey, grease and lint to encourage wound healing [14]. It has been shown that an ointment with one part honey and two parts butter was able to lower a 10^5 *Staphylococcus* and *Escherichia coli* count to less than 10^2 [12].

Wine was another bactericide from antiquity its efficacy is ascribed to both the alcohol content as well as the presence of the pigments, malvoside and oenoside [12]. The Bible describes in Luke 10:34 how the Good Samaritan used a dressing of oil and wine to treat the wounds of the afflicted traveller. The two mentioned pigments become activated during fermentation and are able to kill *Vibrio cholera*, *Escherichia typhi* and *E. coli* [12]. Cornelius Celsus, a Roman physician, documented in *De medicina* a list of 34 dressings and ointments used during the time of Christ. The majority of these dressings and others contained lead and copper salts as well as silver nitrate [12]. Today, the antibacterial properties of silver are well known and this is demonstrated through the variety of silver based dressings that are commercially available. Joseph Lister (1827-1912) introduced the world to the first antiseptic dressing consisting of gauze or lint soaked in phenol. Robert Wood Johnson was present at Lister's presentation in 1876 on aseptic surgical procedures and the presentation of his aseptic dressing soaked with carbolic acid. The result was the mass production of sterile surgical dressings by Johnson and Johnson in 1891 [15]. Work done by Joseph Gamgee in 1880 resulted in the development of an absorbent dressing composed of cotton sandwiched between layers of gauze. The objective of former wound dressings was to keep the wound dry and prevent bacterial infection by serving as a physical barrier [16]. The use of a minimally adherent gauze and non-adherent Tefla followed in 1944 and 1954 respectively [11]. Groundbreaking research by Winter and Hinman [17,18] during the 1960s demonstrated that moist wounds

showed a reduction in inflammation and re-epithelialized faster. Their findings were confirmed by work done during the 1980s [19-21].

Bioengineering research over the past 20 years underwrote the development of effective and advanced wound management products. The applications of these bioengineered skin substitutes include the treatment of: various thickness burn wounds; chronic diabetic ulcers and chronic venous ulcers [22]. The ideal dermal skin substitute has been described and should be non-antigenic, biologically compatible, robust, adherent, easily available and inexpensive [23-35]. This list of prerequisites has expanded over time and now includes: elasticity; provision of a moist environment; effective management of wound exudates; and the ability of non-traumatic removal [26]. Wound management products can be categorized based on their application as wound coverage products and wound closure products. Wound coverage products are intended for superficial burns. These products, through the prevention of dehydration and infection, improve epidermal restoration. It should be noted that the product does not become integrated with the wound. Examples of such products include Biobrane® and Transcyte®. Wound closure products, such as Alloderm® and Integra®, on the other hand, become integrated into the wound bed. This provides the material necessary to restore the dermis and thus serves as a regeneration template [26].

Burke and Yannas published their ground breaking article on the blueprint of Integra®, a biologically active dermal regeneration template, in 1980 [27]. This template was successfully used a year later for the treatment of extensively burnt patients. Their findings were based on the treatment of 10 patients with burn wounds that covered 50-95% of their body surface areas. Other publications by these authors followed in which they described the design and considerations of their acellular artificial skin or dermal regeneration template. They mimicked the extracellular matrix scaffold of living dermis with a covalently bonded collagen-glycosaminoglycan construct. This artificial scaffold was covered with an ultrathin silicone film that served as a physical barrier against infection [28-29].

Integra® was approved by the U.S. Food and Drug Administration in 1996 and has, since then, become synonymous with the treatment of major burn wounds [28]. The stable extra cellular matrix is placed on the excised wound bed and is overgrafted after a few weeks. A very thin skin graft is used from an appropriate donor site such as the posterior aspect of the thigh. This method has been shown to resist the recurrence of scarring compared to the use of traditional skin grafts [29]. The indications for the use of Integra® have widened over the past years and now includes: the treatment of hypertrophic scars and keloids; reconstructive surgery; as well as its application over exposed tendons and bones [30,31]. In order to understand the role of Integra® in the prevention of scarring in contractures it is necessary to comprehend the mechanisms involved in classical wound healing.

2.2 CLASSICAL INFLAMMATORY WOUND HEALING

The continuous process of dermal maintenance is interrupted through injury. Burn injuries can be classified as either partial thickness or full thickness and their severity also depends on the percentage of total body surface area that is affected. The classification correlates to the possibility of healing without surgical intervention. Partial thickness burns can be sub-categorized as either superficial or deep. Superficial burns, unlike deep burns, heal relatively fast (within 14 days) with minimal scarring. The indicators for the determination of the depth of burn wounds are presented in Table 2.1. [32].

Table 2.1. The indicators for the determination of the depth of burn wounds [32].

Burn type	Skin Colour	Blisters	Capillary refill	Sensation	Pinprick	Healing
Epidermal	Red	Absent	Brisk	Painful	Bleeds	Yes
Superficial dermal	Pale pink	Small blisters	Brisk	Painful	Bleeds	Yes
Mid-dermal	Dark pink	Present	Slow	May be painful	Bleeds	Usually
Deep dermal	Dry blotchy red	May be present	Absent	No pain	No bleeding	No
Full thickness	Dry white/black	Absent	Absent	No pain	No bleeding	No

Wound healing is characterized by a sequence of events known as classical inflammatory wound healing. The initial phase is the formation of a haemostatic plug (also known as coagulation), this is followed by inflammation, cellular migration and proliferation, and remodelling (Fig. 2.1) [33].

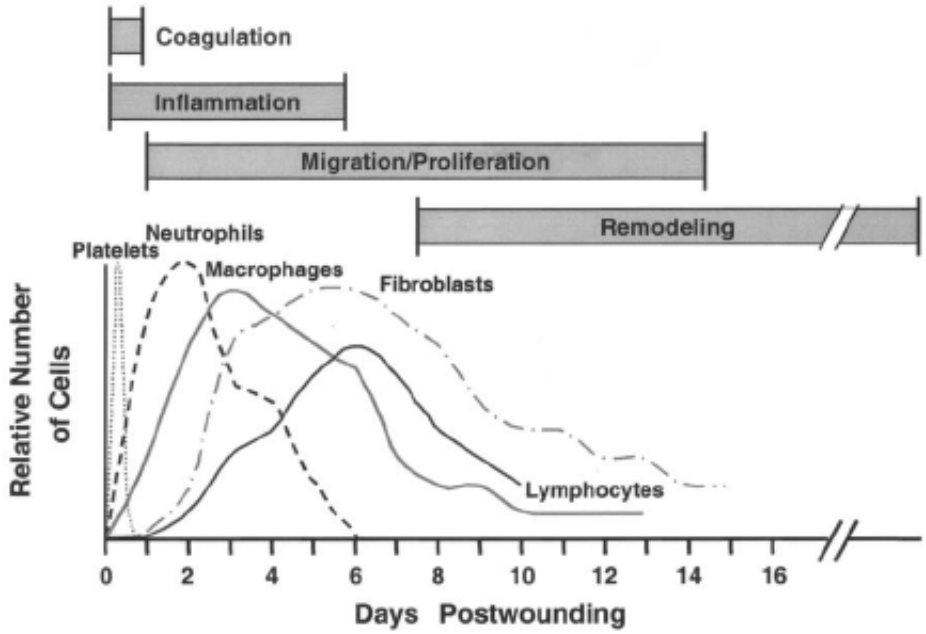

Fig. 2.1. The phases of inflammatory wound healing [33].

Effective wound healing relies on the interaction between cellular components, growth factors and cytokines. The cells involved in the four phases of wound

healing include; fibroblasts, epithelial cells, and endothelial cells as well as leucocytes that migrate to the traumatized area [34]. It is now believed that wound healing is modulated through paracrine and autocrine cytokines of the various skin cells. This is contrary to the idea of macrophages being the composer of wound healing [35-38].

Neutrophils and monocytes permeate to the wound site due to changes in the architecture of endothelial cells lining the damaged area. The Neutrophils have the dual purpose of eliciting an inflammatory response as well as the activation of fibroblasts [39]. The amount of localized neutrophils decline progressively a few days after injury. Mobilized monocytes remain and they are responsible for the removal of debris and pathogens, as well as the release of growth factors and cytokines [40,41].

Fibroblasts seem to play a major role during the proliferation and remodelling phases of wound healing. These phases are characterized by epithelialisation, visualization (angiogenesis) and consequent formation of granular tissue (wound connective tissue). Freshly formed neodermis has a pink granular appearance due to the formation and invasion of capillaries [42]. Angiogenesis is necessary to sustain the granular tissue and is promoted by basic fibroblast growth factor (FGF) and vascular endothelial growth factor (VEGF). FGF is a product of macrophages and damaged endothelial cells [37]. The keratinocytes on the wound edge as well as macrophages are responsible for the release of VEGF. VEGF secretion is thought to be initiated by keratinocyte growth factor (KFG) and transformation growth factor-*α* (TGF-*α*) [43].

Granulation tissue appears four days after injury and it is an accumulation site of cytokines [40,44]. Fibroblasts, macrophages and capillaries infiltrate the wound space at the same time [45]. Wound-edge fibroblasts are stimulated to proliferate, migrate and express integrin receptors. This is achieved through the presence of extracellular matrix molecules, platelet derived growth factor (PDGF) and transformation growth factor-*β2* (TGF-*β2*) [45-47]. PDGF originates from

keratinocytes, platelets and macrophages. Platelets and macrophages are also responsible for the production of TGF-*β2* [48,49].

The provisional matrix (newly formed matrix) with its structural molecules (fibrin, fibronectin, and hyaluronic acid) is a product of fibroblasts and it serves as a scaffold for newly formed cells and blood vessels [35,50,51]. Fibroblasts in the wound are prompted to inhibit local collagen integrin-receptor expression. The expression of this receptor is stimulated, on the other hand, where it is needed for adhesion to the provisional matrix molecules. The up/down-regulation of fibroblast integrin-receptor expression is thus dependent the presence of either growth factors and provisional matrix molecules or growth factors and an existing collagen matrix [47]. Proteolytic serum-derived plasmin and fibroblast-derived enzymes enable the migration of cells through the matrix during the phases of wound healing [52,53]. Fibroblasts undergo a phenotype transformation to myofibroblasts. Myofibroblast wound contraction is mediated by an increase in cytoplasmic actin microfilaments, cell-cell interaction and cell-matrix interaction [54,55].

A collagenous matrix replaces the provisional matrix and the fibroblasts stop with collagen production once enough collagen has been deposited [56]. Fibroblast rich granulation tissue will ultimately make way for acellular scar tissue [35]. The scar tissue is acellular due to chronological apoptosis of endothelial cells and myofibroblasts [44]. It is thus evident that the interplay of various cells and their products result in the progressive advancement of wound healing. Fibroblasts play a critical role during epithelialisation, vascularization and matrix remodelling.

Unassisted wound closure of deep dermal injuries result in excessive scarring and wound contraction. This in return impairs or inhibits the mobility of the affected area. A large full thickness wound that cannot close through contraction or re-epithelialisation can be fatal. This is due to the loss of an intact physical barrier that leads to inflammation and enhanced catabolism [57,58].

Temporary wound closure can be achieved through the use of synthetic biomaterials, allografts, or xenografts. Sequential epidermal closure is accomplished through the use of skin grafts from donor sites (split-thickness or full-thickness) or autologous cultured cells. Harvesting skin grafts from donor sites are usually painful and induces the formation of an additional wound with associated potential scarring, especially in children. Poor healing of donor sites in patients with genetic disorders and the elderly poses another problem. Autologous cultured cells or cultured epithelial autografts (CEA), on the other hand, offers the benefit of generating large quantities of cells from a small biopsy. Large surface areas can thus be covered [59].

A dermal regeneration matrix or template, such as Integra®, serves to mimic the body's extracellular matrix. Research showed that an active highly cross-linked collagen-glycosaminoglycan matrix (CGM) with a collagen:GAG weight ratio of 98:2 and a pore structure of 20-120 μm prevents scar tissue formation and promotes dermal regeneration [60]. A high cross-link density ensures the maintenance of the ECM analogue over a period of 10 days post grafting. It can thus be said that the activity of the biologically active dermal regeneration matrix is highly dependable on the integrity and the maintenance of its three-dimensional structure [60].

The critical features that determine the efficiency of dermal regeneration matrices have been identified as: biochemistry, pore size, pore volume (porosity), and the degradation rate of the matrix [3]. The following sections will focus on the function, efficiency and fabrication of an ECM analogue.

2.3 COLLAGEN-GAG FACILITATION OF WOUND HEALING AND DERMAL REGENERATION

Adult dermal regeneration does not occur spontaneously [3-6]. Aided dermal regeneration of full-thickness dermal injury has been achieved trough the use of

a type I collagen-glycosaminoglycan graft in guinea pigs. The graft, composed of collagen and chondroitin 6-sulfate (a glycosaminoglycan or GAG), served as an extracellular matrix analogue [60-67]. These findings were confirmed in humans [28,29,68]. Histological and ultra-structural studies performed on these results confirmed the formation of neodermis without accessory structures, i.e. sweat glands and hair follicles [59].

The mechanism of dermal regeneration of this biologically active graft was found to be similar to the phases of graft take. The results of the study conducted by Moiemen [69] presented neodermis formation, an organized collagen structure, and an anchored epidermal layer with rete ridges. Chondroitin 6-sulfate, the glycosaminoglycan component of the CGM, was shown to inhibit platelet aggregation and secondary cytokine release. This, in return, prevented an immune cell infiltration as well as an inflammatory response. The dermal regeneration induced by the CGM was further characterized by the controlled migration and proliferation of fibroblasts. Cell density and number were comparable to normal dermis. This also applied to newly formed capillaries. The number of myofibroblasts showed a 10 times reduction compared to granulation tissue. Furthermore, it is believed that glycosaminoglycans are responsible for the prevention of wound contraction. They are believed to bind to TGF-β and thus inhibiting a cascade that leads to wound contraction. The remodelling phase of wound repair is, as a result, distinguished by the formation of neodermis. This is a term used to describe the loose connective tissue that is formed that resembles normal dermal tissue. Coverage of the neodermis with donor epithelium resulted in the formation of rete ridges and rete pegs [69,70].

The efficiency of a CGM or a biologically active artificial skin in dermal regeneration in acute burns is well established [28]. The indications for the use of Integra® has widened over the past years. Integra® has also been used for; the treatment of hypertrophic scars and keloids; reconstructive surgery; as well as for coverage of exposed tendons and bones [30,31].

2.4 THE EFFICIENCY OF COLLAGEN BASED TISSUE ENGINEERING SCAFFOLDS

Prior to 1940 it is known that the majority of burn victims with burn injuries exceeding 40% of their total body surface area (TBSA), died [71]. Later, during the 1970s, work done by Janzekovic showed that early excision and grafting dramatically improved the chances of survival of burn victims [72]. The availability of autologous donor sites in cases where patients presented with 50% TBSA wounds posed another problem. This led to the use of cultured epidermal autografts (CEA) to cover excised areas. The work done by Rheinwald and Green in 1975 [73] on the *in vitro* cultivation of human dermal keratinocytes, made this possible. The ability to culture large volumes of cells from a small biopsy within 3-4 weeks has become valuable for the treatment of burn injuries. Temporary wound coverage until the availability of CEA or donor tissue is still required. This can be achieved through the use of allografts. Allografts have several disadvantages such as, antigenicity, unavailability, risk of disease, and a short shelf life [71]. An artificial skin, such as Integra®, on the other hand is more readily available, shows better healing and mobility, shorter hospitalization of patients, serves as an antimicrobial barrier, prevents wound contraction, and requires thinner epidermal grafts [74,75]. The disadvantages of Integra® include infection, hypersensitivity towards bovine collagen in some cases, and the need for a sequential procedure 74. The latter can potentially be overcome through the seeding of the CGM with autologous keratinocytes.

Loss *et al.* [71] documented their results on the treatment of a 26-year-old male who sustained 93% TBSA burn wounds that ranged from full-thickness (60%) to partial-thickness (33%) in severity (Fig 2.2). A combination of three therapies was employed and included; Integra® dermal regeneration template, split-thickness autografts, and autologous cultured keratinocytes (CEA) (Fig. 2.2). The dermal regeneration template, Integra®, was used to cover the full-thickness injuries on both the left arm and (Fig. 2 and Fig. 2.3) lower limbs (Fig. 2.4).

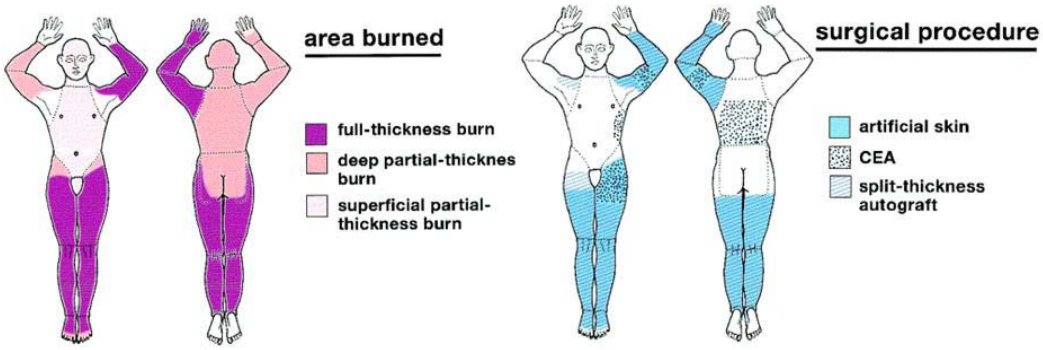

Fig. 2.2. A combination of three therapies was employed to treat a severely burnt (93% TBSA) 26 year old male [71].

Fig. 2.3. The fresh wounds were dressed with Integra® and a 1% silver sulfadiazine [71].

Autologous skin was harvested from an unaffected area of the right arm for CEA. The integrity of the artificial skin was monitored frequently. Minor complications, such as the development of pus and haematomas, were encountered and evacuated in time. The CEA was received after 3 weeks and applied to the patients back, left flank, and the upper part of the left arm. The areas were prepared by debridement prior to the application of the cultured cells. Split-thickness autografts were used to cover most of the left arm, lower left leg and left thigh [71].

Fig. 2.4. An elastic net was used to fixate the artificial skin. The artificial skin was covered with gauze. A silver nitrate solution (0.5%) was applied every 4 hours and this accounts for the black coloration as seen in the photograph [71].

Silver nitrate (0.5% solution) served as a measure against infection and was applied until the silicone sheets were removed after 6 weeks (Fig. 2.5.). Ultrathin split-thickness grafts were applied to the neodermis formed by CGM mediation (Fig. 2.6) [71].

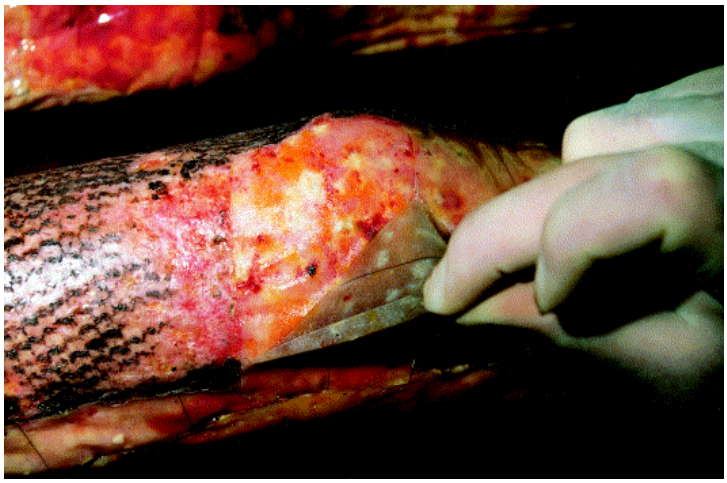

Fig. 2.5. The silicone epidermal equivalent of the CGM was removed after 6 weeks to reveal the neodermis [71].

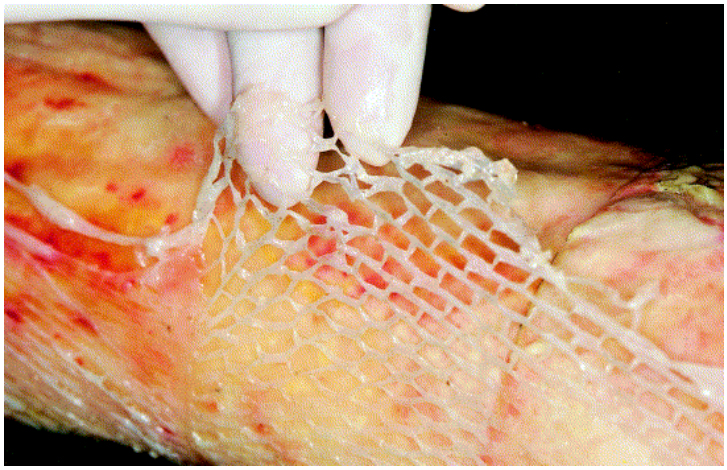

Fig. 2.6. Ultrathin split-thickness grafts were applied once the silicone was removed [71].

The results after 4 months showed that both legs healed completely without excessive scarring (Fig. 2.7). The left arm healed without cubital contractures (Fig. 2.8). The skin of the left cubital fold was thicker and visibly elastic (Fig. 2.9.) [71].

Fig. 2.7. Complete wound healing without severe scarring after 4 months [71].

Fig. 2.8. The cubital surface of the left arm healed with mild hypertrophic scarring without contractures [71].

It was noted that the Integra® covered sites recovered with better results. The skin on these areas was thicker, elastic and no contractures formed. The anterior axillary fold was not covered with Integra® and showed significant contracture after direct treatment with meshed skin autografts [71].

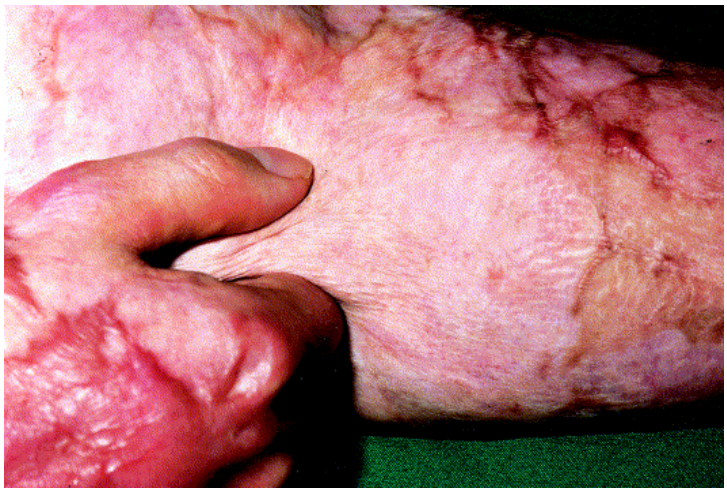

Fig. 2.9. Mild hypertrophic scarring of the left cubital fold with noted elasticity [71].

Fig. 2.10. This photograph was taken 8 months post injury and confirms complete healing without excessive scarring of both legs [71].

The areas treated with CEA indicated uniform healing and the overall cosmetic results were acceptable. The success of an artificial skin such as Integra®, as presented in the case study of Loss *et al.*, relies on the execution of a strict treatment regime. The outcome of the Integra® treated areas was significantly better than that of split-thickness autografts [71]. This was confirmed after an 8 month follow-up (Fig. 2.10). Integra® has become a valuable treatment in the survival of severely burnt individuals. Numerous other clinical results describing the employment of Integra® for the treatment of burn injuries, trauma, and reconstructive surgery, followed the publication of Burke and Yannas in 1981.

2.5 CGM FOR REGENERATION OF SKIN

A study presented by Compton *et al.* [76] used a biologically active CGM for the regeneration of an organized skin. The CGM was applied to full-thickness paraspinal dorsal wounds (4 X 4 cm) on a female Yorkshire pig. The porous side

of the CGM was seeded with keratinocytes with to obtain an approximate density of 5 X 10^5 cells per cm^2. The cells were forced to the silicone-CGM interface by centrifugation at 500 rpm for 15 min. The temperature during centrifugation was maintained at 4°C. This protocol was based on a previous study by Butler *et al*. that used the same seeding density to obtain 75% confluence after 14 days [59,76].

The results presented by Compton *et al.* are of interest when focusing on the integration of the CGM as well as the dermal regeneration mediated by the scaffold. The authors noted complete adherence of the graft with no visible signs of infection during the 35 day study. Histologic sections were prepared with an avadin-biotin peroxidase complex and aminoethylcarbozole as chromogen (Vectastain kit from Vector Laboratories, Burlingame, CA). Counterstaining was done using triple strength hematoxylin. The results obtained on days 4, 8, 12, 15, 19 and 35 are presented [76].

2.5.1 Day 4 post-grafting (Fig. 2.11)

Day 4 showed the intact eosinophilic collagen fibers on top of the wound bed. Stromal cell migration into the inner one-third of the matrix was also evident [76].

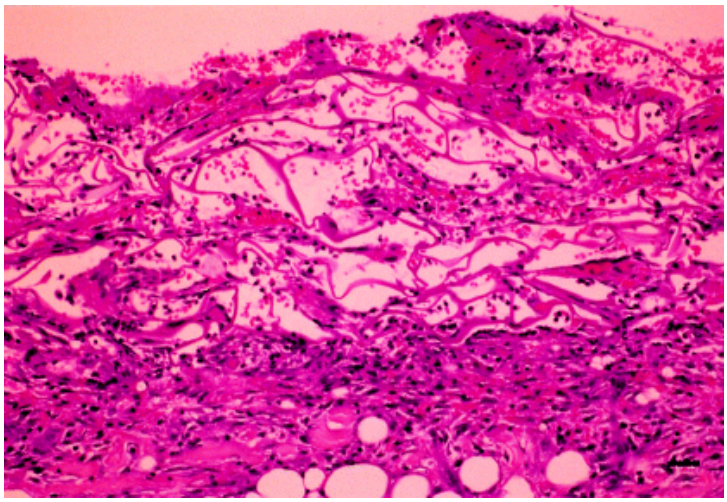

Fig. 2.11. Stromal cells from the wound bed migrated into the inner (deep) one-third of the CGM [76].

2.5.2 Day 8 post-grafting (Fig. 2.12 , Fig. 2.13 and Fig. 2.14)

Day 8 is marked by an increase in graft thickness that measures between 1.5 to 1.6 mm. This is attributed to cellular proliferation. Two-thirds of the CGM is occupied by confluent cells. Giant multinucleated cells, due to a foreign body reaction, have surrounded the fibers of the CGM. The underlying adipose tissue has been infiltrated by fibroblasts. The seeded keratinocytes were more prominent and formed cords and islands [76].

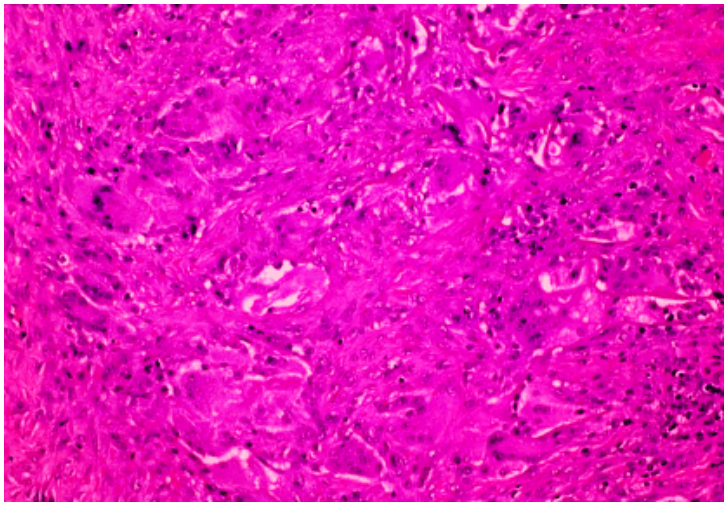

Fig. 2.12. Histologic and immunochemical investigation on day 8 showed foreign body reaction with multinucleate giant cells to the CGM [76].

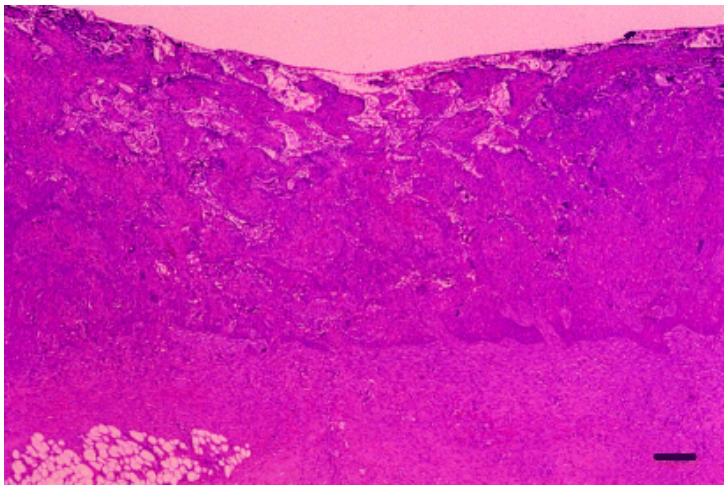

Fig. 2.13. The seeded keratinocytes have increased in number and is now more visible compared to day 4. The underlying adipose tissue has been infiltrated by fibroblasts (Scale bar = 200 μm) [76].

A dense population of spindle shaped stromal cells occupied the spaces between the cords and islands of epithelial cells. Small blood vessels could be seen amongst the stromal cells [76].

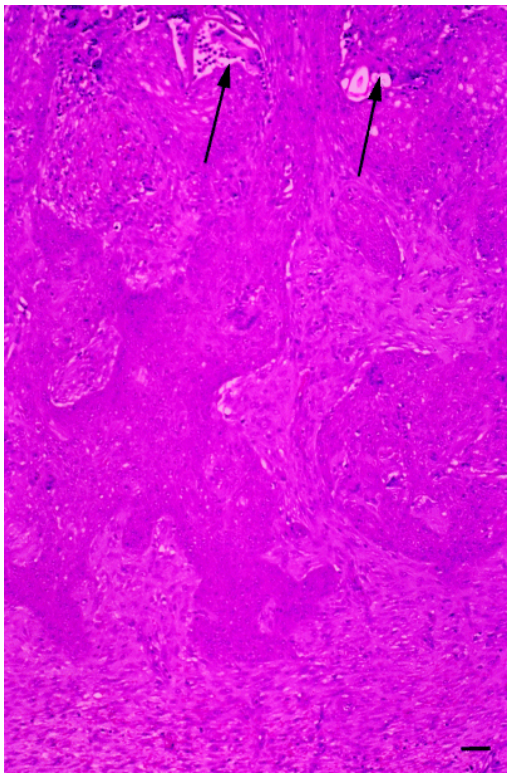

Fig. 2.14. Epithelial cords and islands with small blood vessels (arrows) and spindle shaped stromal cells in between. (Scale bar = 50 μm) [76].

2.5.3 Day 12 post-grafting (Fig. 2.15)

The keratinocyte seeded CGM (K-CGM) had a complex structure of epithelial cords. The surface of the K-CGM is completely covered with a confluent layer of keratinocytes. The graft thickness increased to 2,75 mm. Basement membrane components were also identified [76].

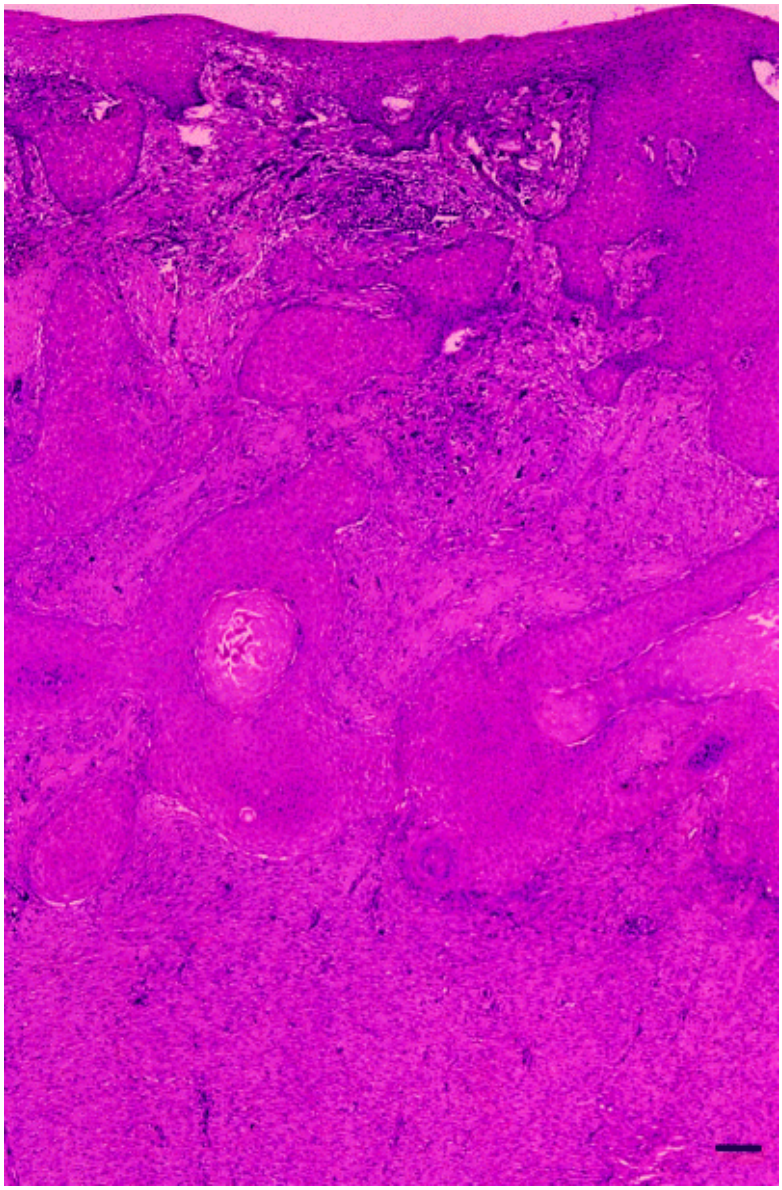

Fig. 2.15. The K-CGM after 12 days post grafting. The superficial keratinocyte layer is completely confluent. (Scale bar = 150 μm) [76].

2.5.4 Day 15 post-grafting (Fig. 2.16)

The graft thickness was equivalent to that of day 12 post grafting.

Histology showed the massive horn cysts (keratin pearls) within the epithelial islands [76].

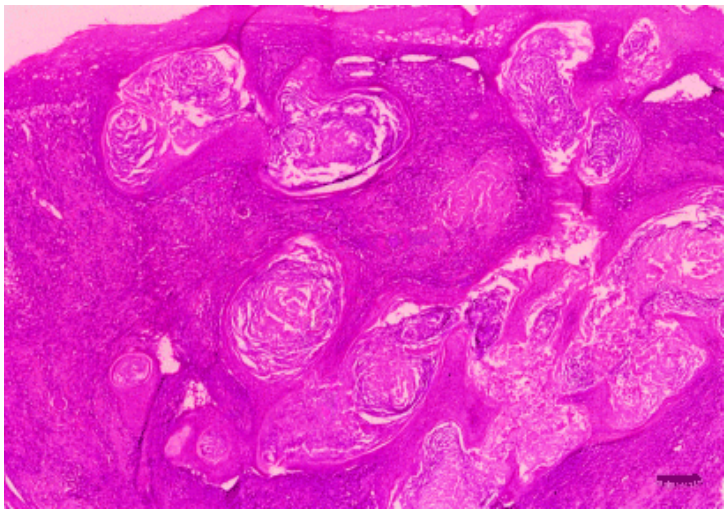

Fig. 16. Massive keratin pearls between the epithelial islands [76].

2.5.5 Day 19 post-grafting

The prominent characteristics of the K-CGM graft on day 19 post grafting are the disappearance of the horn cysts and well as the distinct border between graft and wound bed [76].

2.5.6 Day 35 post-grafting (Fig. 2.17)

The neodermis presented on day 35 post grafting was well organized. Immunostaining was used to compare the structural similarity between the neodermis and normal porcine skin. The results showed a strong correlation in the expression of Keratin 1 and Keratin 14 in both the neodermis and normal porcine skin. The superficial epidermal layer had a well established pattern of rete ridges. The CGM components were completely resorbed and the giant cell foreign body reaction was resolved. The basement membrane components were well established and diffuse [76].

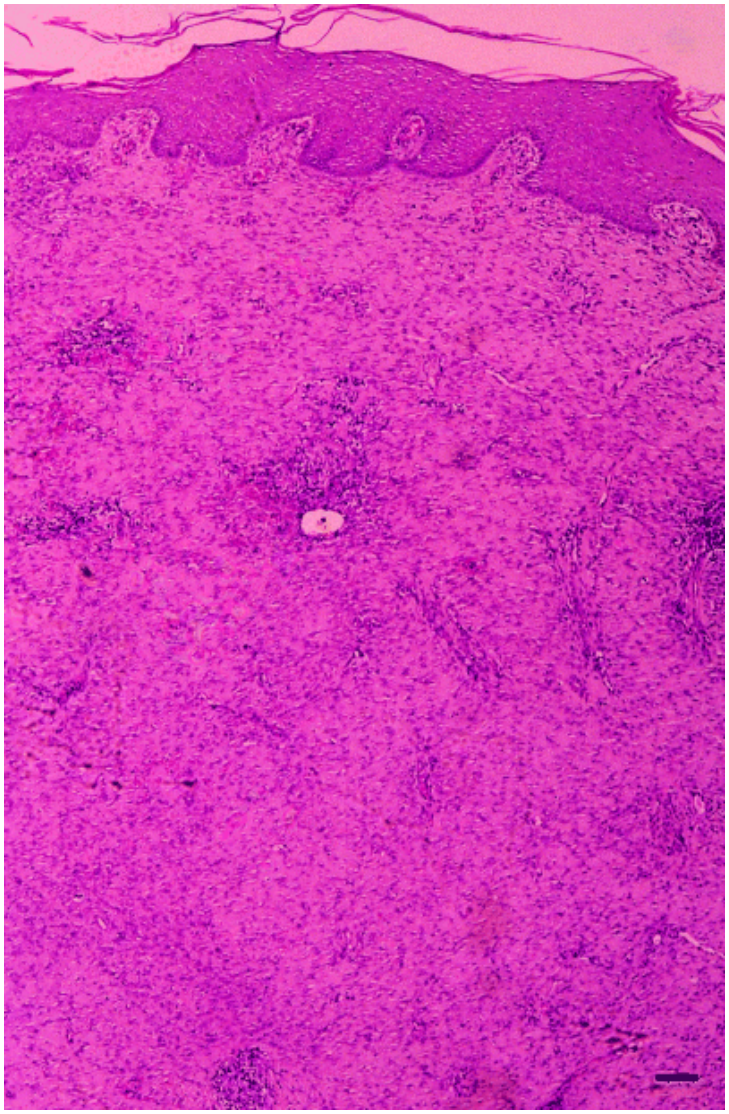

Fig. 2.17. An organized neodermis with blood vessels and associated lymphocytes. The superficial epidermal layer had a well established configuration of rete ridges. The epidermis showed a deep basement membrane as well as a superficial horny layer [76].

The histologic and immunochemical results of this study showed the formation of an organized skin structure. This was obtained using a biodegradable CGM seeded with autologous keratinocytes. Vascularized neodermis formation was accomplished along with the inhibition of wound contraction. Previous studies employing both humans and animals yielded similar results after 2-3 weeks [28,60,65,76].

2.6 ENGINEERING OF A DERMAL REGENERATION MATRIX

2.6.1 The components of an artificial skin

The collaboration between Burke and Yannas resulted in the groundbreaking development of a tissue-engineered artificial skin and their first publication appeared in 1979 in which they discussed the progress in the design of an artificial skin. Numerous other publications on their silicone coated collagen-glycosaminoglycan construct that they developed followed [65,77,78]. Table 2.2 provides the criteria for the design of an artificial skin [28].

Table2.2. The physical and biological prerequisites of a bilaminar artificial skin [28].

Physical properties	Biologic properties
Moisture change and fluid loss	Controlled rate of biodegradation
Bending rigidity	Non-toxic components
Tear strength	Low or minimal antigenicity
Degree of elasticity	Absence of inflammation or a foreign body response
Surface energy	Assist in the infiltration of normal fibroblasts and capillaries
Peel strength	Allow neodermis formation
Epidermal Silastic must be impermeable to bacteria	Prevent infection
Pore structure of the dermal portion must be controllable	Amend contractures
Excellent handling and suturing characteristics	Amend scarring

The bilaminar artificial dermis presented by Burke and Yannas [21] is composed of a porous collagen-glycosaminoglycan construct, which is covered with a disposable silastic (Figure 2.18). Their engineered regeneration template ensured a moist environment; adequate adherence; prevented contamination and fluid loss; biodegradability along with the generation of an extracellular matrix [29].

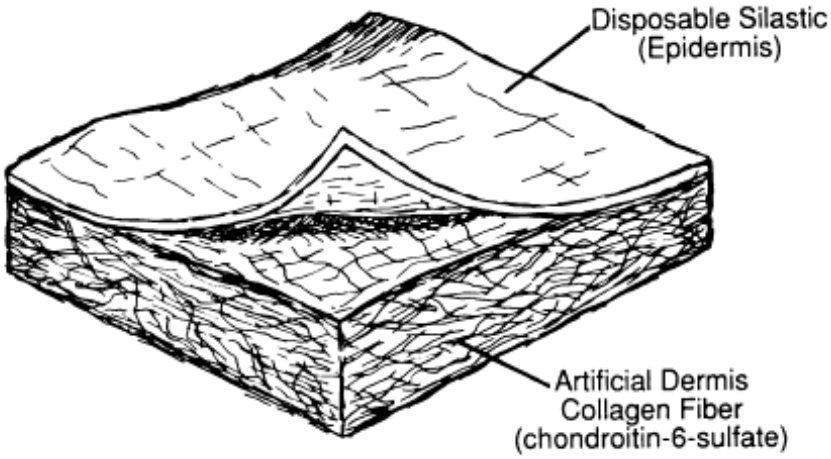

Fig. 2.18. The design template of Integra® as presented by Burke and Yannas [29].

Bovine collagen type I along with glycosaminoglycan and chondroitin 6-sulfate, forms the dermal portion of the construct. Alterations in the chondroitin 6-sulfate content and method of crosslinking were used to control the physiochemical, biochemical and mechanical properties of the matrix. These variables were also known to affect the pore size of the collagen sponge [27].

The epidermal layer consists of a biomedical grade silastic and serves as a physical barrier [28]. This layer thus prevents dehydration as well as bacterial contamination of the wound [27]. Each component necessary for the development of such a dermal regeneration template will be considered in detail. The use of biomaterial in the production of advanced wound management products is summarized in Table 2.3 [26,60].

Table 2.3. The components and applications of advanced wound management products [26,60].

Product	Company	Components	Application
Apligraf®	Organogenesis Inc.	• Neonatal keratinocytes • Collagen seeded with neonatal fibroblasts	• Treatment of chronic ulcers
Biobrane®	Bertek pharmaceuticals	• Silicone • Nylon mesh • Collagen	• Superficial partial-thickness burns • Donor sites
Dermagraft®	Advanced BioHealing	• Fibroblasts seeded onto Polyglycolic acid (Dexon®) or polyglactin 910 (Vycril®)	• Chronic lesions
Transcyte®	Advanced BioHealing	• Silicone • Fibroblasts seeded onto Nylon mesh	• Partial-thickness burn wounds • Excised burn wounds
Alloderm®	LifeCell Inc.	• Human cadaver skin without cellular components	• It serves an allograft (dermal regeneration template) for full-thickness wounds
Integra®	Integra LifeSciences Corp.	• Silicone • Collagen and glycosaminoglycan (GAG) matrix	• Dermal regeneration template for deep partial-thickness and full-thickness wounds

2.6.2 Collagen as biomaterial

Numerous materials have been considered as potential three-dimensional scaffolds for tissue engineering [79]. Collagen is proven to be minimally antigenic with low cytotoxic and inflammatory properties [81,82]. This, along with biodegradability and processability, makes collagen a suitable biomaterial for tissue engineering and reparative medicine [30,77,78,79,81,82]. Collagen sponges are highly porous which yields it effective for cell infiltration and the migration of blood vessels. The biodegradability of these biologically active scaffolds can be adjusted via changes in the formulation and crosslinking [79]. The credibility of collagen sponges has been confirmed in various instances through the

regeneration of skin, connective tissue, adipose tissue, trachea, oesophagus and peripheral nerves [30,65,83-86].

2.6.3 Structure and distribution of collagen in tissue

Collagen is a general term used to describe fibrous proteins, which consist of glycine (33%), hydroxyproline (10-13%), lysine and hydoxylysine. Collagens consist of molecular subsets termed tropocollagens. Each tropocollagen with a molecular weight of circa 300 000 DA, is formed by three left-handed helical peptide chains. The three chains together form a tertiary structure characterized by its right-handed super helix. This super helix is maintained by hydrogen bonds between the individual tropocollagen helixes. All collagens thus consist of three polypeptide chains, each having a molecular weight of 95 000-100 000 DA, termed *α*-chains. Two *α*-chain species exist and are termed *α*1 and *α*2. Type I collagen, for instance, comprises of two similar *α*1-chains and one *α*2-chain [87].

Collagens have been studied extensively especially in relation to specific tissue as an extracellular matrix as well as its correlation among species. The differences between the collagens in specific tissues are attributed to slight modifications in their structure. The same holds true for the majority of vertebrate collagens [87]. The ratio of *α*1-chains to *α*2-chains, in vertebrates, have been found to be 2:1 and can be presented as; $(\alpha 1)_2\alpha 2$ [88]. Research indicated that membrane and cartilage collagens are covalently linked to glycoproteins [89,90]. Skin, tendon and bone collagens, types I and III, have an $(\alpha 1)_2\alpha 2$ polypeptide chain composition [87,91]. Renal glomerular basement membrane collagen has an $(\alpha 1)_3$ configuration [87].

Collagens are considered as ubiquitous proteins that serve as extracellular matrix components that provide strength to various tissues. There is a striking resemblance in collagens found in different tissues and different species [87].

2.6.4 Antigenicity of collagen

Collagen was previously believed to be defectively antigenic but research later showed that it has the ability to initiate both the cellular and humoral immunity [87]. It was demonstrated that collagen's antigenicity was ascribed to the non-helical portions of tropocollagen. These protease susceptible regions are known as telopeptides. Both the *α*1 and *α*2 chains contain telopeptides and it is believed that these regions have undergone more evolutionary change compared to the main triple-helical regions [93].

Haemagglutination studies conducted by Steffen *et al*. showed that three types of species-specific antibody (Table 2.4) react with collagen, namely; A, S and P [94,95].

Table 2.4. Rabbit antibodies specific to calf collagen as demonstrated by Steffen *et al.* [94,95].

Antibody	Specificity
Anti-A	General collagen specificity and specific to protease-treated collagen
Anti-S	Species specific and reacts with both native collagen and protease-treated collagen
Anti-P	Species specific to the P-antigen (telopeptides region) on the C-terminal and only reacts with native collagen (not protease-treated collagen) of both *α*-chains

Additional research by others demonstrated antigenic determinants on both *α*1 and *α*2 chains. The researchers, Lindsley and colleagues, used a radio-immuno-assay and also confirmed the lack of interaction between the different types of *α*-chains. The predominant antigenic regions were shown to be on the C-terminals or telopeptides [96].

Cross-linked collagens, in contrast, have little or no antigenicity. A change in collagen antigenicity has been credited to molecular modifications induced by the binding of aldehydes (such as glutaraldehyde) to the amino group of lysine on the N-terminal of rat collagen *α*2 chain [96].

2.6.5 Collagen and wound healing

The building blocks of extracellular matrices include collagens, proteoglycans, glycoproteins as well as other proteins. Principally collagens provide structural support to tissue and permit the attachment of cells. The beneficial effects of collagen containing dressings can be reviewed as follows [97]:

1. Exogenous collagen stimulates haemostasis through the initiation of platelet aggregation and initiates chemotaxis of granulocytes, macrophages and fibroblasts.
2. Collagen serves as an extracellular scaffold for cell attachment, infiltration, and proliferation.
3. The collagen enhances wound healing by providing a template for collagen production and orientation.

2.6.6 A review on silicones as biomaterials

The silicones (polysiloxanes) used for medical and pharmaceutical applications are macromolecules consisting of silicon, oxygen and an alkane. The backbone of the macromolecule is formed through repeating units of Si bound to O. Research done by Kipping [98] laid the foundation of organosilicon chemistry and he coined the term “silicone” after recognizing structural similarities to that of ketones. “Siloxane” refers to the basic repeating unit of silicones. Numerous publications followed (1940s) which illustrated the potential of siloxanes as biomaterials.

Jaques *et al.* [99] (1946) conducted a study in which they found that silicone coated glassware and needles delays blood coagulation. The information they obtained was later (1949) confirmed by Margulies and Barker. They found that silicone-coated needles had no significant effect on the blood coagulation time after the blood was collected in these needles [100]. The majority of contemporary hypodermic needles are either coated or lubricated by silicone for this exact reason and it has also been found that they are less painful. Syringes and vials

are some of the other current blood collecting devices that are either lubricated or coated with medical grade silicone [98].

Elasticity and chemical stability are the key features that make silicones suitable for long- and short-term implantation. The first published report on implanted silicone was made by Lahey in 1946. Dr. Frank Lahey [101] used silicone obtained from the General Electric Company (GE) as a biomaterial for bile duct repair. De Nicola reported on the first successful artificial urethra implant in 1950. The artificial urethra was a construct made of a narrow catheter covered by silicone tube [102].

The "Spitz-Holter" hydrocephalus shunt was another silicone implant breakthrough. This silicone shunt was developed by John D. Holter in 1956 in a desperate attempt to save the life of his son, Casey, who suffered from congenital lumbosacral myelomeningocele associated hydrocephalus. Dr. Eugene Spitz successfully implanted a shunt catheter that drained excess cerebrospinal fluid from Casey's ventricle into the right atrium of his heart. The polyethylene shunt contained a double silicone slit valve and was connected to catheters on either side. It prevented backflow of CSF by acting as a one-way valve and is considered to be a landmark in the treatment of hydrocephalus [98,103].

Silicone materials have been proven as indispensable in the field of medicine. This holds true for its use in: orthopaedics (such as finger joint implants); components of blood-oxygenators and heart-bypass machines; heart valves; and aesthetic implants (e.g. mammaplasty) [98].

Polysiloxanes are formed when siloxanes are polymerized. One such polymer is polydimethylsiloxane $[SiO(CH_3)_2]_n$ or PDMS (Fig 1.). PDMS is highly biocompatible and this is attributed to its hydrophobicity, low reactivity and a lack of surface energy [98].

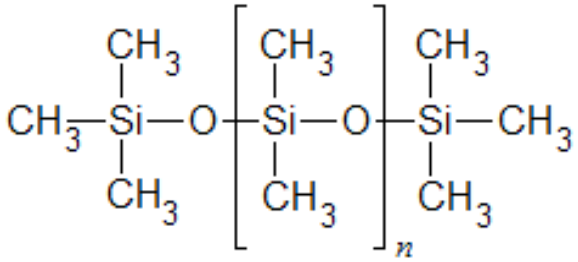

Fig 2.19. The structure of polydimethylsiloxane which has been used as an epidermal equivalent [98].

2.6.7 Silicones in wound dressings and dermal regeneration templates

The value of PDMS as a biomaterial can be further exemplified by referral to its function in an artificial skin. Dow Corning® silastics are typically used to form the epidermal portion of these collagen-glycosaminoglycan copolymers [27].

Another example for the use of silicones in wound dressings is Biobrane®. Woodroof developed Biobrane® in 1979 (published in 1983). This cell-free product consists of an ultrathin silicone film bound to a knitted-nylon fabric. The dressing is coated with collagen, which makes it both biocompatible and hydrophilic [104].

The choice of biomaterial ultimately determines the effectiveness of the product. Biomaterial science has led to the development of advanced wound management products. A variety of these products exist today (Table 2.3) and they all have specified clinical applications [26,60].

2.7 SUMMARY

From the literature presented it is thus evident that wound management has advanced form archaic coverings to bioengineered skin substitutes. Today clinicians are offered a variety of products. These products employ various biomaterials, such as collagen, that serve to both facilitate and promote wound healing. The proven efficiency of bioengineered dressings has led to a greater

demand of similar for more advanced products. One such advanced product is Integra®. Research and clinical data has proven the efficiency of this biologically active scaffold.

This thesis will further address the following research objectives in order to obtain an advanced engineered dermal regeneration matrix:

A. Preparation of an optimal collagen-GAG suspension.

B. Scaffold architecture - The influence of freezing rate on the pore structure.

C. The influence of freezing container on the scaffold porosity.

D. Formation of an artificial epidermal layer.

E. Optimal procedure for crosslinking of the scaffold.

F. Procedures for removal of unbound aldehydes.

G. Optimal packaging, terminal sterilisation and storage.

H. Cytotoxicity analysis to asses the effectiveness of free aldehyde removal.

I. Determination of the rate of degradation of the scaffold.

J. Electron microscopic analysis of the engineered scaffold.

CHAPTER 3

ENGINEERING OF A DERMAL REGENERATION SCAFFOLD

3.1 INTRODUCTION

The following sections aim to address a detailed description of the fabrication considerations and steps necessary to obtain a dermal regeneration matrix or bioengineered artificial skin. The protocol that will be used is based on the extensive work done by Burke and Yannas. Their bilayered artificial skin is fabricated through a series of events which include: formation of a collagen and chondroitin 6-sulfate coprecipitate; casting of the coprecipitate; freeze drying; dehydrothermal crosslinking; glutaraldehyde crosslinking; elution of aldehydes; and finally the formation of an epidermal layer [28]. Each of these steps will we reviewed and used to generate an optimal and reproducible method for the fabrication of an equivalent dermal regeneration template.

3.2 PREPARATION OF AN OPTIMAL COLLAGEN-GAG SUSPENSION

The tensile strength, elasticity and compressibility of normal skin are attributed to a gel-like matrix known as the extracellular matrix (ECM). This is a network of covalently cross-linked macromolecules and forms the largest component of the dermal skin layer [105,106]. The ECM not only serves as a three dimensional scaffold for cells, but also mediates cellular function through cell adhesion. There are two main classes of ECM molecules that are secreted by fibroblasts and epidermal cells [107]:

- Fibrous structural proteins. These proteins include collagen types I and III, as well as the basement membrane component, collagen type IV.
- Proteoglycans (such as hyaluronic acid and dermatan sulphate). These hydrophilic macromolecules are composed of numerous glycosaminoglycans and serve to protect cells in the ECM.

The predominant protein in the body is collagen and it consequently forms the largest component of non-wounded normal skin [107]. The dermal matrix collagens type I (80-85%) and type III (8-11%) can either be fibrillar or rod-shaped. Self-assembly of fibrillar collagen molecules results in the formation of microfibrils. The assembly occurs in a head-to-tail and spread out side-to-side lateral fashion. Crosslinking of collagen molecules to other collagen molecules result in enhanced strength and stability of collagen fibers [108].

The basic structural unit of collagen, tropocollagen (Fig. 3.2) as described previously, has an average molecular weight of 300 000 Daltons [109]. A tropocollagen fibre (300 nm long) is formed by three left-handed helical peptide chains. The three chains combine to form a tertiary structure characterized by right-handed super helix. Hydrogen bonds uphold the super helix between the individual tropocollagen helixes. All collagens thus consist of three polypeptide chains, each having a molecular weight of 95 000-100 000 DA, and are termed *α*-chains (Fig. 1). There are two types of *α*-chains, namely, *α*1 and *α*2. Type I collagen, a heterotrimer, consists of two similar *α*1-chains and one *α*2-chain. Each polypeptide chain, in its turn, is made up of repeating units of three amino acids which can be represented as follows, $(Gly\text{-}X\text{-}Y)_n$ [96,110].

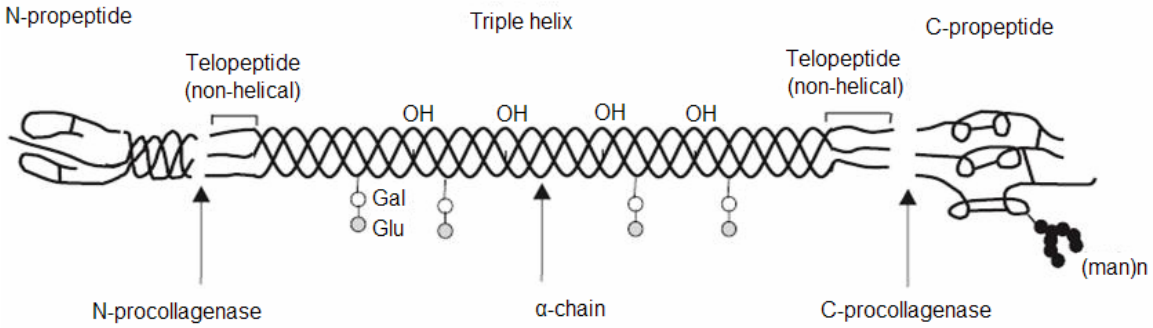

Fig. 3.2. The triple helix structure of a tropocollagen fiber along with its terminal telopeptides. Tropocollagen consists of three polypeptide chains termed *α*-chains [110].

The supramolecular assembly of the fibril forming collagens (types I, II, III, V, and XI) yield a characteristic banding pattern. The resultant is also known as

native collagen. The banding is a result of the quarter-staggered configuration of several monomers or collagen fibers as depicted in Fig. 3.3. The frequency of the banding is every 65-67 nm (Fig. 2.). A combination of a light and dark band is known as a D-period (Fig. 3.3) [111].

Fibril forming collagens, through chemical manipulation, have the ability to reassemble to their native state after disintegration. This, along with other chemical and physical properties has led to the use of collagen in medicine and other disciplines such as the food industry [112].

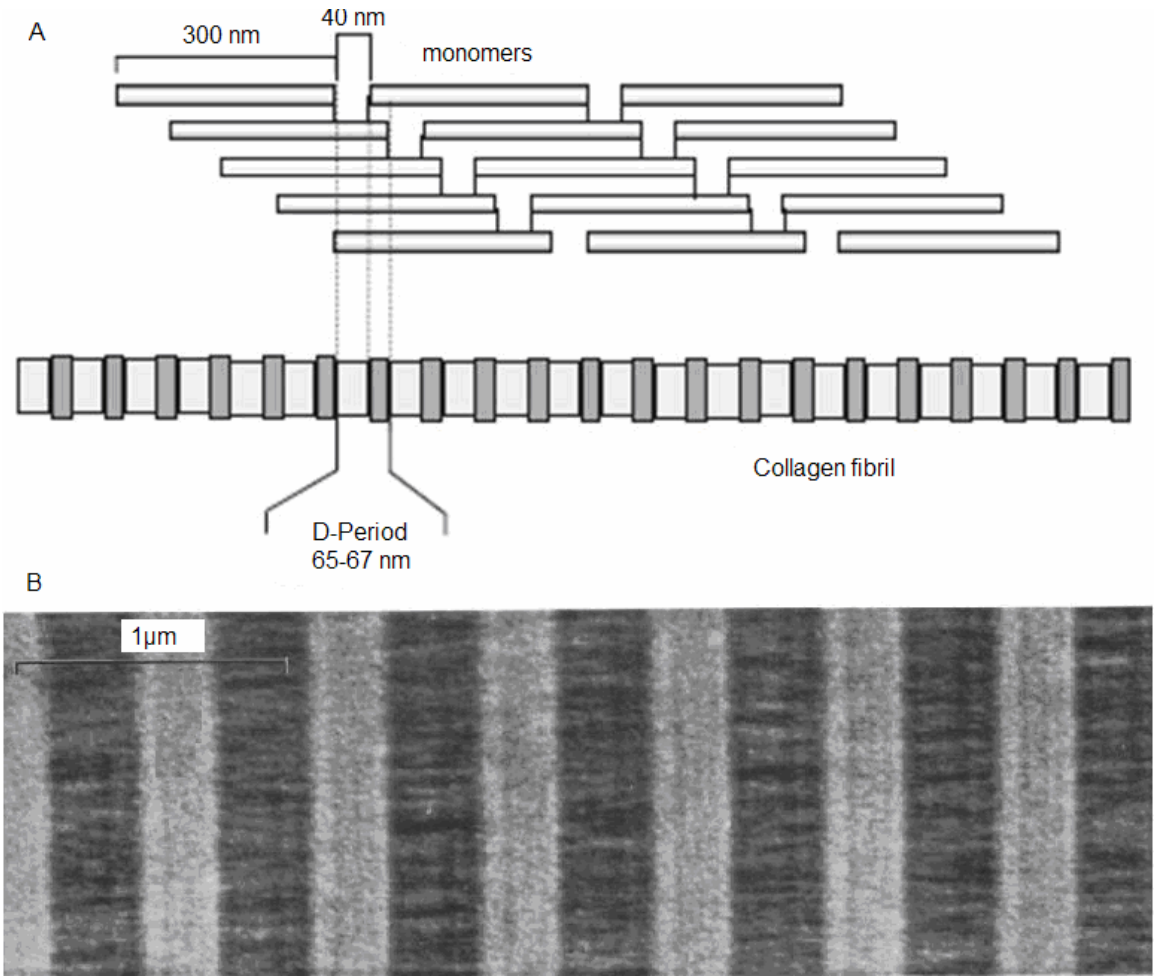

Fig. 3.3. The supramolecular assembly of fibrillar collagen as a result of quarter stagger configuration of collagen monomers (A). Successive light and dark banding is known as a D-period (A) and can be seen in the micrograph (B) of native rat tail collagen [110,113].

The regeneration capacity of collagen is largely dependant on the quality and uniformity of the extracted raw product. A study conducted by Miller *et al*. found that solubility and amount of extracted bovine hide collagen decreased proportional to the biological age of the animal. It is believed that the results obtained are due to an increase in collagen-collagen crosslinks in biologically older hides. Extraction of bovine dermal collagen was done through three different solubilisation techniques which used pepsin, acetic acid and a neutral salt respectively. Miller and colleagues concluded that more collagen can be extracted from a very young animal, but would lack adequate intermolecular cross-links. The opposite can be said for collagen extracted from a very old animal. The dermis of an old animal will yield small amounts of highly cross-linked collagen which will reconstitute into a high tensile strength structure [112]. It is thus clear that the source of extracted collagen will ultimately determine the quality of an artificial ECM.

The collagen used in this study is atelocollagen. Atelocollagen is collagen extracted by using proteolytic enzymes other than collagenase. The telopeptides, which are antigenic, are consequently removed whilst the basic triple-helical structure of collagen remains unchanged [87]. The common terms used in collagen research and their use in relation to biomaterials are provide in Table 3.1 [87].

Table 3.1. The various terms used in collagen research [87].

Term	Definition
Collagen	A general term to encompass al fibrous proteins consisting of 33% glycine, 10-13% hydroxyproline, and that shares the physicochemical properties of collagen.
Tropocollagen	Triple helical molecular subunit of collagen
Telopeptides	The nonhelical polar portions of tropocollagen that is responsible for the antigenicity of collagen.
Atelocollagen	Enzyme extracted collagen that lacks the telopeptides portion.
Gelatine	Denatured collagen obtained by heating collagen dissolved in acid.
α-chains	The polypeptide chains of tropocollagen that can be further subdivided as *α*1 and *α2*.

Glycosaminoglycans, the second chief component of the ECM, are made up of straight polysaccharide chains. Examples of ECM glycosaminoglycans include hyaluronic acid, heparin, heparin sulphate, dermatan sulphate and keratin sulphate. Glycosaminoglycans are hydrophilic and the association of water with these molecules results in the formation of a rigid structure. This structure allows for the migration of both cells and nutrients. The majority of glycosaminoglycans, except hyaluronic acid, are bound to a protein core. The resultant is known as proteoglycans [112]. Research has also indicated that glycosaminoglycans serve as co-receptors for growth factors and in so doing promotes cellular growth and differentiation [114].

The glycosaminoglycan of interest in this study is chondroitin-6-sulfate (Fig. 3.4). This compound, used by Yannas *et al.* for the development of their collagen-glycosaminoglycan scaffold, consists of alternating residues of *β*-D-glucuronate and *β*-D-N-acetylgalactosamine residues. Both the mentioned residues are sulphated in different regions [115]. Chondroitin-6-sulfate is known to play an important role during wound healing.

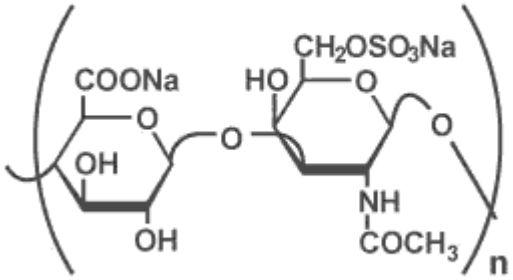

Fig. 3.4. The repeat unit of shark cartilage extracted chondroitin-6-sulfate. It has been found that this glycosaminoglycan is responsible for the promotion of cell adhesion and proliferation [116].

Zou and colleagues showed that chondroitin-6-sulfate plays an important role during wound healing [117]. Rabbit palatal fibroblasts were employed in their study. They found that chondroitin-6-sulfate promoted cellular adhesion and proliferation in a dose dependant manner. They also showed that the biological activity of chondroitin-6-sulfate depended both on the presence and location of the sulphate groups. These findings were confirmed when it was shown that inhibition of the sulphation of glycosaminoglycans, through the action of chlorate, resulted in a reduction of cell adhesion and proliferation. Furthermore, the authors also found that chondroitin-4-sulfate inhibited cell adhesion [117].

Additional motivation for the incorporation of chondroitin-6-sulfate into the scaffold arises from data that showed that collagen-glycosaminoglycan (collagen-GAG) had an increased resistance to collagenase degradation [117,118]. Furthermore, the porosity and elasticity were also enhanced compared to scaffolds that did not contain chondroitin-6-sulfate [117,119]. Yannas noted that the mentioned benefits along with its lack in antigenicity, credits chondroitin-6-sulfate as a valuable addition [117,120].

With this in mind, Yannas and colleagues stressed that in order for an artificial ECM or collagen-glycosaminoglycan scaffold to be biologically active, it had to comply with the following [121]:

- A collagen/glycosaminoglycan ratio of 92/8 (w/w).
- An average pore diameter between 20 and 120 μm.
- Highly cross-linked in order to resist degradation of its three-dimensional structure for between 5 to 15 days.

It is worth mentioning that the earlier work by Yannas *et al*. [28,60] used a collagen/glycosaminoglycan ratio of 98/2 whilst the more recent work employed a ratio in the order of 92/8 [121, 122].

Both the fibrous protein component and the proteoglycan component of normal ECM are included in the fabrication of an artificial ECM. This study will employ bovine hide collagen type I and chondroitin-6-sulfate to represent macromolecular components respectively. The information provided motivates for the use of both these molecular components. It should also the stressed that the quality and quantity of the collagen and chondroitin-6-sulftae that is used, will contribute towards the quality and suitability of the final dermal regeneration matrix or artificial ECM.

.

3.3 SCAFFOLD ARCHITECTURE

Tissue engineering relies on three-dimensional scaffolds for both *in vitro* and *in vivo* applications. A typical example of such a scaffold is the well known collagen-glycosaminoglycan (CG) construct of Burke and Yannas [27-29]. The efficiency of tissue engineering scaffolds rests upon a few vital key features. They include biocompatibility, controlled biodegradability, low or no antigenicity and, a suitable micro-structure or architecture.

The scaffold architecture in turn relies on three variables, namely, the pore size, pore structure, and the surface area of the scaffold. These variables must be manipulated in order to yield a suitable homogenous three-dimensional construct that will allow cellular phenotype, growth, migration and adhesion [122]. This has been confirmed based on studies conducted on endothelial cells, fibroblasts, osteoblasts, vascular smooth muscle cells, rat marrow cells, chondrocytes, preadipocytes, and adipocytes [123-130]. It is worth mentioning that a scaffold used for dermal regeneration should have a porosity ranging between 20 μm and 120 μm. Any pore size on either side of this critical range was found to be ineffective for dermal regeneration [60].

The uniformity of the scaffold architecture greatly influences the biomechanical outcome of the newly formed tissue. Tissue formed in a homogenous scaffold has superior biomechanical properties compared to tissue formed in a non-uniform scaffold [131]. The following literature will focus on the relevant variables that can be altered in order to obtain the ultimate bioactive collagen-glycosaminoglycan scaffold.

Doillon and colleagues [131] conducted a study in which they examined the effects of the collagen-glycosaminoglycan (collagen-GAG) co-precipitate pH, freezing temperature, and the viscosity on the pore structure and morphology of collagen scaffolds. The authors used scanning electron and light microscopy to obtain their published results. The viscosity of the collagen-GAG suspension was altered by changing the blending speed. Low blending speeds for short periods yielded low-viscosity dispersions. This method led to the formation of a fibrous structure with an average pore size of 300 μm. High-viscosity solutions, on the other hand, were achieved through high velocity mixing for 3 to 5 minutes. The result was a highly porous structure with an average pore diameter of 30 μm [131].

The effect of freeze temperature on the porosity of the resulting scaffold was examined by placing the collagen-GAG dispersion containing plastic tray on a

shelf of a freezer, or in an ethanol bath. The temperature of the freezer was maintained at -25°C while that of the ethanol bath ranged between -20°C and-90°C. Adjusting the freezing temperature between -60°C and -80°C led to the formation of a homogenous sponge. This methodology, unfortunately, had a sample loss of 25% due to the formation of cracks. Temperatures between -40°C and -60°C, on the other hand, formed a homogenous scaffold that did not crack. An average pore size of 27 μm was achieved at a temperature of -50°C. An interesting observation made by Doillon *et al*. was that the surface topography, at temperatures between -20°C and -40°C, depended on the topography of the freezing surface. Samples with an average pore size of 64 μm were obtained at a freezing temperature of -30°C using an ethanol bath (Fig. 3.5) [131].

The above mentioned results were obtained by using a conventional freeze-drying method. This method results in variable cooling rates throughout the freezing process. This technique is also known as rapid quenching and relies on the sequence of events where a collagen-GAG suspension is placed in a pre-cooled freezer or ethanol solution. The temperature of either the freezer or the ethanol solution is then regulated as required [131].

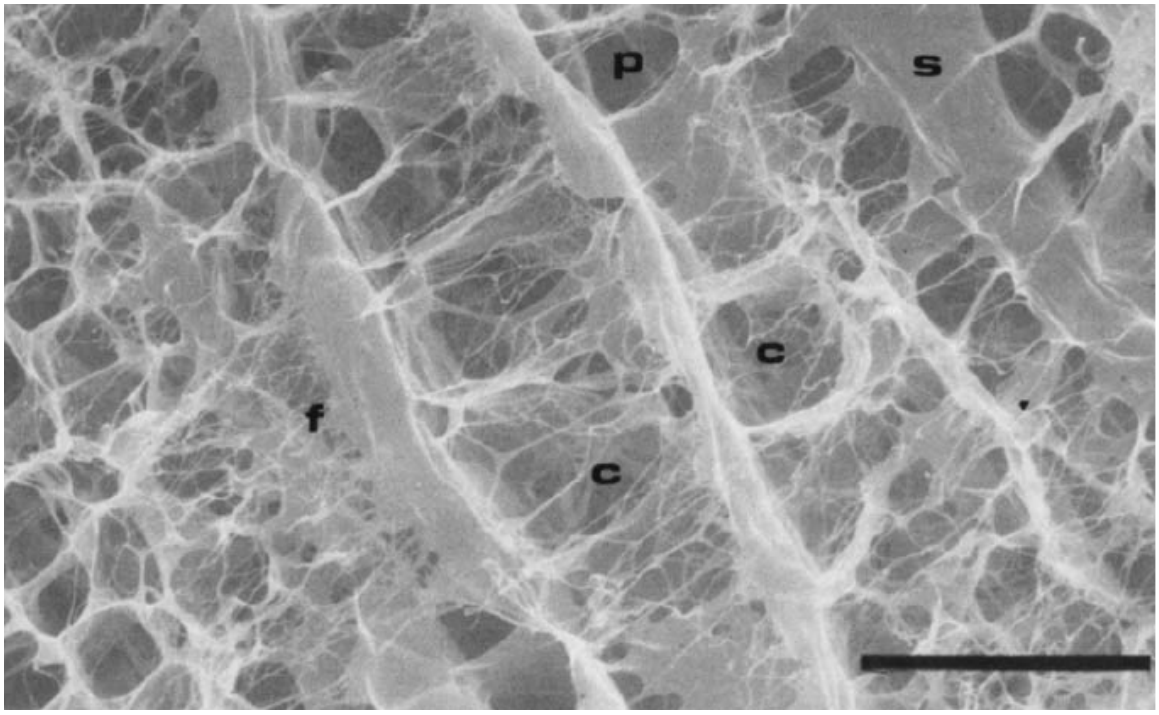

Fig. 3.5. A collagen-glycosaminoglycan scaffold with an average pore size of 64 μm obtained after freezing at -30°C using an ethanol bath. This illustrates the effect of freezing temperature on the average pore size (scale bar = 100 μm). The alphabetical letters represents collagen fibres (f), sheets-like structures (s), channels (c), and pores (p) [131].

The third parameter that affects the porosity, as described by Doillon *et al*. is the pH. The authors used a pH range of 2.0 to 3.75. No significant change in sponge morphology was observed at temperatures below -35°C. However, significant architectural changes were observed within a -35°C and -20°C temperature range. The morphology of the sponge was found to be a combination of sheets and fibers when the dispersion pH was 2 (Fig. 3.6). An increase in pH to 3.5 resulted in a more fibrous architecture [131].

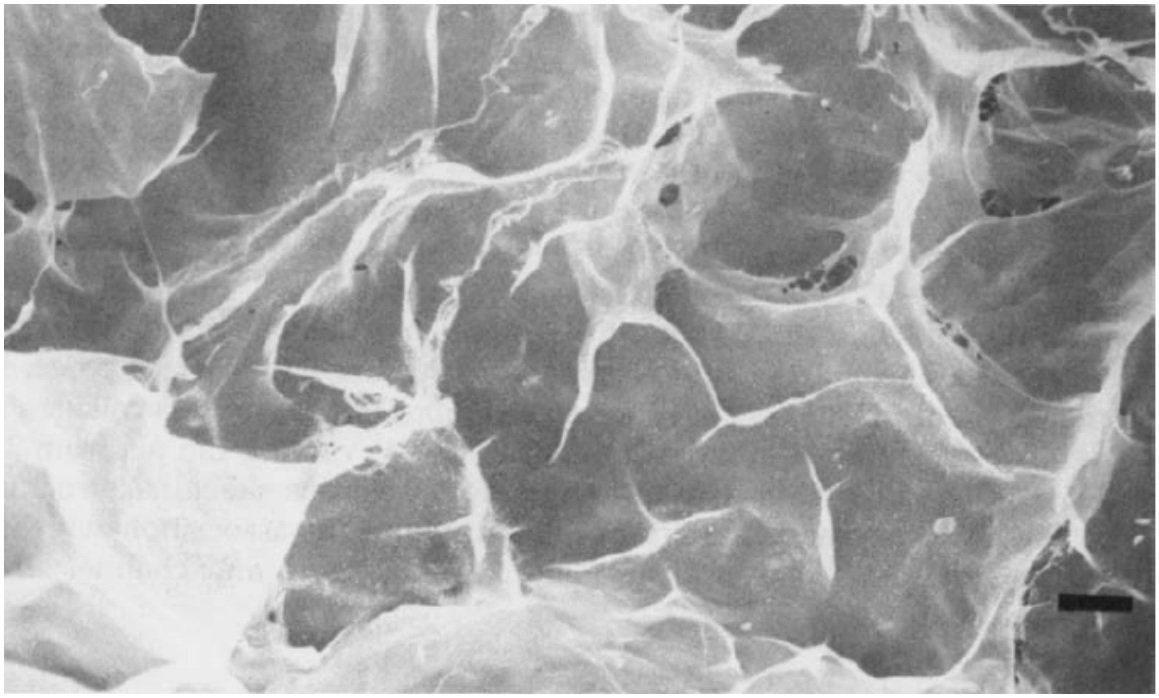

Fig. 3.6. The morphology of the sponge was altered by a pH of 2 and resulted in a combination of sheets and fibers [131] (scale bar = 100 μm).

More recent work done by O'Brien *et al.* [122] in 2003 focused on the development of a homogenous collagen-GAG scaffold. O'Brien and colleagues believed that the method of freezing of the collagen-GAG suspension is the most important determinant for the formation of a uniform or homogenous scaffold. The authors consequently developed a new freezing process which increased the homogeneity. Their research deviated from the conventional quenching technique of freezing by modelling a more controlled and slower freezing process. The cooling rate used by O'Brien *et al.* was 0.9 °C/min [121]. It was also found that the pores of the scaffold, produced by a constant cooling rate, were more regular in structure and uniform in size. Results provided by the authors, as depicted in Fig. 3.7, showed that conventional quenching with a freeze rate of 4.1 °C/min produced the least uniform scaffold with a coefficient of variance of 0.173. The most uniform scaffold, with a coefficient of variance of 0.128, was obtained using a constant cooling rate of 0.9 °C/min.

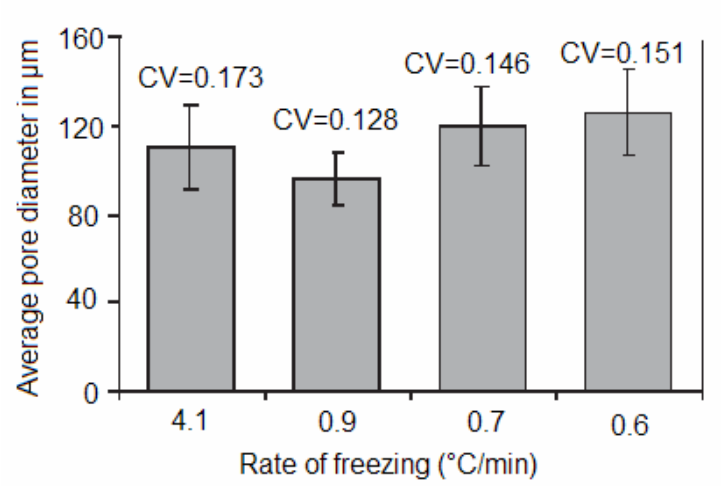

Fig. 3.7. The results obtained after comparing scaffolds manufactured through the conventional quenching process and controlled freezing. The quenching process resulted in a less homogenous scaffold with a coefficient of variance (CV) of 0.173. A cooling rate of 0.9 °C/min (CV = 0.128), on the other hand, produced a scaffold that was more uniform compared to cooling rates of 0.6 (CV = 0.151) and 0.7 °C/min (CV = 0.146) [122].

The importance of a constant freeze rate was further emphasized when the authors noted less variability among scaffolds prepared at the same rate of 0.9°C/min (Fig. 3.8).

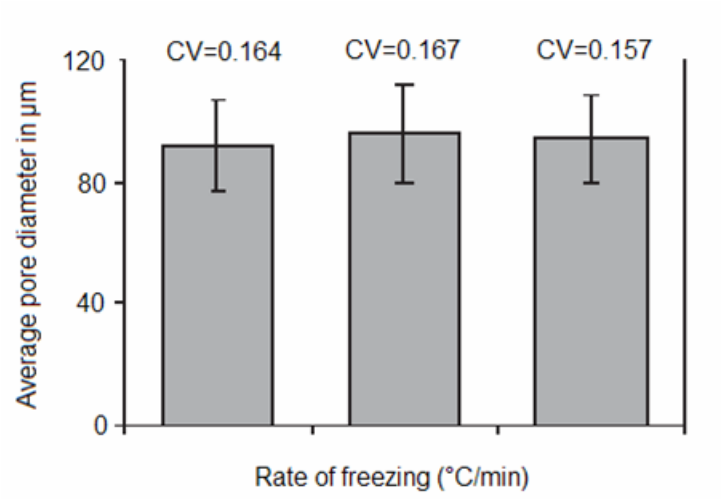

Fig. 3.8. Three scaffolds were prepared by using a constant freeze rate of 0.9 °C/min. This experiment indicated no significant difference ($p = 0.257$) in the average pore size of the collagen-GAG scaffolds [122].

An additional factor that was considered by O'Brien *et al.,* is the geometry of the pan in which the suspension was poured and frozen. Two different sized stainless steel containers were used; a small 12.4 cm X 12.4 cm pan and a larger 16.9 cm X 25.3 cm pan. The results of their study indicated that smaller stainless steel pans yielded a homogenous scaffold without areas of uneven ice crystal formation or nucleation between the collagen-GAG coprecipitates. In addition, the smaller pans underwent less warping compared to the larger containers. The results are depicted in Fig. 3.9. The CV of the pore size of the small non-compliant pan (0.173), was significantly smaller ($p < 0.05$) than that of the larger compliant pans [122].

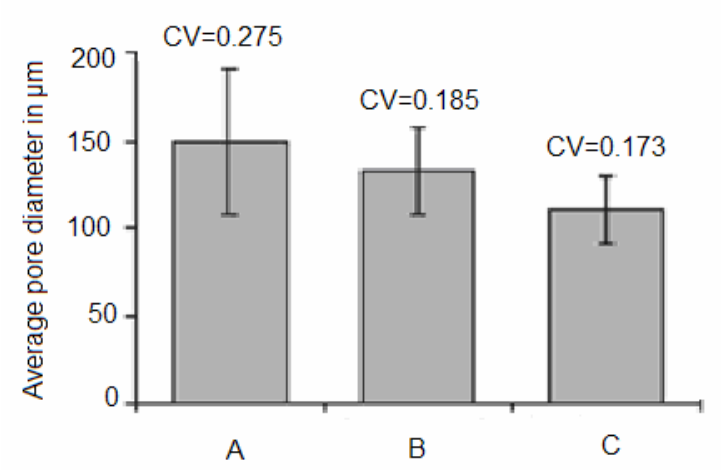

Fig 3.9. The effect of the pan size and pan compliance on the average pore size. Three different samples were selected from two different pan sizes (A-C). Pan A: Large and compliant and the sample selected included variable homogeneity; B: Large compliant pan where the sample was selected from a homogenous area; C: Small stiff pan where the sample was selected from a homogenous area [122].

In summary it can be said that an optimal and homogenous architecture of a collagen-GAG scaffold relies on:

- The collagen concentration of the collagen-GAG suspension.
- The collagen:GAG ratio.
- The pH of the collagen-GAG suspension.
- The duration and blending speed of the collagen-GAG suspension.
- The compliance and material of the container used for freezing.

- A constant freeze rate.
- The final temperature reached during freezing.
- Effective sublimation of ice crystals from the frozen scaffold.

The effect of crosslinking on the architecture of collagen-GAG scaffolds will be considered in a separate chapter.

3.4 FORMATION OF AN ARTIFICIAL EPIDERMAL LAYER

The epidermal portion of the artificial skin orchestrated by Yannas and colleagues is a uniform layer of medical grade Silastic® [28]. Silastic® is a morpheme of silicone and plastic and became a registered trademark of Dow Corning in 1948 [132]. The relevant and irreplaceable silicone for medical use is polydimethylsiloxane (PDMS) or $Me_3SiO(Me_2SiO)_nSiMe_3$. The unique physico-chemical attributes of this semi-organic molecule contribute its versatility [133,134]. In addition, the purity, toxicological profile and biocompatibility make PDMS a suitable component for biomedical use [135].

Polydimethylsiloxanes (PDMSs) are derived from the polymerization of octamethylcyclotetrasiloxane through hydrolysis and condensation. Catalysts for this polymerization can either be an acid or a base, and are removed by means of filtration after neutralization. Polymerization through condensation results in a mixture of two products. One being high-molecular-weight polymers and the other, low-molecular weight-products, are removed through distillation. Substitution of methyl groups can be achieved through the addition of functional siloxane groups, such as vinyl, hydrogen, phenyl, during re-equilibration or condensation. The resulting PDMSs can have various physical forms, namely, resins, gums, and liquids with different viscosities. The majority of medical silicones are thermally cured using platinum as a catalyst. This entails the crosslinking of PDMSs by vinyl hydrosilylation (Fig. 3.10). The result is the formation of an elastomer without any secondary product [135].

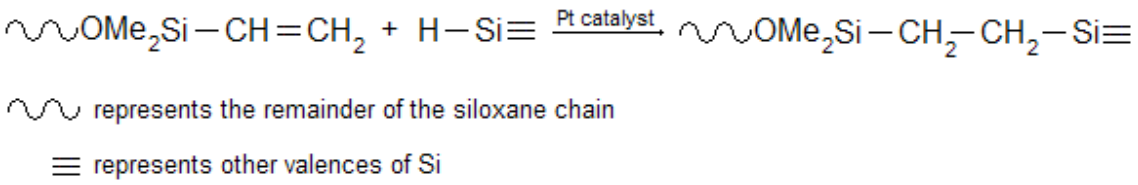

Fig 3.10. Crosslinking of PDMSs by vinyl hydrosilylation.

The versatility of silicones as biomaterials is evident from the classification introduced by the International Standards Organization (ISO) as well as the Tripartite Guidance [135]:

- direct contact of silicones with healthy skin (oxygen masks, and teats for babies; bottles)
- temporary contact with body fluids (drains, catheters, tubes in heart surgery and dialysis)
- extended and permanent contact with the body (joint prosthetics, contact lenses, protective sheaths, and isolative coatings for leads and circuits)

PDMS is thus the preferred choice in this instance as an epidermal layer. It serves to prevent the loss of moisture from the wound bed and also acts as a physical barrier against bacterial infection [28].

3.5 CROSSLINKING

Crosslinking of collagen based medical devices is achieved through three methodologies, namely, chemical crosslinking, physical crosslinking, and biological or enzymatic crosslinking. Chemical crosslinking relies on water soluble crosslinking agents such as glutaraldehyde and carbodiimide. This form of crosslinking can prevent the denaturation of the protein to be crosslinked through the manipulation of the environmental conditions during crosslinking [136]. Physical crosslinking is achieved through either high temperature vacuum dehydration or irradiation. Irradiation in the form of Co-60 γ-ray and electron beam induces simultaneous crosslinking and scission of collagen and other proteins [136]. Disruption of the three-dimensional structure of proteins thus

demerits irradiation as crosslinking method. The destructive nature of γ-rays will be further addressed in section 3.6 that deals with the method of terminal sterilisation. UV photo-induced crosslinking, unlike γ-ray and EB, on the other hand is limited by poor penetration capabilities and only the surface of a material can consequently be crosslinked [136]. High temperature vacuum dehydration or dehydrothermal (DHT) treatment ensures removal of water from collagen scaffolds which in turn results in crosslinking through esterification or amide formation [137]. The removal of water prevents denaturation of the collagen [122]. The choice of crosslinking methodologies in this study is in accordance with the work done by Burke and Yannas [28]. The mechanism of glutaraldehyde will be addressed in further detail in the following sections. More attention will be paid to this chemical crosslinker due to the complex nature of the induced crosslinking as well as the existence of possible side effects.

Glutaraldehyde, introduced by Sabatini *et al*. [138] in 1962, is known to be an invaluable fixative for the preparation of tissue for microscopy. Glutaraldehyde rapidly penetrates small tissue and it consequently renders proteins insoluble [138]. It is a small molecule consisting of two polar aldehydes, which are linked by three methylene bridges (Fig 3.11). The –CHO groups account for the crosslinking ability of the molecule [139]. It is known that glutaraldehyde polymerizes in aqueous solution [140]. The polymer form of glutaraldehyde (GA) also serves as a potent crosslinking agent due to free side-chain –CHO groups (Fig 3.12) [139].

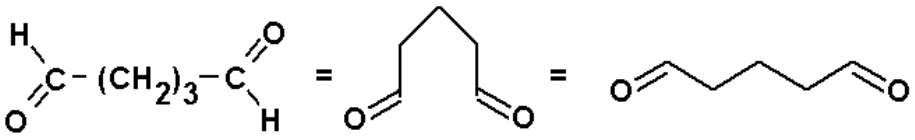

Fig. 3.11. Various notations of glutaraldehyde. The molecules' crosslinking ability is ascribed to free –CHO groups [139].

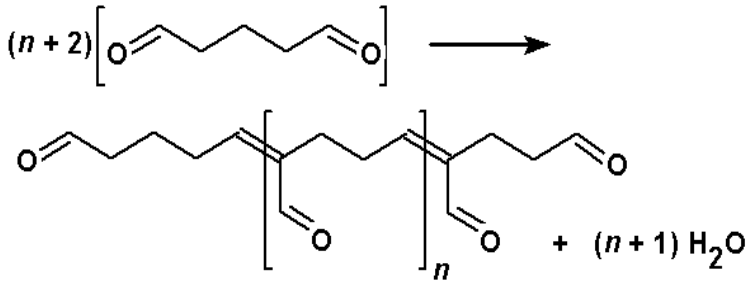

Fig. 3.12. The polymerization of glutaraldehyde results in polymers that serve as potent crosslinking agents [139].

Furthermore, GA is well known as a crosslinking agent for collagen-based biomaterials [141-144]. The use of glutaraldehyde (GA) as a crosslinking agent for these biomaterials has been studied in detail by Olde Damink *et al.* [145]. Their study focused on the formation of Schiff bases during glutaraldehyde crosslinking of dermal sheep collagen. GA is known to react with the free amine groups of lysine or hydroxylysine of the protein backbone of collagen to form Schiff base intermediates. Both the stability and reactivity towards GA, of these resultant Schiff bases were considered as depicted in Fig. 3.13 [145]. The initial intermediate (III) that forms after the interaction between collagen (I) and GA (II), is an unstable imine from which several subsequent reactions can originate before crosslinking [146]. The intermediate III can react with another imine to form the hydrolytically unstable GA polymer, IV. The formation of a cyclic aminal XII can occur in an aqueous environment. Crosslinking in the presence of water and GA can give rise to XIII [145].

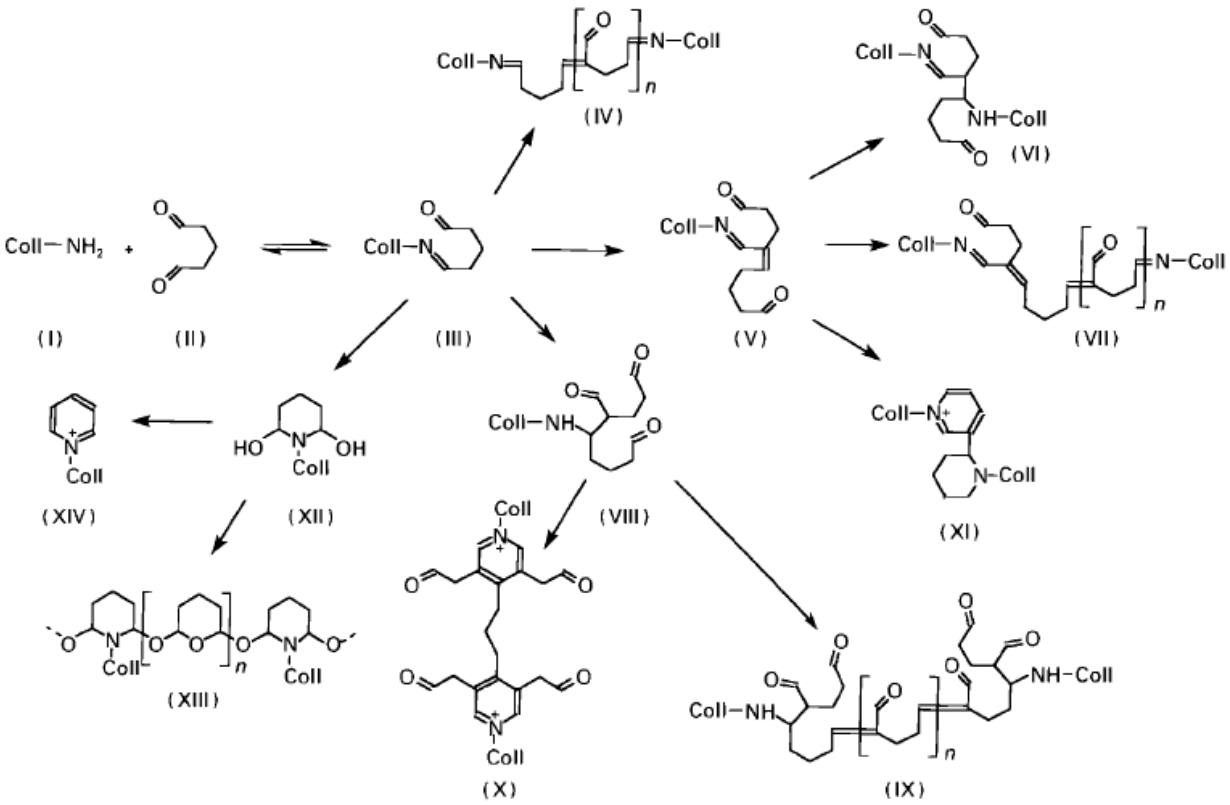

Fig 3.13 GA is known to react with the free amine groups of lysine or hydroxylysine of the protein backbone of collagen to form Schiff base intermediates. [145].

The interaction between GA and intermediate III can also give rise to products V and VIII. Product V, a stable *α-β*-unsaturated imine, is formed through an aldol-type condensation reaction. An acidic environment though, would lead to the hydrolysis of V. The same applies to products VI and VII [145]. Product VIII, a secondary amine, results from a Mannich type reaction between a protonated Schiff base and a GA-related enol [148,149]. Aliphatic crosslinks, as depicted in IX, are possible after aldol condensation and reaction with the amines of collagen. Further interaction between an additional GA molecule and VIII will form a dihydropyridine [148]. Oxygen present in the crosslinking solution can lead to the oxidation of dihydropyridine crosslinks. This in turn will result in the formation of substituted quaternary pyridinium crosslinks as depicted in X [150]. Structure XI is the consequence of the interaction between a free amine of collagen and V [151]. Finally, Lubig *et al*., [152] suggested that the condensation of XII (N-alkyl-2,6-

dihydroxy piperidine) and cyclic monohydrated GA would form XIII (*α*-oxo-N-alkyl piperidine) crosslinks. The pyridinium XIV as a side reaction was also mentioned.

Olde Damink *et al.* concluded that Schiff bases are formed rapidly once GA reacted with the free amines of lysine and hydroxylysine. GA is also responsible for the stabilization of hydrolysable Schiff bases through the formation of crosslinks. More importantly, the authors deduced that pendant-GA-molecules rather than crosslinks will result from the use of high GA concentrations over longer reaction times. Less pendant GA molecules were introduced when the crosslinking solution had an acidic pH. Crosslinking at a lower pH was also further motivated after they found the same amount of crosslinking when the pH of the crosslinking solution ranged between 5 and 9. The study also found no evidence for the formation of polymeric GA arrangements during crosslinking [145].

The benefits of GA as a crosslinking agent can be summarized as follow;

- Reduces the resorption and antigenicity of collagen related and other proteins [141,153,154].
- GA serves as a chemical sterilant and makes the material less prone to bacterial and fungal contamination [28,155].

The cytotoxicity of GA crosslinked tissue and collagen based scaffolds are well documented [156-158]. Both cytotoxicity and inflammation are ascribed to the presence of residual aldehydes in these tanned (crosslinked) materials [157,158]. Mechanisms employed to reduce or limit the cytotoxic effects of aldehyde residues, include washing and capping. Vigorous washing has been proven to have limited benefits since only the unbound aldehydes are removed. Free aldehydes that remain after GA has reacted with the scaffold collagen are not removed [159]. Capping, as suggested by Seifter and Frater, uses pure (99%) liquid polyols to react with free aldehydes in the GA tanned tissue. The polyols mentioned include, propylene glycol, 1,3-propanediol, glycerol, and 2,3-butylene

glycol. The inventors of this method noted no significant impairment of the mechanical strength of the polyol treated tissue [159]. Others advise to post-treat the GA crosslinked scaffold with 8% L-glutamic acid in order to reduce the effect of free aldehydes [160]. The study by Speer *et al.* noted that the pH of the aqueous carrier, of the collagen scaffold, influenced the amount of free aldehydes. They noted a tenfold increase in free aldehydes when the pH decreased form 7 to 4.5 [156]. Thus, although GA crosslinking in an acidic environment at 4°C allows for the control of the formation of inter- and intramolecular crosslinks, it is important that the final pH of the scaffold affects the amount of aldehyde that is leached [156,161]. Furthermore, the authors found that treatment of GA crosslinked collagen sponges with Eagle's Minimum Essential Medium (EMEM) with Earl's salts and 10% foetal calf serum completely eradicated the cytotoxicity of GA. The EMEM treatment of the collagen scaffold followed an intermediate wash phase in tap water [156].

GA crosslinking, as mentioned earlier, reduces the bioscaffold resorption rate. Research has shown that the *in vivo* scaffold degradation rate affects dermal regeneration significantly and a critical rate of 1.5 weeks has been emphasized [60,116,121]. Evidence motivates that an insoluble or crosslinked scaffold inhibits wound contraction through inhibition of the organization of contractile cells [162,163]. The degradation rate is also, independent of GA crosslinking, reduced through the integration of glycosaminoglycan chains into the scaffold architecture [61]. Resistance of collagen-GAG to degradation by collagenase increases with crosslinking and crosslink density [164-169]. Crosslinking in combination with chemical composition thus determines the rate of degradation and consequent effectiveness of collagen-GAG scaffolds.

From the literature presented it is evident that effective GA crosslinking and reduced cytotoxicity depends on a strict protocol. The sequential key elements of such a protocol are: GA crosslinking in an acidic environment (pH 3-4) at 4ºC;

washing of the scaffold to remove free aldehydes; transfer of the scaffold to a complete EMEM solution [156].

3.6 PACKAGING, TERMINAL STERILISATION AND STORAGE

The packaging material employed depends on the method of sterilisation and the latter will thus be discussed first. Sterilisation methods used in the medical device industry include (Fig. 3.14); dry heat, autoclaving, irradiation and gaseous chemicals.

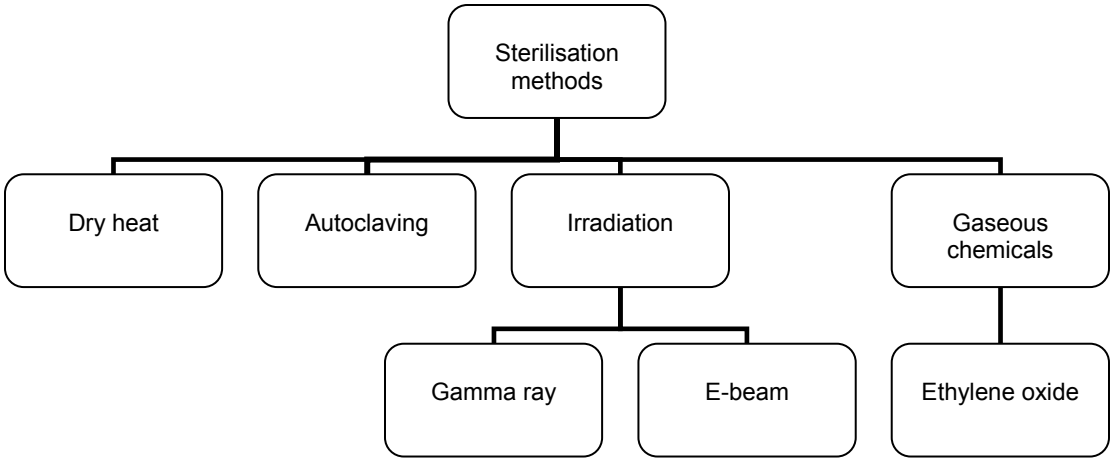

Fig. 3.14. Methods of sterilisation employed in the medical device industry [170].

Collagen containing sponges, in general, are sterilized by either EO (ethylene oxide) or gamma irradiation. Conventional sterilisation methods such as autoclaving and dry heat are known to be inappropriate for these heat and water sensitive biomaterials. Earlier research addressed the physical and chemical modifications induced by EO and gamma sterilisation. EO sterilisation imparts minimal structural alterations but has the detriment of toxic residues [171,172]. Sterilisation through gamma irradiation on the other hand imparts no toxins but dramatically affects chemical bonds, tensile strength and consequently the scaffold architecture [173,174]. Gamma irradiation depends on a Co-60 (an artificial radioactive isotope) source to generate ionizing photons that irrevocably disrupts and fragments the deoxyribose nucleic acid (DNA) of living microbes [175]. The penetration depth of γ-rays is dependent on the density of the material [170].

Extensive work has been done on the effect of gamma irradiation on both native and crosslinked collagen [176-178]. Furthermore recent (2002) work done by Noah and colleagues specifically focused on stability and porosity of collagen sponges after EO and gamma sterilisation. Their study used a collagen sponge with a homogeneous pore size of 20 µm. Gamma irradiation at 25KGy or 25 000 J/kg caused a collapse of the porous architecture and the scaffold showed a decreased resistance against enzymatic degradation. The structure and stability of EO-sterilized sponges, on the other hand, remained virtually unchanged [179]. Gamma irradiation, because of its simplicity and effectiveness [173,174], will be employed in this study. A few key elements of gamma irradiation will be addressed and considered.

The predominant effect of gamma irradiation in air on collagen is a combination of random crosslinking and breakdown of the tropocollagen molecules. Analysis of the optical rotation of collagen after irradiation shows degradation of the collagen helix [177]. It is worth noting that GA crosslinking of collagen provides a degree of protection against irradiation induced degradation at doses ranging between 25 and 50 X 10^4 J/kg. It was also found that collagen that was irradiated dry after crosslinking showed more morphological changes than crosslinked collagen that was irradiated in water. Resistance to collagenase digestion was seen in crosslinked collagen (wet) after irradiation in the range of 5 and 25 X 10^4 J/kg [178]. Degradation of collagen scaffolds can be reduced when irradiation is performed under an inert gas such as nitrogen. Gamma irradiation under nitrogen not only delayed degradation but also increased crosslinking of collagen [177]. The irradiation tolerance level of the epidermal portion of the bioengineered artificial skin should also be considered. Available data (Table 3.2) shows that the majority of elastomers have an irradiation tolerance ranging between 50 to 200 kGy [180].

Table 3.2. Gamma irradiation tolerances for elastomers used in the medical industry [180].

Elastomer		
Material	**Tolerance Level (KGy)**	**Comments**
Butyl	50	Tends to release particles after irradiation.
Ethylene-Propylene Dienne Monomer (EPDM)	100-200	Crosslinks, but yellows slightly.
Fluoro Elastomer	50	
Natural Rubber (Isoprene)	100	Multiple sterilisations should be avoided.
Nitrile	200	Natural rubber tends to be very stable when sulphur or resin cure systems are used. Stressing of the product should be avoided.
Polyacrylic	50-200	Multiple sterilisations should be avoided.
Polychloroprene (Neoprene)	200	Multiple sterilisations should be avoided.
Silicones (Peroxide & Platinum Catalyst System)	50-100	Multiple sterilisations should be avoided.
Styrene-Butadiene	100	The crosslinking density increases more in peroxide systems than in platinum systems. Prevent creasing and warping when packaged since it is known that silicone will retain its shape post-irradiation.
Urethanes	100- 200	Multiple sterilisations should be avoided.

Packaging material is also significantly altered by gamma irradiation. Polymers used in packaging, interact with radiation in a similar fashion compared to a biological polymer such as collagen. The result is a combination of chain scission and crosslinking. Chain scission reduces the tensile strength as well as the elasticity of the polymer. Crosslinking improves the tensile strength but reduces the elasticity of the polymer [180]. The most common thermoplastics used in the medical device industry are listed in Table 3.3 [180]:

Table 3.3. Gamma irradiation tolerances for thermoplastics used in the medical industry [180].

Thermoplastic		
Material	**Tolerance Level (KGy)**	**Comments**
Acrylonitrile / Butadiene / Styrene (ABS)	1 000	These thermoplastics are protected by a benzene ring structure. Butadiene impact modifier degrades above 100 kGy. High doses on high impact grades should be avoided.
Aromatic Polyesters (PET, PETG)	1 000	Polyesters remain exceptionally stable and retain excellent clarity.
Esters and Ethers	50	Thin films of both esters and ethers brittle above 50 kGy.
Paper, Card, Corrugated Fibers	100- 200	Paper tends to discolour and become brittle. Acceptable for single use.
Cellulose, Acetate, Propionate, and Butyrate	50	Plasticsed versions of these materials slowly embrittle above 50 kGy.
Fluoropolymers		
Tetrafluoroethylene (PTFE)	5	The use of PTFE should be avoided since it tends to liberate fluorine gas and disintegrates to powder.
Polychlorotrifluoroethylene (PCTFE)	200	
Polyvinyl Fluoride	1 000	
Polyvinylidene Fluoride	1 000	
Ethylene-Tetrafluoroethylene (ETFE)	1 000	
Fluorinated Ethylene Propylene (FEP)	50	
High Performance Engineering Resins	1 000-10 000	Resins tolerate radiation well.
Polyacetals (Delrin, Celcon)	15	The use of polyacetals should be avoided due to the fact that it becomes brittle.
Polyacrylics		
Polymethylmethacrylate	100	This thermoplastic turns yellow at 20 – 40 kGy, but recovers partially with aging.
Polyacrylonitrile	100	Turns yellow between 20 and 40 kGy.
Polycyanoacrylate	200	Polycyanoacrylate adhesives perform well at 100 kGy and show less than 30% degradation.
Polyamides (Nylons)		
Aliphatic & Amorphous Grades	50	This Nylon discolours and should never be resterilised. It should be noted that Nylon 11 and 12 perform better.
Aromatic Polyamide-imide	10 000	Another benzene ring stabilised thermoplastic.
Polycarbonate	1 000	Polycarbonates discolour once irradiated but its clarity recovers with aging.
Polyethylene (LDPE, LLDPE, HDPE, UHMWPE)	1 000	Polyethylenes undergo crosslinking and gain strength, but lose some elasticity. All polyethylenes tolerate radiation well. Low density is the most resistant. HDPE packaging film including spin-bonded porous packaging which may lose 40-50 % elongation at doses of 50 kGy.
Polyamides	10 000	

Polymethylpentene	20	Avoid the use of this material since it degrades due to oxidation.
Polyphenylene Sulphide	1 000	
Polypropylene, Radiation Stabilized		Shows higher tolerance levels when using e-beam.
Homopolymer	20-50	Homopolymers have been used with marginal success in syringes. The material becomes brittle due to oxidation and degrades over time. Real time aging should be used to validate the material. The use of non-stabilized polypropylene should be avoided.
Copolymers of Propylene-Ethylene	25-60	The copolymer is more stable than homopolymer.
Polystyrene	10 000	All styrenes are stabilized by a benzene ring structure.
Polysulfone	10 000	Polysulfones have an amber colour before irradiation.
Polyurethane, Polyether and Polyester	100- 200	Excellent physical and chemical resistance to stress-cracking.
Rigid and flexible		Drying is essential to success. Good in luer connectors. All types show irreversible yellowing.
Polyvinylbutyral	100	This thermoplastic turns yellow.
Polyvinylchloride (PVC)	100	This thermoplastic turns yellow but can be tinted in order to compensate for the discolouration. Successful use of PVC depends on quality of material, formulation and processing. PVC tubing is known to crosslink and this will affect the elasticity of the material.
Polyvinylidene Chloride (PVDC)	100	Turns yellow and releases HCl.
Styrene / Acrylonitrile (SAN)	1 000	Turns yellows at 40 kGy.

From Table 3.3 it is thus evident that the majority of thermoplastics have acceptable irradiation tolerances. Polyurethane will be used as backing on either side of the fabricated scaffold and the primary packaging will be made of a foil-lined paper pouch. The backing will prevent warping of the product and will also ensure easy handling. The secondary packaging will be a peelable pouch commercially available from Safmed (Pty) Ltd, South Africa. The lowest acceptable terminal sterilisation dose of 10KGy under an inert gaseous environment was chosen because it is known that GA also serves as a sterilant [155,157].

3.7 SUMMARY

The considerations for the design and development of an artificial skin or tissue engineering scaffold are vast. The key elements of biocompatibility, pore volume and diameter, effective crosslinking, and the optimal rate of degradation are influenced by a multitude of variables. These variables, ranging from the method used to prepare the collagen suspension to the sterilisation protocol, ultimately determine the efficiency of an engineered dermal regeneration scaffold. An optimized protocol has been compiled from the presented literature and will be implemented in Chapter 4.

CHAPTER 4

MATERIALS AND METHODS

4.1 INTRODUCTION

This chapter will focus on the materials and methods applied in this study. Collagen-GAG scaffolds were prepared through a series of sequential steps (Fig. 4.1) that include: the formation of the collagen-GAG coprecipitate; poring of the suspension into appropriate containers; controlled freezing; freeze drying; addition of the epidermal layer; heat crosslinking under vacuum; additional crosslinking with GA; removal free unbound aldehydes; packaging; and finally terminal sterilisation and storage.

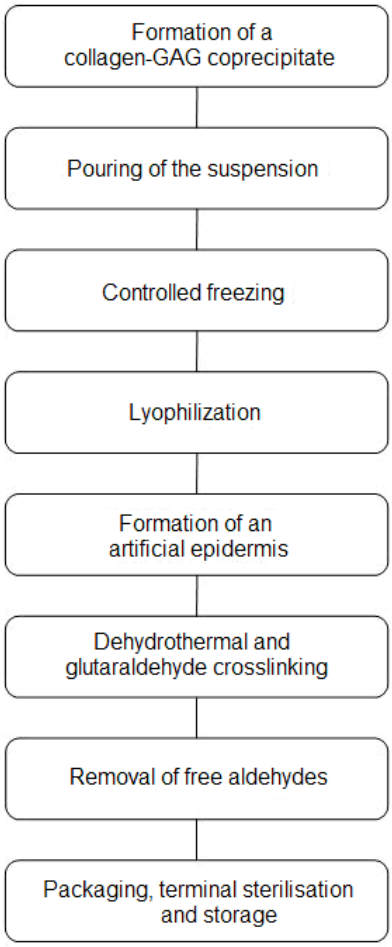

Fig. 4.1. The sequential steps used to obtain a dermal regeneration matrix.

4.2 SCAFFOLD PREPARATION

4.2.1 Collagen-GAG coprecipitate formation and pouring

BSE-free (Bovine spongiform encephalitis free) type I collagen was provided by Southern Biologics (Pty).Ltd. and combined with chondroitin-6-sulfate (Sigma-Aldrich Chemical Co., St. Louis, MO) to form a co-precipitate as described below.

Two separate collagen suspensions were prepared in 0.05 M acetic acid to yield concentrations of 0.56% and 1.11% (w/v) respectively. Both solutions were subjected to high speed blending for an hour at 4°C. Chondroitin-6-sulfate in 0.05 M acetic acid was added to each of the prepared collagen suspensions to result in a final collagen wieght:GAG weight ratio of 92:8. The final solutions, with end collagen concentrations of 0.5% and 1.0% (w/v) respectively, were blended for an additional 90 minutes to form a homogenous coprecipitate. Again the temperature was regulated to prevent denaturation of the collagen. The co-precipitates had a pH of 3 and were transferred to two 50 ml centrifuge tubes and centrifuged at 4000 rpm for 5 minutes to remove any trapped air bubbles. The suspensions were poured into two different pans. One set of pans were Teflon-coated and measured 120 X 240 mm. The second set of stainless steel pans measured 110 X 220 mm. A total of 6 samples for each set of pans were prepared. Each sample was labelled for later identification. All the samples were allowed to reach a final temperature of 20ºC. It should be noted that the collagen-GAG coprecipitate can be stored for up to 4 months at 4°C, but should be blended prior to use [122, 181].

4.2.2 Controlled freezing

Biofreeze DV 50, version 1.30.2, software package (*CONSARCTIC, GmbH*) was pre-programmed (Fig. 4.2) to produce a freezing rate of 0.92 °C/min which was similar to that used by Yannas *et al*. [122] The default freezing rate for collagen sponges of 1.3 °C/min (Fig.4.3), provided by *CONSARCTIC*, was used as a control. Each pan was frozen separately using a *CONSARCTIC* liquid nitrogen cryopreservation chamber (Fig.4.4). The program had an initial temperature of

20°C and reached a final temperature of -40°C. The result of each freezing cycle was recorded and compared in order to ensure reproducibility of the scaffolds.

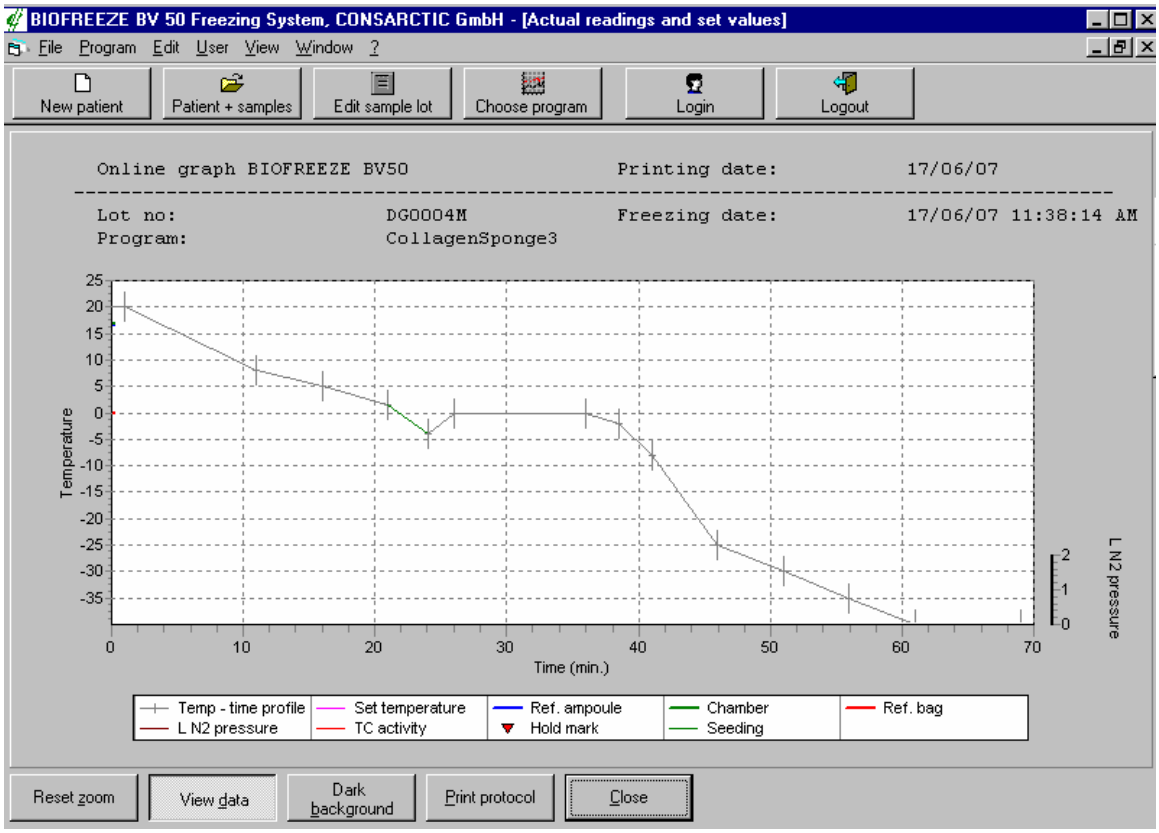

Fig. 4.2. A screenshot of the freeze program that was programmed, using the *Biofreeze* DV 50, version 1.30.2, software, to produce an average freeze rate of 0.92°C/min.

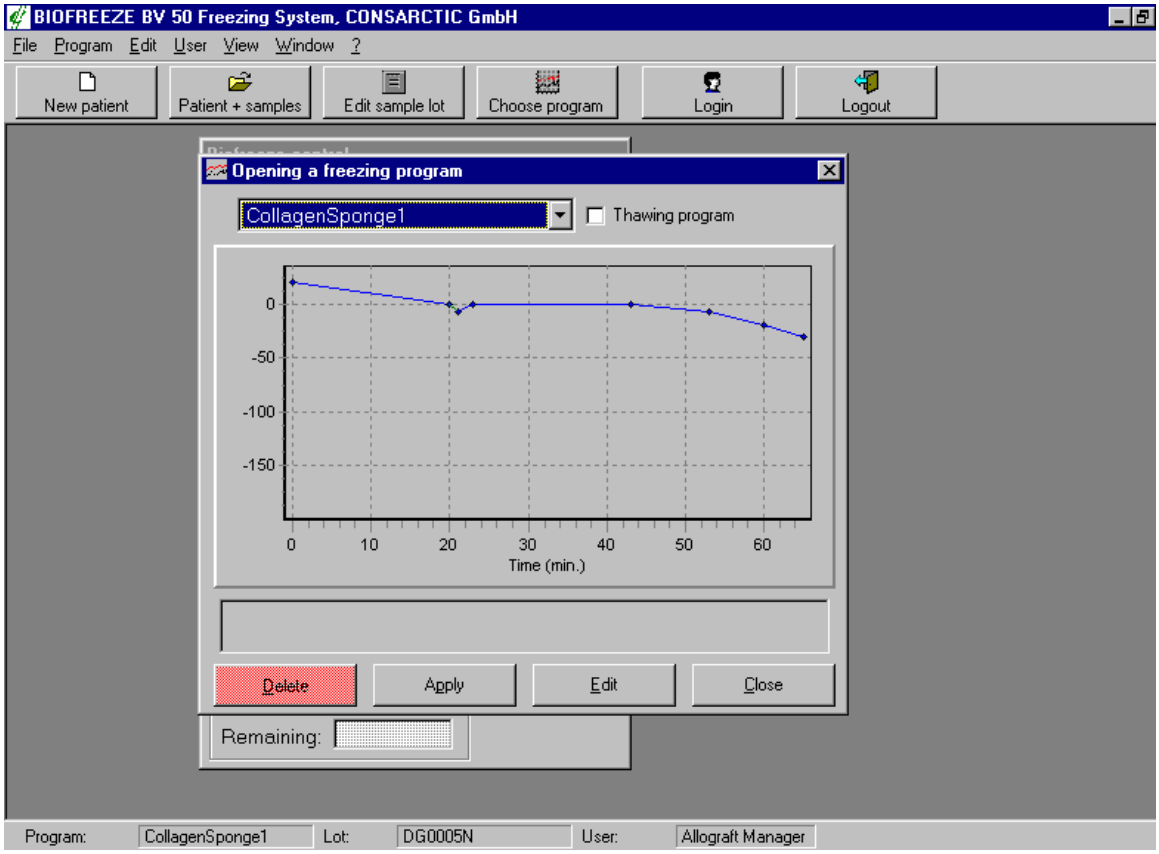

Fig. 4.3. A screenshot of the freeze default curve for collagen sponges which is provided by the *Biofreeze* DV 50 (version 1.30.2) software. This program had an average freeze rate of 1.3°C/min.

Fig. 4.4. The cryopreservation chamber and liquid nitrogen storage tank that was used to perform the controlled freezing of the collagen-GAG co-precipitates. An initial temperature of 20°C was lowered at a controlled rate of 0.92°C/min to reach a final temperature of -40°C.

4.2.3 Lyophilization

Sublimation through lyophilization was performed in an *INSTRAVAC*® lyophilization chamber (Air & Vacuum Technologies (Pty) Ltd, South Africa), after immediate transfer of the frozen pan (Fig.4.5). Each pan was lyophilized separately once a freeze-dryer shelf temperature in the order of -50ºC was reached. The frozen scaffolds were subjected to lyophilization for at least 17 hours in order to ensure total sublimation of the ice crystals [128,181].

Fig. 4.5. The *INSTRUVAC*® lyophilization chamber that was used for the sublimation of ice crystals from the prepared collagen-GAG scaffolds. The prepared scaffolds were lyophilized for at least 17 hours.

4.2.4 Formation of an artificial epidermal layer

Dry collagen-GAG sponges were formed once lyophilization was completed. Each specimen was once again labelled and handled separately. The silicone epidermal portion of each of the scaffolds was prepared as described below. Biomedical grade silicone rubber (Dow Corning, Silastic®, Q7-4840) will be used

to form a 0.2 mm thick film on an acetate based backing. Precision coating will be performed by using a spreader with a 0.2 mm aperture. The thickness was selected due to the fact that the polymerization will result in a 10% loss in thickness which will result in a final film of 0.18 mm. Equal amounts of solution A and B were thoroughly mixed prior to application. The acetate backing will ensure easy removal after the silicone had polymerized. The surface of the collagen sponge that was in contact with the atmosphere was placed onto the wet unpolymerized silicone. Polymerization occurred at 105ºC for 30 minutes. This temperature will not denature the collagen as long as all the moisture has been removed during lyophilization [128,182]. The samples were then removed and allowed to cool down. Once cooled, the samples were transferred to appropriate plastic containers and prepared for crosslinking. The epidermal portion of each sample will be measured, up to two decimal places, at three different locations to ensure consistency. A calibrated digital calliper will be used and the means and standard deviations of the intra- and inter epidermal layer thicknesses will be calculated.

4.2.5 Optimal glutaraldehyde crosslinking

Freshly prepared GA in 0.05 M acetic acid was used for crosslinking [145]. Crosslinking was done at 4°C for 12 hours in a dark environment [156,161,182]. Additional crosslinking was done for another 12 hours in a fresh change of GA. The samples (Table 4.1) were exposed to one of two different GA concentrations, namely; 0.25% and 0.50% [145,181].

4.2.6 Removal of free aldehydes

The procedure that was followed was based on the work done by Speer *et al*. [156]. The samples were washed in three changes of 500 ml MilliQ water which was filtered through a 0.2 µm filter. The water is available from Glycar (Pty) Ltd, and a Stuart orbital shaker was used to ensure efficient rinsing. Each wash cycle lasted 10 minutes. An additional wash was done in 500 ml Dulbecco's Phosphate Buffered Saline (DPBS), available from Whitehead Scientific (Pty) Ltd, to ensure

that the scaffold reached a pH in the order of 7. The pH was confirmed using a CRISON pH meter. The final wash entailed the use of Fibroblast Basal Medium (FBM) supplemented with 10% foetal calf serum for 10 minutes. The efficacy of the wash procedure was verified through exposure of sample extracts to normal foreskin dermal fibroblasts as described in section 4.3.

4.2.7 Packaging, terminal sterilisation and storage

The artificial skin samples were rinsed in DPBS prior to packaging. Excess fluid was allowed to drain and the moist scaffolds were placed between two polyethylene sheets and into the primary foil-lined paper pouch (available from BLESSTON (Pty) Ltd. Air was removed from the packaging under vacuum and replaced with pure nitrogen and hermetically sealed (Gammatron (Pty) Ltd) (Fig. 4.4). A peelable pouch, commercially available from Safmed (Pty) Ltd, was used as secondary packaging. Terminal sterilisation was done by ISOTRON SA (Pty) Ltd at 10 KGy as indicated in Table 4.1. Control samples were prepared as described above, but will remain in an air atmosphere.

Table 4.1. Terminal sterilisation was done by ISOTRON SA (Pty) Ltd at 10 KGy under pure nitrogen gas. A control group was irradiated under an air environment.

No	Description and collagen concentration (% m/v)	Crosslinking method	Terminal sterilisation
1	Generic scaffold (0.5%)	0.25% GA, pH 3-4, at 4°C	10 KGy γ-irradiation, hermetically sealed under pure nitrogen
2	Generic scaffold (0.5%)	0.50% GA, pH 3-4, at 4°C	10 KGy γ-irradiation, hermetically sealed under pure nitrogen
3	Generic scaffold (1.0%)	0.25% GA, pH 3-4, at 4°C	10 KGy γ-irradiation, hermetically sealed under pure nitrogen
4	Generic scaffold (1.0%)	0.50% GA, pH 3-4, at 4°C	10 KGy γ-irradiation hermetically sealed under pure nitrogen
5	Generic scaffold (0.5%)	0.25% GA, pH 3-4, at 4°C	10 KGy γ-irradiation
6	Generic scaffold (0.5%)	0.50% GA, pH 3-4, at 4°C	10 KGy γ-irradiation
7	Generic scaffold (1.0%)	0.25% GA, pH 3-4, at 4°C	10 KGy γ-irradiation
8	Generic scaffold (1.0%)	0.50% GA, pH 3-4, at 4°C	10 KGy γ-irradiation

The opaque primary packaging will ensure that the product will be UV-protected. The terminally sterilized dermal regeneration matrices will then be subjected to further SEM analysis as described below.

4.3 ELECTRON MICROSCOPIC ANALYSIS

Scanning electron microscopy was performed on the prepared uncrosslinked collagen-GAG scaffolds (Table 4.2). The architecture of these scaffolds was compared with the data available on the scaffolds prepared by O'Brien *et al.* [122].

Table 4.2. Scanning electron microscopy were done on selected uncrosslinked scaffolds and compared with the dry scaffold of Integra®.

No	**Description and collagen concentration (% m/v)**	**Collagen concentration (%w/v)**	**Freeze rate (**°C/min)
1	Integra®	0.5% (w/v)	0.9
2	Generic scaffold	0.5	0.92
3	Generic scaffold	1.0	0.92
4	Generic scaffold	0.5	1.3

The "pan-side" surfaces of the scaffolds were prepared in accordance with the study by Doillon *et al*. [131]. Uncrosslinked dry scaffolds were prepared by fixation with 2.5% glutaraldehyde in 0.1 M phosphate buffer (pH 7.4) for 90 minutes. Postfixation was done in a 0.5% aqueous osmium tetroxide solution for 60 minutes. Critical point CO_2 freezing followed in order to dry the samples after which they were coated with gold. The samples were viewed and photographed by using a JEOL (JSM-840) Scanning Microscope [131,182]. Each sample was examined for the presence of the following; collagen fibre aggregates or strands, collagen sheets, and the polygonal shapes of open pores [131]. The diameters of were obtained through measurement of the largest distance between adjacent vertices (Fig. 4.6). These diameters were measured after calibration and analysed using the UTHSCSA *ImageTool* program (developed at the University of Texas Health Science Centre at San Antonio, Texas and available from the Internet by anonymous FTP from maxrad6.uthscsa.edu). SEM micrographs and

information on the uncrosslinked Integra® scaffolds were obtained from previous literature [122,181,183] and used as a reference. The data sets were compared with each other and any statistical significance was assessed through a paired *t*-test. The probability value used to determine statistical significance was 95% ($p<0.05$). Errors in both the text and figures were reported as standard deviation.

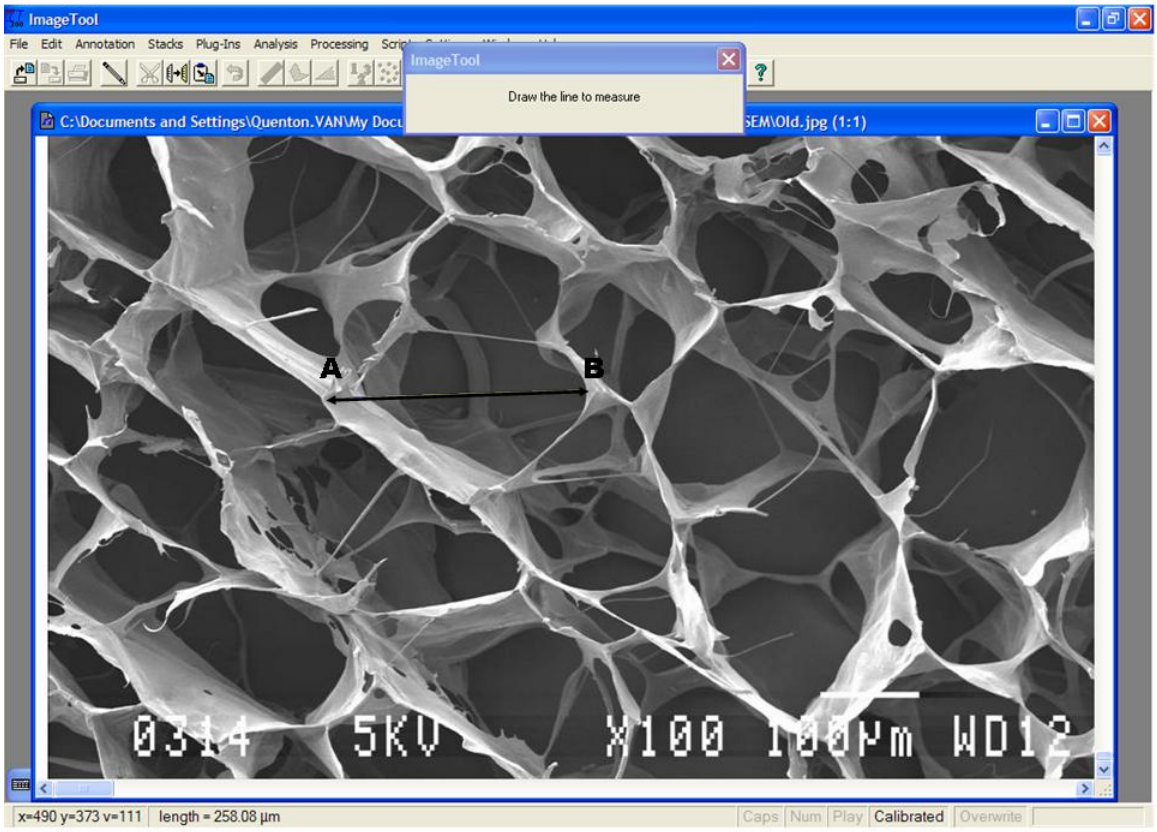

Fig. 4.6. The pore diameters of the prepared scaffolds (line AB in the above micrograph) were obtained through measurement of the largest distance between adjacent vertices. Each micrograph was analysed, post calibration, using the UTHSCSA *ImageTool* program.

The final product, consisting of both an epidermal and dermal portion, was also viewed and photographed by using a JEOL (JSM-840) Scanning Microscope. These samples were examined to asses the impact of γ-irradiation on the scaffold integrity and microstructure.

4.4 ENZYMATIC DEGRADATION ASSAY

The assay that was performed was based on earlier work done by Moore and Stein in 1948 [184] as well as that of Mandl *et al*. [185] in 1948 and more recent (2004) work by Pek *et al*. [186]. Table 4.3 represents the samples that were subjected to the enzyme degradation assay. The principle of the test rests on the fact that collagenase I (Sigma, C-9891) cleaves two of the three helical chains of collagen. The absorbance of the resulting peptides is then measured calorimetrically at 570 nm [184,185].

Table 4.3. The sample selection for the collagenase degradation assay.

No	Description and collagen concentration (% m/v)	Crosslinking method	Terminal sterilisation
1	Integra® (0.5%)	Thermal crosslinking under vacuum followed by 0.25% GA [181]	Electron beam [181]
2	Generic scaffold (0.5%)	N.A.	N.A.
3	Generic scaffold (0.5%)	0.25% GA, pH 3-4, at 4°C	N.A.
4	Generic scaffold (0.5%)	0.25% GA, pH 3-4, at 4°C	10 KGy γ-irradiation, hermetically sealed under air
7.	Generic scaffold (0.5%)	0.25% GA, pH 3-4, at 4°C	10 KGy γ-irradiation, hermetically sealed under pure nitrogen
5	Generic scaffold (0.5%)	0.50% GA, pH 3-4, at 4°C	N.A.
6	Generic scaffold (0.5%)	0.50% GA, pH 3-4, at 4°C	10 KGy γ-irradiation, hermetically sealed under pure nitrogen

Only the most suitable samples were tested. The selection was based on the electron microscopic analysis of scaffold architecture and porosity. The samples were cut into 10 mm X 10 mm pieces, thoroughly washed and placed in a 15 ml centrifuge tube. Buffer (5 ml of a 50 mM of TES buffer) with calcium chloride with a final pH of 7.4 was added to the sample material. This was done in triplicate and the average of the three representative values of each sample was used for the data analysis.

Freshly prepared collagenase (100 µl at 0.1mg/ml) was supplemented and this was followed by incubation at 37°C over 120 minutes. The containers were frequently swirled. The blank contained 100 µl buffer instead of collagenase and native collagen (Sigma, C9791) was used as sample material. Extraction of 200 µl of the supernatant was done over four, 30 minute time intervals. Thus, for each sample extracts were done after 30, 60, 90, and 120 minutes. Each of the extracts was thoroughly marked. Freshly prepared ninhydrin colour reagent (2 ml of a 4% ninhydrin solution and 200 mM citrate buffer) was added to each sample and this was followed by boiling for 30 minutes. Isopropanol (10 ml of a 50% v/v) was combined with the test material once the container cooled down to room temperature. A standard curve was prepared using 4.0 mM L-Leucine in 10 mM hydrochloric acid. Again, freshly prepared ninhydrin colour reagent (4% ninhydrin solution and 200 mM citrate buffer) was added according to the L-Leucine samples and this was followed by boiling for 30 minutes. Isopropanol (10 ml of a 50% v/v) was combined to the test material once the container cooled down to room temperature. Finally, 200 µl of the coloured solutions were transferred to a 96 well plate for absorbance reading at 570 nm using a Bio-Tek, model ELx800 plate reader.

A standard curve was compiled by plotting the corrected absorbance (ΔA_{570nm}) of the L-leucine standard solution versus the µmoles of L-leucine. This curve was used to determine the µmole of L-leucine liberated through the enzymatic action of collagenase. A subsequent curve was compiled that represented the µmole of L-leucine liberated over the four time intervals for each sample. The rate of degradation was extrapolated from the rate of product formation.

4.5 CYTOTOXICITY ASSAY

Normal foreskin dermal fibroblasts were used to determine the efficacy of the washing procedure. Second passage cells were counted and cell viability seeded was assed using the trypan blue dye exclusion assay. These cells were then seeded into 24 well plates at a density of 5×10^4 cells per well. Incubation for 48

hours (at 37°C and 5% CO_2) in supplemented FBM followed. Extracts were prepared by placing 1 mm X 1mm sample pieces in test tubes containing 8 ml supplemented FBM. The samples were incubated for 24 hours at 37 °C in order to obtain extracts. The culture medium of the incubated cells was replaced after the 48 hour incubation period with sample extract. Further incubation for 48 hours followed after which the MTT assay was performed. The assay relies on the vital mitochondrial reduction of yellow MTT [3-(4,5-Dimethylthiazol-2-yl)-2,5-diphenyltetrazolium bromide] to purple formazan. A control group was included and received fresh culture medium instead of sample extract when the sample change of the test batch was done. Cell viability was measured by this colorimetric assay after the incubation period. The culture medium in each well was replaced with a 5% MTT solution and incubated for 3 hours at 5% CO_2 and 37°C. The MTT solution was then removed and replaced with 100µl of DMSO and transferred into a 96-well plate. The absorbance at 450 nm was read using a Bio-Tek, model ELx800 plate reader [156,187]. The data was graphically depicted to represent the cell viability versus sample type and also included. The standard deviation of each data set was included and a probability value of 95% was used to determine statistical significance.

CHAPTER 5

RESULTS AND DISCUSSION

5.1 INTRODUCTION

The results of the study will be presented in this chapter and will comprise of four sections. The first section, titled “Collagen-GAG scaffold architecture”, will address the micro- and macro-architecture of the scaffolds and will include the data obtained from the microscopic analysis of the various samples prior to crosslinking and terminal sterilization. This section will consequently combine the results of the steps employed to fabricate the artificial skin. Attention will be paid to the results of: the scaffold morphology after controlled freezing and lyophilization of the collagen-GAG coprecipitate; the influence of freezing container on the scaffold porosity; the formation of an artificial epidermal layer; and scanning electron microscopic analysis.

The second section, “Enzymatic degradation assay”, will discuss the results of the collagenase degradation assay. In this section attention will be paid to the rate of degradation of each of the scaffolds as well as the effectiveness of the crosslinking methods and how the latter is altered by the terminal sterilization.

The third, “Cytotoxicity assay”, will reveal the efficacy of free aldehyde removal based on the results of the cell viability assay. All the data obtained will then be amalgamated and summarized in the fourth and a final section. Here more attention will be paid to the most equivalent collagen-GAG copolymer.

5.2 COLLAGEN-GAG SCAFFOLD ARCHITECTURE

The study managed to obtain intact collagen-GAG scaffold from the Teflon-coated pans once freezing and lyophilization was completed. These scaffolds, depending on the freeze rate employed, had either a homogenous or a varied

appearance upon visual inspection and easily released from the pan surface. The set of scaffolds obtained from the stainless steel pans, on the other hand, did not allow for easy removal. These scaffolds adhered to the pan and tore upon removal.

The three-dimensional structure of the scaffold produced by the default *Biofreeze DV 50* program is depicted in Fig. 5.1. The average freeze rate was 1.3 °C/min and represented the conventional quenching technique. The 0.5% collagen-GAG scaffold presented with a pore diameter ranging between 93.43 and 278.07 µm (mean = 174.08 µm with a standard deviation of 54.24). The scaffold had an open pore structure with a small amount of collagen sheets. Numerous collagen strands contributed towards the scaffold architecture.

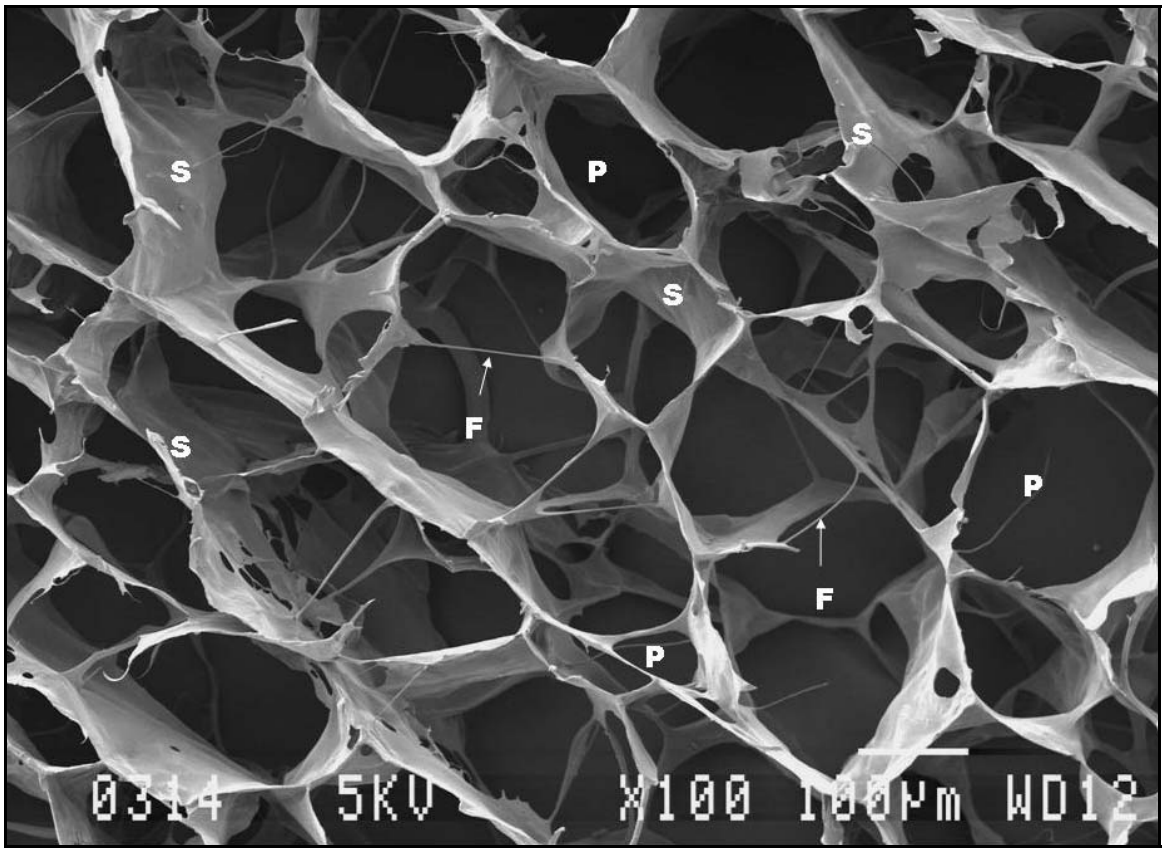

Fig. 5.1. SEM micrograph of the scaffold produced by the conventional quenching technique. The pore diameter ranged between 93.43 and 278.07 µm with a mean of 174.08 µm. The scaffold presented with an open pore (P) structure, few collagen sheets (S) and numerous collagen fibres (F).

The second set of 0.5% collagen-GAG scaffolds (Fig. 5.2), produced using a freeze rate of 0.92 °C/min, had an average pore diameter of 87.32 µm (standard deviation = 26.14). Their pore diameters ranged form 52.47 to 136.44 µm. The scaffolds had a closed appearance with more collagen sheets, pores and fibres per surface area than the previous scaffold.

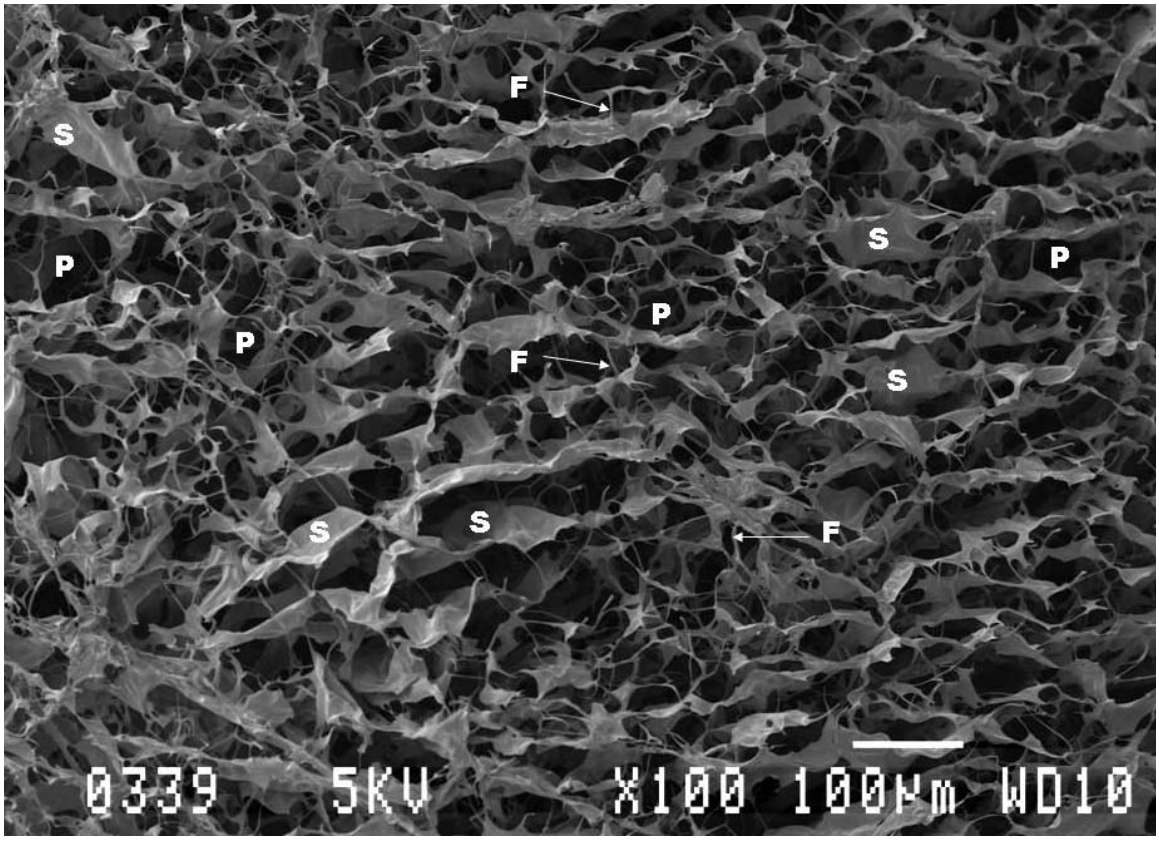

Fig 5.2. SEM micrograph of the scaffold produced by a controlled freeze rate of 0.92°C/min. Their pore diameters ranged form 52.47 to 136.44 µm with an average of 87.32 µm. The scaffolds presented with more collagen sheets (S), pores (P) and fibres (F) per surface area.

Statistical analysis (Fig. 5.3) of the two data sets showed that the rate of freezing significantly influences the resulting average pore diameter of the scaffolds ($p = 0.000$). Uncontrolled freezing (1.3 °C/min) produced scaffolds with larger average pore diameters (mean = 174.08 µm) and more open pore structure. Controlled freezing resulted in a smaller mean pore size (87.32 µm).

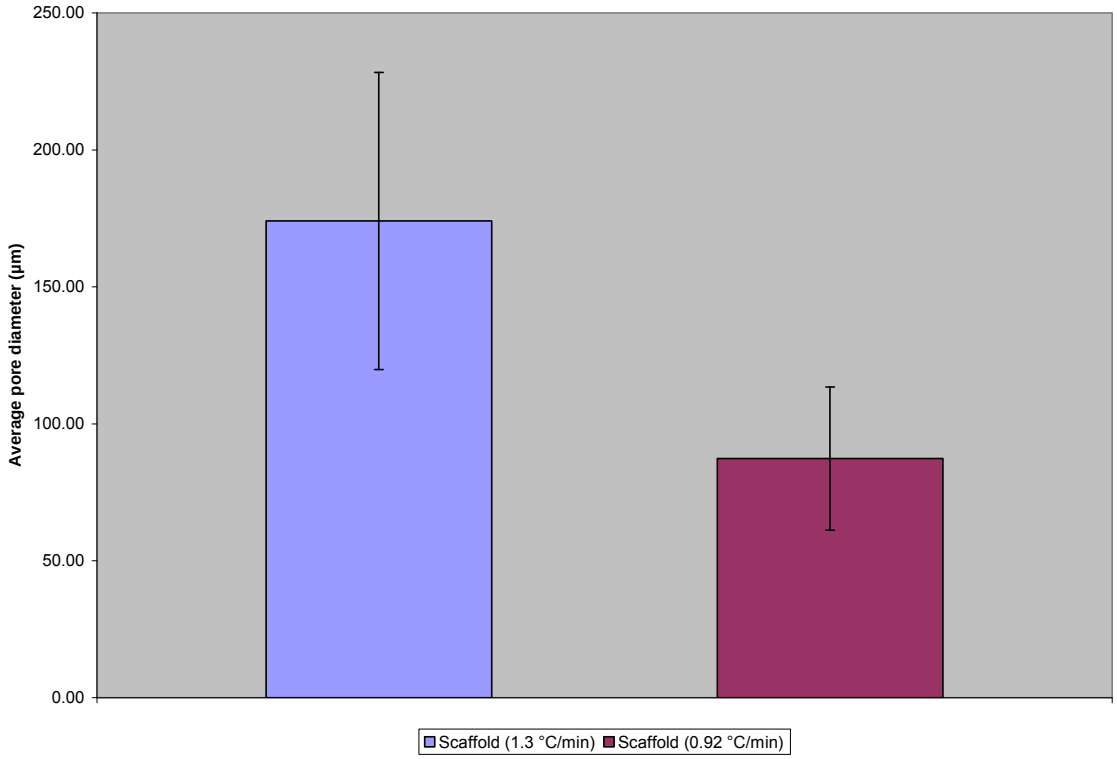

Fig. 5.3. Statistical analysis showed that the rate of freezing significantly ($p = 0.000$) influences the average pore diameter of the scaffolds produced. Conventional quenching resulted in scaffolds with an average pore diameter of 174.08 µm (standard deviation = 54.24). Controlled freezing, on the other hand, produced scaffolds with an average pore diameter of 87.34 µm (standard deviation = 26.14).

An increase in collagen concentration with the same controlled freeze rate led to the production of a denser scaffold with less and smaller pores (mean pore diameter = 56.51 µm). This scaffold distinctively had more collagen sheets (Fig. 5.4). There was a significant difference ($p < 0.050$) in average pore diameter between the 1.0% and 0.5% collagen scaffolds (Fig. 5.5).

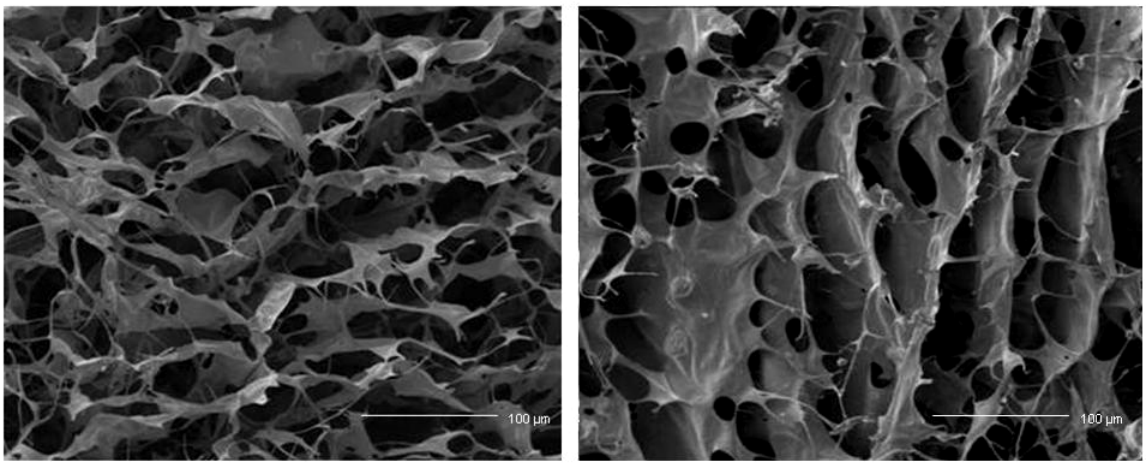

Fig. 5.4. A comparison between two scaffolds showing the influence of altering the collagen concentration. The scaffold on the left was fabricated by using a 0.5% collagen-GAG coprecipitate (average pore size = 87.32 µm). The scaffold on the right was produced with double (1.0%) the amount of collagen and had an average pore size of 56.51 µm.

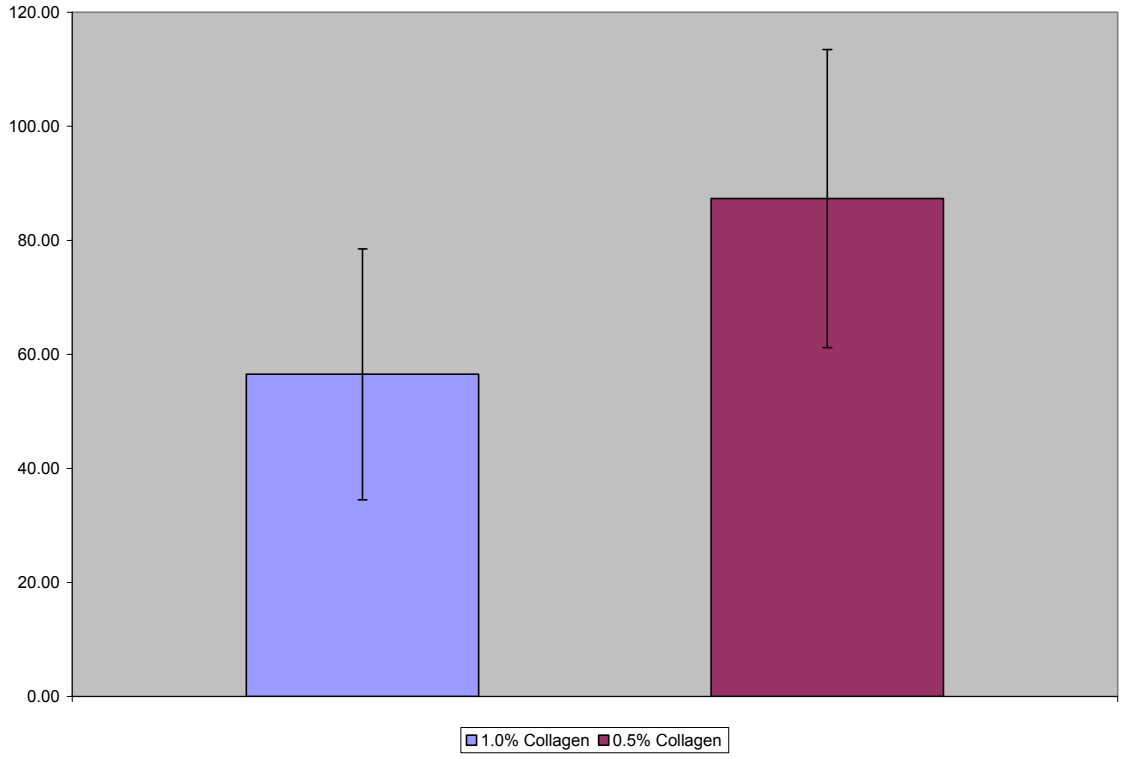

Fig. 5.5. 1.0% collagen under controlled freezing (0.92°C/min) resulted in an average pore diameter of 56.51 µm (standard deviation = 22.00). 0.5% collagen scaffolds produced by the same rate of freezing had a larger mean pore diameter (mean = 87.32 µm, standard deviation = 22.00). This difference was statistically significant with $p < 0.050$.

The most suitable scaffold was compared to the uncrosslinked Integra® collagen scaffold. The Integra® template, fabricated by using a controlled freeze rate of 0.9 °C/min, had an average pore diameter of 80.71 µm ranging between 36.17 and 139.61 µm. Comparing Integra® with the scaffold produced by employing a controlled freeze rate of 0.92 °C/min reveals similar scaffold microstructures (Fig. 5.6). Both consist of a combination of polygonal pores, collagen sheets, and collagen fibres. There was no significant difference ($p = 0.424$) between the average pore diameters resulting from the two slightly different rates of freezing (Fig. 5.7).

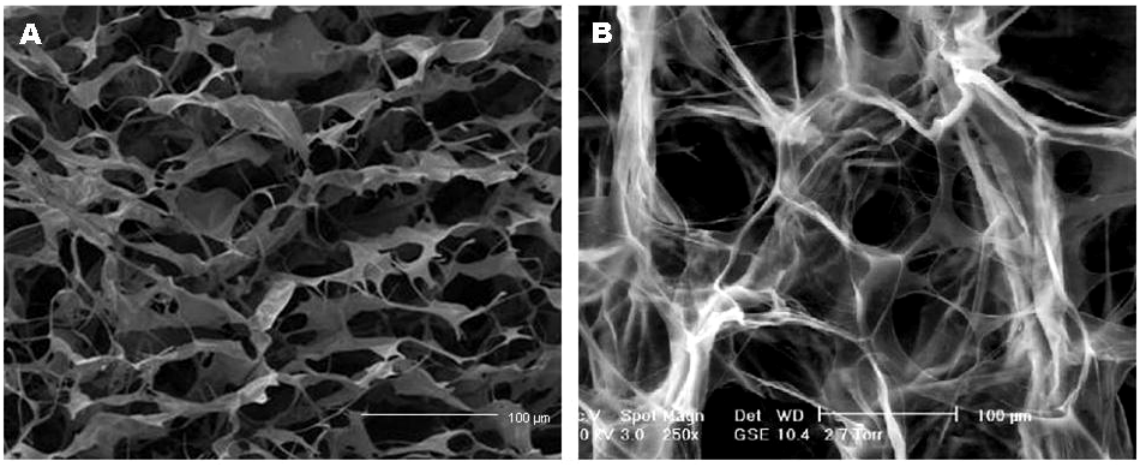

Fig. 5.6. A comparison between two scaffolds produced by controlled rate of freezing. The SEM micrograph A reveals a similar microstructure than that of the environmental scanning electron microscopy (ESEM) micrograph B. Both scaffolds comprise of a combination of pores, collagen sheets and collagen filaments.

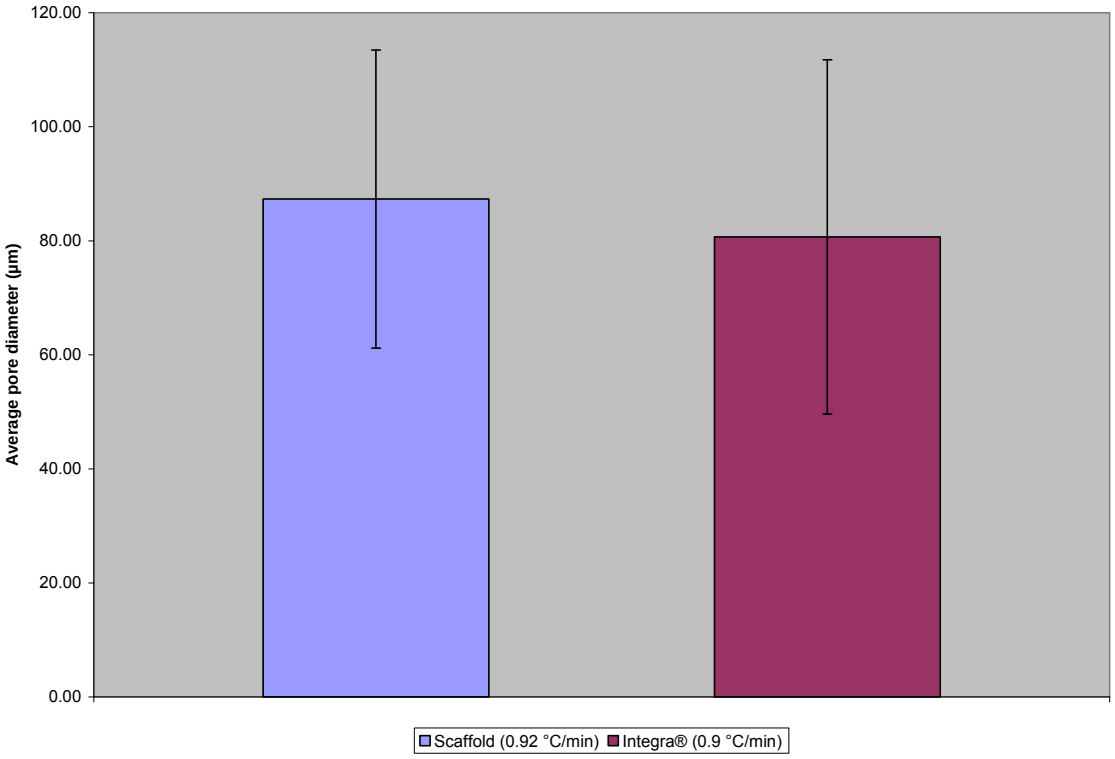

Fig 5.7. Statistical analysis of mean pore sizes revealed no significant architectural difference (p = 0.424) between the generic scaffold (0.92 °C/min) and the Integra® scaffold (0.9 °C/min). The generic scaffolds (left) had a mean pore diameter of 87.32 µm while that of Integra® (right) ranged between 36.17 and 139.61 µm (mean = 80.71 µm, standard deviation = 31.06).

The following was found when the epidermal portion was considered. Both the intra- and inter-epidermal layer thicknesses ranged from 0.15 to 0.19 mm and averaged 0.176 mm (standard deviation = 0.012). This compares well with that of Integra® with a documented thickness of 0.1 mm [28]. This layer not only serves as physical barrier against infection but also allows for easy manipulation of the collagen-GAG copolymer. Moisture transfer can be enhanced by meshing the scaffold prior to its application.

Fig. 5.8. This photo demonstrates the crosslinked artificial skin which consists of an epidermal portion (the exposed inferior surface) and a dermal portion (superior).

The crosslinked collage-GAG copolymer (Fig. 5.8) had a white appearance prior to packaging and sterilization and showed good structural integrity. No separation of the bilaminate construct was observed after handled.

5.3 ENZYMATIC DEGRADATION ASSAY

The results of the collagen degradation assay indicate that efficient crosslinking is dependent on the glutaraldehyde concentration as well as the method of sterilisation. After 30 minutes of incubation it was found that the uncrosslinked and un-irradiated scaffolds completely degraded. This sample was therefore eliminated from the test group. The rest of the sample group, including Integra®, showed good resistance against the enzymatic degradation of collagenase after the first 30 minutes (Fig. 5.9). There was no visible separation of the two layers of the scaffolds. After 120 minutes, visual inspection revealed that some of the specimens underwent extensive enzymatic degradation compared to Integra®.

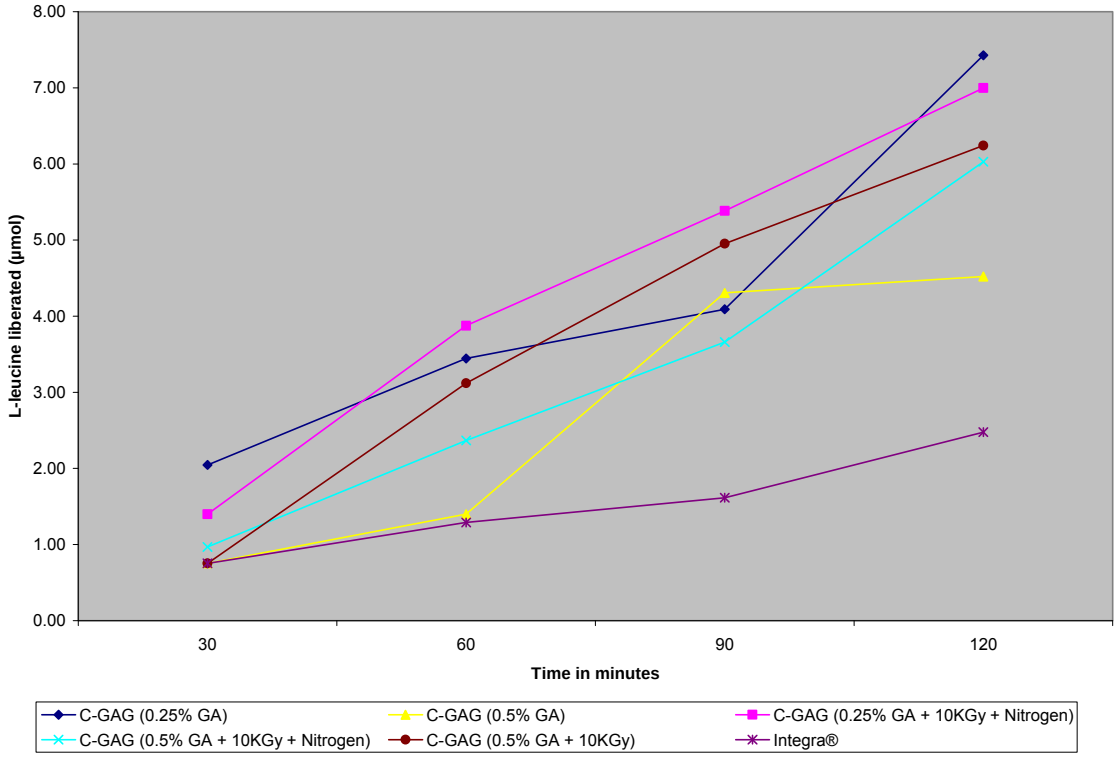

Fig. 5.9. The results of the enzymatic degradation of variable crosslinked and sterilised collagen-GAG scaffolds. The data reveals that each set of variables dramatically influence the rate of degradation.

The trendlines (Fig. 5.10) of the line graph in Fig. 5.9 provides a clearer comparison of the rate of degradation of each collagen-GAG scaffold. Scaffolds that were crosslinked with 0.5% GA degraded at a rate of 1.15 µmol/min. The collagen-GAG matrices crosslinked with 0.25% GA degraded at a rate of 1.15 µmol/min 1.16 µmol/min. These results confirm that a higher GA concentration improves crosslinking and consequently reduces the rate of scaffold degradation. Although there is a slight difference in the rates of degradation between the 0.25 % GA (1.69 µmol/min) and 0.5 % GA (1.15 µmol/min) crosslinked scaffolds, it is clear that deterioration increases upon terminal sterilisation. Irradiation under pure nitrogen, however, reduces collagen degradation as described by Miyata *et al.* [177]. This can be seen when comparing the rate of degradation of 1.56 µmol/min and 1.36 µmol/min. Integra® presented with a rate of degradation of 0.60 µmol/min.

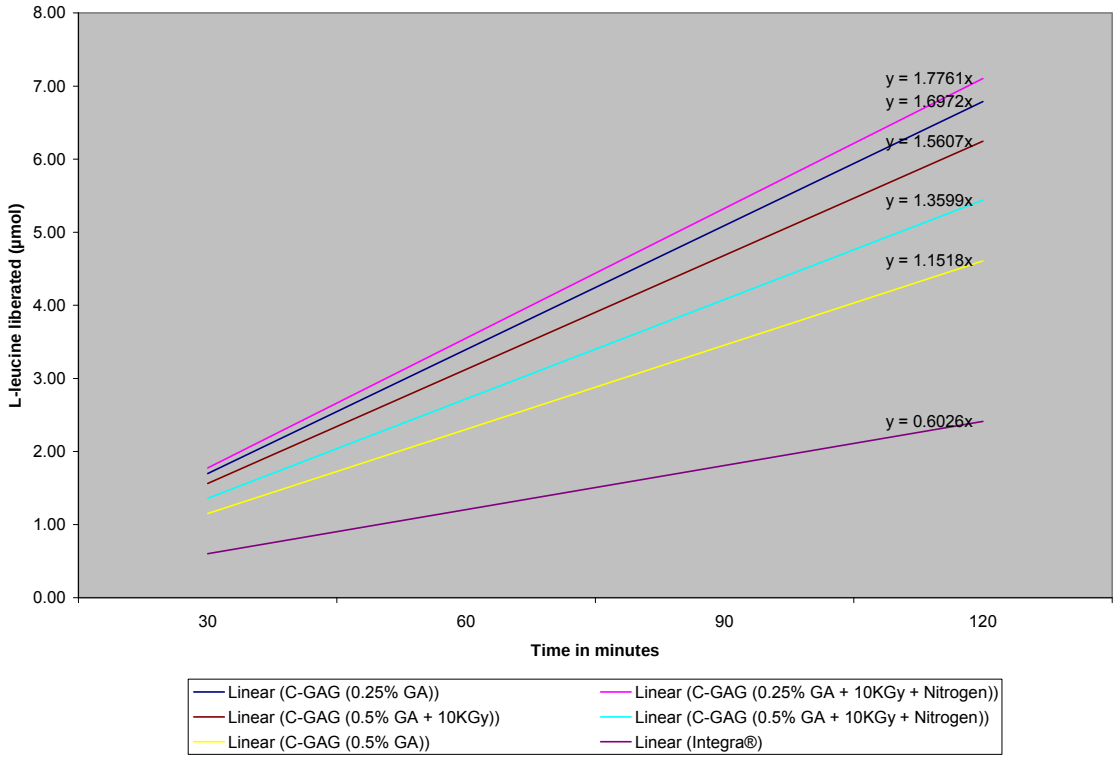

Fig. 5.10. The linear representations of the rates of degradation of each scaffold. Terminal sterilization dramatically increases the rate of degradation even though nitrogen gas has been used to reduce oxidation during the process. The unsterilised and highly crosslinked scaffold has the slowest rate of degradation compared to rest but does not compare well to that of Integra® and is 1,9 times faster.

It is thus clear that sterilisation by γ-irradiation significantly increases the rate of scaffold degradation. The irradiation induced random crosslinking and breakdown of the tropocollagen molecules results in the disruption of the collagen-GAG scaffolds architecture as can be seen in the SEM micrographs in Fig. 5.11. This is in accordance with the work done by Noah *et al.* [179]. Integra® is represented by A in figure 5.11. Sample B shows the closest resemblance to Integra®. This sample has not been terminally sterilised. Distinct architectural disruption is induced by γ-irradiation (samples C and D). Scaffold D is rendered impermeable due to additional γ-irradiation induced and this will ultimately influence tissue regeneration.

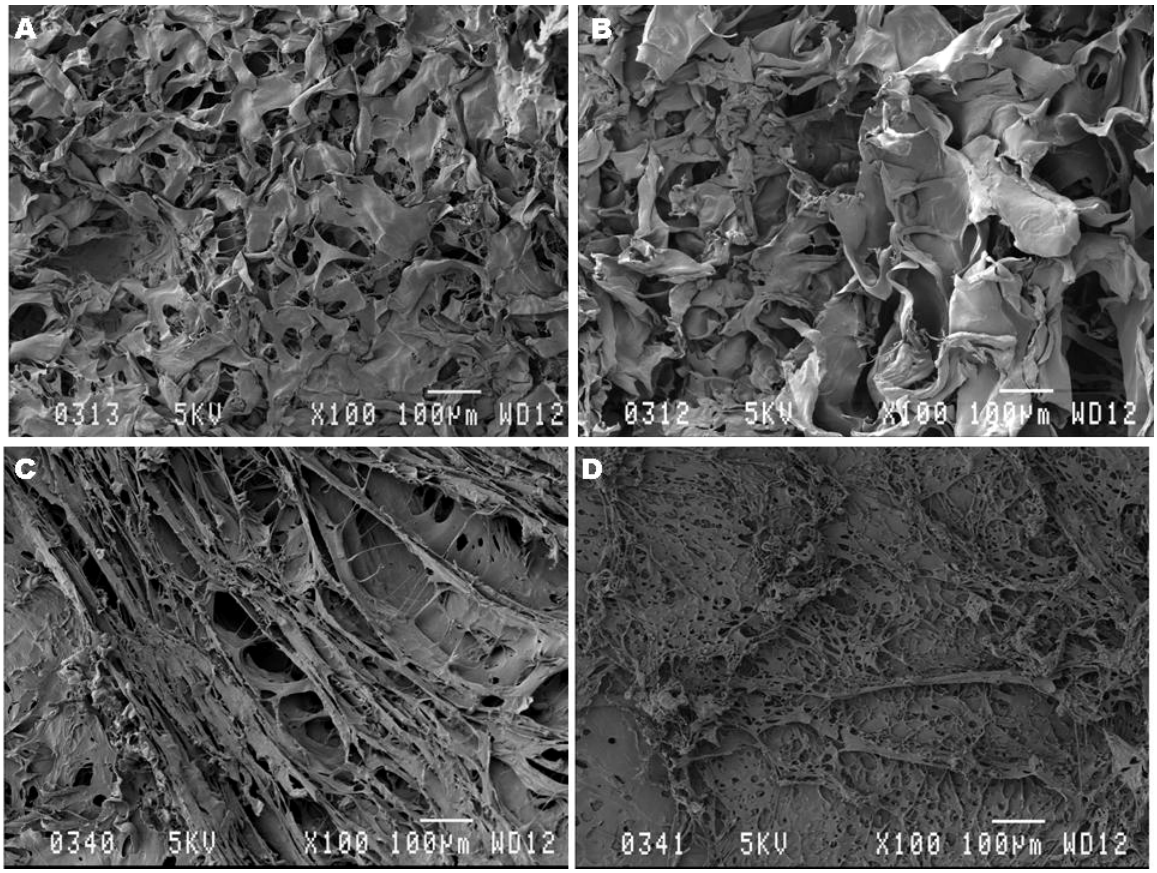

Fig 5.11. This series of SEM micrographs reveals the effect of γ-irradiation on the integrity of the scaffold architecture. The closest resemblance to Integra® is portrayed by B which has not been terminally sterilised. Distinct architectural disruption is induced by γ-irradiation as can be seen by upon inspection of C and D.

5.4 CYTOTOXICITY ASSAY

The results of the cytotoxicity assay confirmed effective removal of free aldehydes. There was no significant difference in the cell viability between the control group and the test group ($p = 0.098$). The data obtained correlates with the study by Speer *et al*. [156]

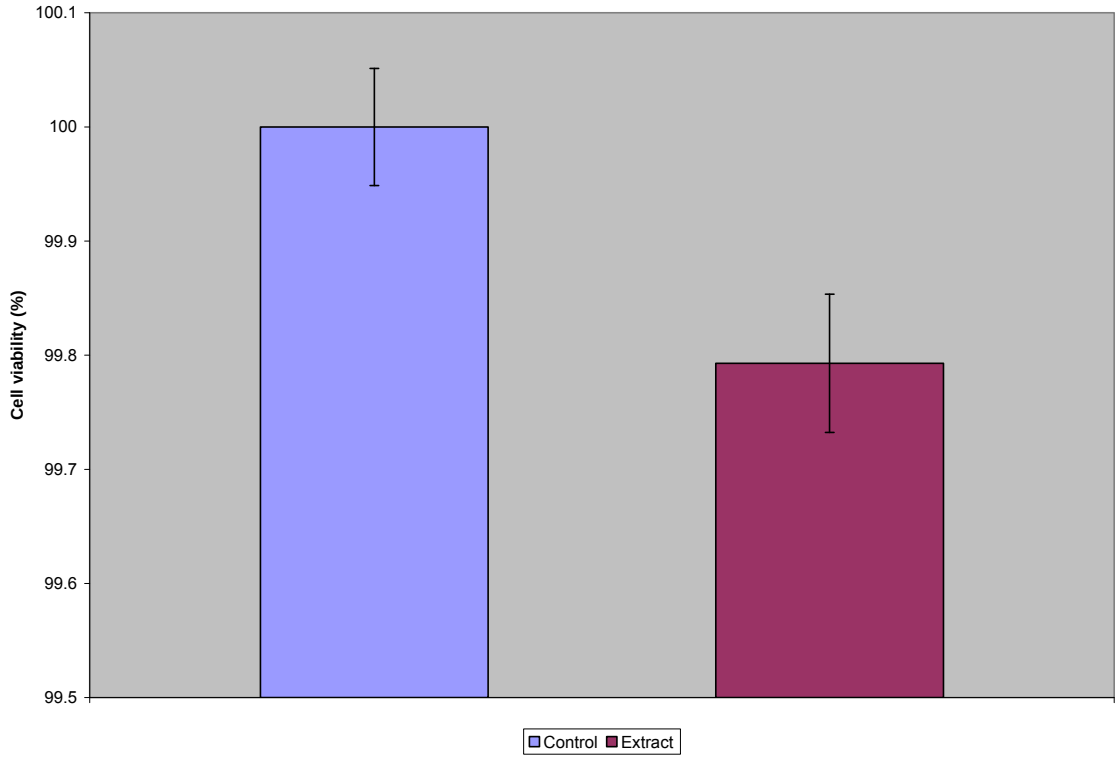

Fig 5.12. The results obtained from the cytotoxicity assay indicates no significant difference (p = 0.098) in cell viability between the test group and the control group.

5.5 SUMMARY

The results of study show that it is possible to obtain a biologically active crosslinked collagen-GAG copolymer that resembles Integra®. Data reveals that it is possible to obtain an Integra® equivalent scaffold with an average pore diameter of 87.32 µm. There was no significant difference (p = 0.424) in the mean pore diameters between the most equivalent scaffold micro structure compared to Integra® (mean = 80.71 µm).

An epidermal layer of with an average thickness of 0.176 mm (standard deviation = 0.012) was obtained. This layer did not separate from the underlying collage-GAG sponge and thus indicated that a sufficient mechanical bond was generated. The most effective crosslinking was achieved using a 0.5% GA solution at an acid pH and 4 °C. This was confirmed via a calorimetric assay after exposure of the scaffolds to 0.1mg/ml collagenase at 37 °C. The rate of

degradation of the most equivalent un-irradiated scaffold (1.15 µmol/min) as well as the most equivalent irradiated (1.36 scaffold µmol/min) is higher compared to that of Integra® (0.60 µmol/min).

GA removal through the method proposed by Speer *et al*. [156] proved to be efficient. Extracts prepared post-treatment did not have a significant effect on cell viability ($p = 0.098$). No adverse host reaction in the form of inflammation would thus be expected *in vivo*.

The initial crosslinking was insufficient as suggested by the current research. This would implicate that either additional crosslinking is required or that the method of terminal sterilization should be questioned. The collagen purity would also affect crosslinking since the amount of available amine groups of lysine or hydroxylysine, with which GA reacts, would be reduced [145]. However, it should be noted that the determination if an *in vivo* degradation rate, in the form of an animal study, will aid to confirm the efficiently of the biologically active regeneration matrix.

CHAPTER 6

CONCLUSION

An extracellular analogue such as Integra® has become an invaluable resource for the treatment of massively burnt patients. Skin substitutes not only saves lives as in the case of full-thickness burn wounds but also improves the quality of live of those affected. Today the application of this reliable product extends to serve as a tissue engineering scaffold in plastic and reconstructive surgery. The perfect artificial skin should be non-antigenic, biocompatible, robust, and adherent, easily available and inexpensive [23-35]. More specifically such device must have: an average pore diameter between 20 and 120 µm; be highly crosslinked to resist degradation; and present with a collagen/glycosaminoglycan ratio of 92/8 [121]. The continuous need for cost-effective treatment of severely burnt patients and an efficient tissue engineering scaffold developed on African soil motivated this study.

The main objectives of this study were to describe and evaluate the efficacy of collagen based tissue engineering scaffolds and to review collagen-GAG facilitated dermal regeneration mediated by Integra®. Furthermore an attempt was made to generate such an equivalent scaffold or biocompatible artificial skin. An elaborate protocol was prepared and included information on: the preparation of an optimal collagen-GAG suspension; factors affecting the scaffold architecture; the influence of the freezing container on the scaffold porosity; formation of an artificial epidermal layer; optimal procedure for crosslinking of the scaffold; procedures for removal of unbound aldehydes; optimal packaging, terminal sterilization and storage; the cytotoxicity analysis to asses the effectiveness of free aldehyde removal; the determination of the rate of degradation of the scaffold; and electron microscopic analysis of the engineered scaffold.

This study managed to obtain a homogenous, highly porous and crosslinked collagen-GAG tissue engineering scaffold. The crosslinking, however, proved to be inadequate since the rate of degradation was found to be 1.9 times faster than that of Integra®. The rate of scaffold degradation can be extended, either by additional crosslinking or the prevention of degradation induced by irradiation. The latter is achieved trough the prevention of oxidation by replacing the oxygen rich atmosphere of the packaging with an inert gas such as nitrogen. Additional research is proposed where initial crosslinking is done by using high temperature vacuum dehydration crosslinking through esterification or amide formation [137]. This would then be followed by conventional GA crosslinking which is known to react with the free amine groups of lysine or hydroxylysine of the protein backbone of collagen [145]. By enhancing the crosslinking it would be possible to compensate for the irradiation induced degradation.

CHAPTER 7

REFERENCES

1. Vacanti CA. History of Tissue Engineering and A Glimpse into Its future. Tissue Engineering 2006; 12(5); 1137-1142.

2. Pachence JM. Collagen-Based Devices for Soft Tissue Repair. Journal of Biomedical Materials Research 1996; 33: 35-40.

3. Bansky R. The use of dermal template INTEGRA in scalpation injury of the hand. Bratisl Lek Listy 2005; 106(6-7): 221-225.

4. Billingharm E, Medawar PB. The technique of free skin grafting in mammals. Journal of Experimental Biology 1951; 28: 385-394.

5. Billingharm E, Medawar PB. Contracture and intussusceptive growth in the healing of extensive wounds in mammalian skin. Journal of Anatomy 1955; 89: 114-123.

6. Peacock EE, Van Winkle W. Wound repair. 2nd edition. Philadelphia: W. B. Saunders; 1976.

7. Saffle JR, Davis B, Williams P. Recent outcomes in the treatment of burn injury in the United States: A report from the American Burn Association Patient Registry. Journal Burn Care and Rehabilitation 1995; 16: 219-232.

8. Williams W. Pathophysiology of the burn wound. In: Total Burn Care.
2nd ed. London: Saunders; 2002.

9. Sipe JD. Tissue engineering and reparative medicine. Annals of the New York Academy of Sciences 2002; 961: 1-9.

10. Jones L, Currie L, Martin R. A guide to biological skin substitutes. British Journal of Plastic Surgery 2002; 55: 185-193.

11. Broughton G, Janis JE, Attinger CE. A brief history of wound care. Plastic and Reconstructive Surgery 2006; 117 (Suppl): 6S-9S.

12. Manjo G. The healing hand: Man and wound in the ancient world. Cambridge: Harvard University Press; 1975.

13. Lionelli GT, Lawrence WT. Wound dressings. Surgery Clinics of North America 2003; 83(3): 617-638.

14. Henry G. Garner W. Inflammatory mediators in wound healing. Surgery Clinics of North America 2003; 83: 483.

15. Johnson S. Early years: Our History [Online]. 2005; [4 screens]. Available from: URL: http:// www.jnj.com/our_company/history/history_section_1.htm.

16. Ho W. Skin substitutes: An overview. Annals of the College of Surgeons Hong Kong 2002; 6: 102-108.

17. Winter RD. Formation of the scab and the rate of epithelialization of superficial wounds in the skin of the young domestic pig. Nature 1962; 193: 293-294.

18. Hinman CD, Maibach H. Effect of air exposure and occlusion on experimental human skin wounds. Nature 1963; 200: 377-379.

19. Alvarez OM, Mertz PM, Eaglestein WH. The effect of occlusive dressings on collagen synthesis and re-epithelialization in superficial wounds. The Journal of Surgical Research 1983; 35: 142-148.

20. Caldwell Jr FT, Bowser BH, Crabtree JH. The effect of occlusive dressings on the energy metabolism of severely burned children. Annals of Surgery 1981; 193: 579-591.

21. Barnett A, Berkowitz RL, Mills R, Vistnes LM. Comparison of synthetic adhesive moisture vapor permeable and fine mesh gauze dressings for split-thickness skin graft donor sites. The American Journal of Surgery. 1983; 145: 379-381.

22. Eisenbud D, Huang NF, Luke S, Silberklang M. Skin substitutes and wound healing: current status and challenges. Wounds 2004; 16(1): 2-17.

23. Pruitt BA. The evolutionary development of biologic dressings and skin substitutes. Journal Burn Care and Rehabilitation 1997; 18: s2-s5

24. Tompkins RG, Burke JF. Burn wound closure using permanent skin replacement materials. World Journal of Surgery 1992; 16: 47-52.

25. Turner, TD: Semiocclusive and occlusive dressings. In: An Environment for Healing: The Role of Occlusion. Royal Society of Medicine International Congress and Symposium Series No. 88; Published by the Royal Society of Medicine; 1984.

26. Bar-Meir E, Mendes D, Winkler E. Skin Substitutes. The Israel Medical Association Journal, March 2006; 8: 188-191.

27. Yannas IV, Burke JF. Gordon PL *et al*. Design of an artificial skin: II. Control of chemical composition. Journal of Biomedical Material Research 1980; 14: 107-132.

28. Burke JF, Yannas IV, Quinby WC, Bondoc CC, Jung WK. Successful use of a physiologically acceptable artificial skin in the treatment of extensive burn injury. Annals of Surgery 1981; 194(4): 413-428.

29. Heimbach D, Luterman A, Burke J.F, *et al*. Artificial dermis for major burns: a multi-center randomized clinical trial. Annals of Surgery 1988; 208(3): 313-320.

30. Moiemen NS, Vlashou E, Staiano JJ, Thawy Y, Frame FD. Reconstructive Surgery with Integra Dermal Regeneration Template: Histologic study, Clinical Evaluation, and Current practice. Plastic and Reconstructive Surgery 2006; 117(7S): 160S-174S.

31. Clayman MA, Clayman SM, Mozingo DW. The use of Collagen-Glycosaminoglycan Copolymer (Integra) for the Repair of Hypertrophic Scars and Keloids. Journal of Burn Care and Research 2006; 27(3): 404-409.

32. Benson A, Dickson W, Boyce DE. ABC of wound healing. Burns. British Medical Journal 2006; 332: 649-652.

33. Witte MB, Barbul A. General principles of wound healing. Surgery Clinics of North America 1997; 77: 509-528.

34. Garner WL, Ann AM. Epidermal Regulation of Dermal Fibroblast Activity, Plastic and Reconstructive Surgery July 1998; 102(1): 135-139.

35. Eisinger M, Sadan S, Flick RB. Growth regulation of skin cells by epidermal cell-derived factors: Implications for wound healing. Proceedings of the National Academy of Sciences March 1988; 85(6): 1937-1941.

36. Eisinger M, Sadan S, Soehnchen R, Silver IA. Wound healing by epidermal-derived factors: Experimental and preliminary clinical studies. Progress in Clinical and Biological Research 1988; 266:291-302.

37. Silver, I. A., and Eisinger, M. Influence of an epidermal cell extract on skin healing and scar formation. International Journal of Tissue Reactions 1988; 10: 381.

38. Kratz G, Haegerstrand A, Dalsgaard CJ. Conditioned medium from cultured human keratinocytes has growth stimulatory properties on different human cell types. Journal of Investigative Dermatology 1991; 97: 1039-1043.

39. Hübner G, Brauchle M, Smola H, Madlener M, Fässler R, Werner S. Differential regulation of pro-inflammatory cytokines during wound healing in normal and glucocorticoid-treated mice. Cytokine 1996; 8: 548-556.

40. Martin P. Wound healing - aiming for perfect skin regeneration. Science 1997; 276: 75-81.

41. Leibovich SJ, Ross R. The role of the macrophage in wound repair. A study with hydrocortisone and antimacrophage serum. American Journal of Pathology 1975; 78: 71-100.

42. Madri, J. A., Sankar, S., and Romanic, A. M. Angiogenesis. In: Clark RAF, ed. The Molecular and Cellular Biology of Wound Repair. 2nd edition. New York: Plenum; 1995: 355-371.

43. Brown LF, Yeo KT, Berse B, et al. Expression of vascular permeability factor (vascular endothelial growth factor) by epidermal keratinocytes during wound healing. The Journal of Experimental Medicine 1992; 176: 1375-1379.

44. Clark RAF. Wound Repair: Overview and General Considerations. In: Clark RAF, ed. The Molecular and Cellular Biology of Wound Repair. 2nd edition. New York: Plenum Press; 1996: 3-50.

45. Desmouliere A, Geinoz A, Gabbiani F, Gabbiani G. Transforming growth factor-beta 1 induces alpha-smooth muscle actin expression in granulation tissue myofibroblasts and in quiescent and growing cultured fibroblasts. The Journal of Cell Biology 1993; 122: 103-111.

46. Gray AJ, Bishop JE, Reeves JT, Laurent GJ. A alpha and B beta chains of fibrinogen stimulate proliferation of human fibroblasts. Journal of Cell Science 1993; 104: 409-413.

47. Xu J, Clark RA. Extracellular matrix alters PDGF regulation of fibroblast integrins. The Journal of Cell Biology 1996; 132: 239-249.

48. Eriksson A, Siegbahn A, Westermark B, Heldin CH, Claesson-Welsh L. PDGF alpha- and beta-receptors activate unique and common signal transduction pathways. The European Molecular Biology Organization Journal 1992 February; 11(2): 543-550.

49. Roberts AB, Sporn MB, Frank S, Madlener M, Werner S. Transforming growth factors beta1, beta2, and beta3 and their receptors are differentially regulated during normal and impaired wound healing Journal of Biological Chemistry 1996; 271(10188): 275-308.

50. Greiling D, Clark RA. Fibronectin provides a conduit for fibroblast transmigration from collagenous stroma into fibrin clot provisional matrix. Journal of Cell Science 1997; 110(7): 861-870.

51. Toole BP. Proteoglycans and hyaluronen in morphogenesis and differentiation. In: Hay ED, ed. Cell Biology of Extracellular Matrix. 2nd edition. New York: Plenum Press; 1991: 305-341.

52. Mignatti P, Rifkin DB, Welgus HG, Parks WC. Proteinases and tissue remodeling. In: Clark RAF, ed. The Molecular Biology of Wound Repair, 2nd edition. New York, NY: Plenum Press; 1996: 427–474.

53. Vaalamo M, Mattila L, Johansson N, Kariniemi AL, Karjalainen-Lindsberg ML, Kähäri VM, Saarialho-Kere U. Distinct populations of stromal cells express collagenase-3 (MMP-13) and collagenase-1 (MMP-1) in chronic ulcers but not in normally healing wounds. Journal of Investigative Dermatology 1997; 109: 96-101.

54. Welch MP, Odland GF, Clark RA. Temporal relationships of F-actin bundle formation, collagen and fibronectin matrix assembly, and fibronectin receptor expression to wound contraction. The Journal of Cell Biology 1990; 110: 133-146.

55. Desmoulière A, Gabbiani G. The Role of the Myofibroblast in Wound Healing and Fibrocontractive Diseases. In: Clark RAF, ed. The Molecular and Cellular Biology of Wound Repair. 2nd edition. New York: Plenum Press, 1996: 391-423.

56. Desmouliere A, Redard M, Darby I, Gabbiani G. Apoptosis mediates the decrease in cellularity during the transition between granulation tissue and scar. American Journal of Pathology 1995; 146: 56-66.

57. Saffle JR, Davis B, Williams P. Recent outcomes in the treatment of burn injury in the United States: A report from the American Burn Association Patient Registry. Journal of Burn Care and Rehabilitation 1995; 16: 219-232.

58. Williams WG, Phillips LG. Pathophysiology of the burn wound. In: Total Burn Care. Hernndon DN ed. 2nd edition. Philadelphia: WB Saunders Company; 1996: 63-70.

59. Compton CC, Butler CE, Yannas IV, Warland G, Orgill DP. Organized Skin Structure Is Regenerated *In Vivo* from Collagen-GAG Matrices Seeded with Autologous Keratinocytes. The Journal of Investigative Dermatology 1998; 110(6): 908-916.

60. Yannas IV, Lee E, Orgille DP, Skrabu M, Murphy TGF. Synthesis and characterization of a model extracellular matrix that induces partial regeneration of adult mammalian skin. Proceedings of the National Academy of Sciences of the USA 1989; 86: 933-937.

61. Yannas IV, Burke JF, Huang C, Gordon PL. Suppression of *in vivo* degradability and of immunogenicity of collagen by reaction with glycoaminoglycans. Polymer Preprints, American Chemical Society 1975; 16: 209-214.

62. Yannas IV, Burke JF, Gordon PL, Huang C, inventors; Massachusetts Institute of Technology (Cambridge, MA), assignee; Multilayer membrane useful as synthetic skin. US Patent 4060081. 1977.

63. Yannas IV, Burke JF, Umbrei T, Stasikelis P. Progress in design of an artificial skin. Federation Proceedings 38: 988.

64. Yannas IV, Burke JF, Warpehoski M, Stasikelis P, Skrabut EM, Orgill D, Giard DJ. Prompt, long-term functional replacement of skin. Transactions - American Society for Artificial Internal Organs. 1981; 27: 19-23.

65. Yannas IV, Burke JF, Orgill DP, Skrabut EM. Wound tissue can utilize a polymeric template to synthesize a functional extension of skin. Science 1982; 215(4529): 174-176.

66. Yannas IV, Orgill DP, Skrabut EM, Burke JF. Skin regeneration with a bioreplaceable polymeric template. Polymeric Materials and Artificial Organs. Gebelein CG (editor). Washington DC: American Chemical Society; 1984; 191-197.

67. Murphy GF, Orgill DP, Yannas IV. Partial dermal regeneration is induced by biodegradable collagen-glycosaminoglycan grafts. Laboratory Investigation 1990; 63(3): 305-313.

68. Stern R, McPherson M, Longaker MT. Histologic study of artificial skin used in the treatment of full-thickness thermal injury. Journal of Burn Care Rehabilitation 1990; 11: 7-13.

69. Moiemen N, Staiano J, Ojeh N, Thway Y, Frame J. Reconstructive surgery with a dermal regeneration template: Clinical and histological study. Plastic Reconstructive Surgery 2001; 108: 93-103.

70. 2nd European Symposium of Dermal Regeneration. Dublin 16-18 May; 2002; Abstract book, p7.

71. Loss M, Wedler V, KuÈnzi W, Meuli-Simmen C, Meyer VE. Articial skin, split-thickness autograft and cultured autologous keratinocytes combined to treat a severe burn injury of 93% of TBSA. Burns 2000; 26: 644-652.

72. Janzekovic ZA. A new concept in the early excision and immediate grafting of burns. The Journal of Trauma 1970; 10: 1103-1108.

73. Rheinwald JG, Green H. Serial cultivation of strains of human epidermal keratinocytes: the formation of keratinizing colonies from single cells. Cell 1975; 6: 331-344.

74. Fette A. Integra artificial skin® in use for full-thickness burn surgery: Benefits or harms on patient outcome. Technology and Health Care 2005; 13: 463-468.

75. Ryan C, Schoenfield D, Malloy *et al*., Use of Integra Artificial Skin is associated with decreased length of stay for severely injured adult burn survivors, Journal of Burn Care and Rehabilitation 2002; 23: 311-317.

76. Butler CE, Orgill DP, Yannas IV, Compton CC. The effect of keratinocyte seeding of collagen-glycosaminoglycan membranes on the regeneration off skin in a porcine model. Plastic and Reconstructive Surgery 1998; 101(6): 1572-1579.

77. Raultt I, Frei V, Herbage D, Abdul-Makak N, Huc AE. Evaluation of different chemical methods for crosslinking collagen gel, films, and sponge. Journal of Materials Science: Materials in Medicine 1996 7: 215-221.

78. Friess, W. Collagen: Biomaterial for drug delivery. European Journal of Pharmaceutics and Biopharmaceutics 1998; 45: 113-136.

79. Hiraoka Y, Kimura Y, Hiroki U, Yasuhiko T. Fabrication and biocompatibility of collagen sponge reinforced with Poly (glycolic acid) Fiber. Tissue Engineering 2003; 9(6): 1101-1112.

80. Nicolas FL, Gagnieu CH. Denatured thiolated collagen II . Crosslinking by oxidation. Biomaterials 1997; 18: 815-821.

81. Goissis G, Marcantonio EJ, Marcantonio RA, Lia RC, Cancian DC, de Carvalho WM. Biocompatibility studies of anionic collagen membranes with different degree of glutaraldehyde crosslinking. Biomaterilas 1999; 20: 27-34.

82. Miyata T, Taira T, Noishiki Y. Collagen engineering for biomaterial use. Clinical Materials 1992; 9: 139-148.

83. Teramachi M, Nakamura T, Yamamoto Y, Kiyotani T, Takimoto Y, Shimizu Y. Porous-type tracheal prosthesis sealed with collagen sponge. Ann. Thorac. Surg 1997; 64: 965-969.

84. Natsume T, Ike O, Okada T, Takimoto N, Shimizu Y, Ikada Y. Porous collagen sponge for esophageal replacement. Journal of Biomedical Materials Research 1993; 27: 867-875.

85. Yamamoto Y, Nakamura T, Shimizu Y, Takimoto Y, Natsumoto K, Kiyotani T, *et al*. Experimental replacement of the thoracic esophagus with a bioabsorbable collagen sponge scaffold supported by a silicone stent in dogs. American Society of Artificial Internal Organs Journal. 1999; 45: 311-316.

86. Chamberlain LD, Yannas IV, Hsu HP, Strichartz GR, Spector M. Near-terminus axonal structure and function following rat sciatic nerve regeneration through a collagen–GAG matrix in a ten-millimeter gap. Journal of Neuroscience Research 2000; 60: 666-677.

87. Piez KA. In Treatise on collagen. London and New York: Academic 1967; 1: 207-252.

88. Spiro RG. Characterization and Quantitative Determination of the Hydroxylysine-linked Carbohydrate Units of Several Collagens. The Journal of Biological Chemistry 1969; 244: 602-612.

89. Stark M, Miller EJ, Kühn K. Comparative Electron-Microscope Studies on the Collagens Extracted from Cartilage, Bone, and Skin. European Journal of Biochemistry 1972; 27: 192-196.

90. Krieg T. Collagen in wound healing. Wounds 1995; 7Suppl A (5): 5A-12A.

91. Miller EJ, Matukas VJ. Chick Cartilage Collagen: A New Type of 1 Chain not Present in Bone or Skin of the Species. Proceedings of the National Academy of Sciences 1969; 64: 1264-1268.

92. Bornstein P, Nesse R. The comparative biochemistry of collagen: The structure of rabbit skin collagen and its relevance to immunochemical studies of collagen. Archives of Biochemistry and Biophysics 1970; 138: 443-450.

93. Steffen C, Timpl R, Wolff I. Immunogenicity and specificity of collagen
V. Demonstration of three different antigenic determinants on calf collagen Immunology 1968; 15(1): 135-144.

94. Timpl R, Wolff I, Wick G, Furthmayer H. Steffen C. Immunogenicity and Specificity of Collagen: VII. Differences Between Various Collagens Demonstrated by Cross-Reaction Studies. The Journal of Immunology 1968; 101: 725-729.

95. Lindsley H, Mannik M, Bornstein P. The distribution of antigenic determinants in rat skin collagen. The Journal of Experimental Medicine 1971; 133(6):1309-1324.

96. Furthmayer H, Timpl R. Structural requirements of antigenic determinants in the aminoterminal region of the rat collagen α2 chain. Biochemical and Biophysical Research Communications 1972; 47: 944-950.

97. Purna SK, Babu M. Collagen based dressings – a review. Burns 2000; 26: 54-62.

98. Coals A, Curtis J. Silicone Biomaterials: History and Chemistry and medical Applications of Silicones [Online]. Available from: URL: http://www.pubmedcentral.nih.gov/picrender.fcgi?artid=1409420&blobtype=pdf

99. Jaques LB, Fidlar E, Feldsted ET, MacDonald AG. Silicones and blood coagulation. Canadian Medical Association Journal 1946; 55: 26-31.

100. Margulies, H., and Barker, NW. The coagulation time of blood in silicone tubes. The American Journal of The Medical Sciences. 1949; 218: 42.

101. Lahey FH. Comments made following the speech “Results from using Vitallium tubes in biliary surgery” read by Pearse HE before the American Surgical Association, Hot Springs, VA. Annals of Surgery 1946; 124: 1027.

102. De Nicola RR. Permanent artificial (silicone) urethra. The Journal of Urology 1950; 63(1): 168-172.

103. Aschoff A. John D Holter and his century valve. Cerebrospinal Fluid Research 2004; 1(Suppl 1) : S13

104. Woodroof EA. Biobrane: a new biosynthetic skin substitute.Care of the burn wound, International Congress; Geneva; 1983.

105. Alberts B, Johnson A, Lewis J, Raff M, Roberts K, Watson JD. Cell junctions, cell adhesion, and the extracellular matrix. Molecular biology of the cell. New York: Garland Science, 2002; 1065-1125.

106. Lodish H, Berk A, Zipursky SL, Matsudaira P, Baltimore D, Darnell J. Integrating cells into tissues. Molecular cell biology. New York: Freeman & Co, 2000; 968-1002.

107. Smith BD. Expression and regulation of the collagen family in skin. In: Falanga V (editor). Cutaneous wound healing. London: Martin Dunitz, Ltd, 2001; 57-80.

108. Schultz GS, Ladwig G, Wysocki A. Extracellular matrix: review of its roles in acute and chronic wounds. World Wide Wounds, August 2005; 1-20.

109. Lehninger AL. Biochemistry. 2nd edition. New York: Worth and Co.; 1975; 337.

110. Gelsea K, E. Poschl E, Aigner T. Collagens-structure, function, and biosynthesis. Advanced Drug Delivery Reviews 2003; 55 (12): 1531-1546.

111. Hulmes DJ, Miller A. Molecular packing in collagen, Nature 1981; 293: 234-239.

112. Miller AT, Karmas E, Fu Lu M. Age-related changes in collagen of bovine corium: studies on extractability, solubility and size distribution. Journal of Food Science 1983; 48: 681-686.

113. Cox RW, Grant RA, Kentan CM. Electron-microscope study of the reaction of collagen with some monoaldehydes and bifunctional aldehydes. Journal of Cell Science. 1973; 13: 933-949.

114. Couchman JR, Hook M. Proteoglycans and wound repair. In: Clark RAF, Henson PM (editors). The Molecular and Cellular Biology of Wound Repair. New York, NY: Plenum Press; 1988: 437-470.

115. Rapraeger AC, Krufka A, Olwin BB. Requirements of heparin sulfate for bFGF-mediated fibroblast growth and myoblast differentiation. Science 1991; 21: 1705-1708.

116. Yannas N, Burke JF. Design of an artificial skin. I. Basic design principles. Journal of Biomedical Materials Research 1980; 14: 65-81.

117. Zou XH, Foong WC, Cao T, Bay BH, Ouyang HW, Yip GW. Chondroitin sulfate in palatal wound healing. Journal of Dental Research 2004; 83(11): 880-885.

118. Murata K, Yokoyama . Enzymatic analysis with chondrosulfatases of constituent disaccarides of sulfated chondroitin sulfate and dermatan sulfate isomers by high performance liquid chromatography. Analytical Biochemistry 1985; 149: 261-268.

119. Suzuki S, Isshiki N, Tamada Y, Ikada Y. A new bilayer artificial skin composed of an outer layer of silicone and inner layer of collagen and GAG. The Japanese Journal of Plastic and Reconstructive Surgery 1986; 6: 221-231.

120. Matsuda K, Suzuki S, Isshiki N, Yoshioka K, Okada T, Ikada Y. Influence of glycosaminoglycans on the collagen sponge component of a bilayer artificial skin. Biomaterials 1990; 11: 351-355

121. Yannas IV. Models of organ regeneration process induced by templates. Annals of the New York Academy of Science 2002; 961: 280-293.

122. O'Brien FJ, Harley BA, Yannas IV, Gibson L. Influence of freezing rate on pore structure in freeze-dried collagen-GAG scaffolds. Biomaterials 2004; 25: 1077-1086.

123. Zeltinger J, SherwoodJK , Graham DA, Mueller R, Griffith LG. Effect of pore size and void fraction on cellular adhesion, proliferation, and matrix deposition. Tissue Engineering 2001; 7(5): 557-572.

124. Wake MC, Patrick Jr. CW, Mikos AG. Pore morphology effects on the fibrovascular tissue growth in porous polymer substrates. Cell Transplant 1994; 3(4): 339-343.

125. Salem AK, Stevens R, Peason RG, Davies MC, Tendler SJ, Roberts CJ, Willams PM, Shakesheff KM. Interactions of 3T3 fibroblasts and endothelial cells with defined pore features. Journal of Biomedical Materials Research 2002; 61(2): 212-217.

126. Nehrer S, Breinan HA, Ramappa A, Young G, Shortkroff S, Louie LK, *et al*. Matrix collagen type and pore size influence behavior of seeded canine chondrocytes. Biomaterials 1997; 18(11): 769-776.

127. LiVecchi AB, Tombes RM, LaBerge M. In vitro chondrocyte collagen deposition within porous HDPE: substrate microstructure and wettability effects. Journal of Biomedical Materials Research 1994; 28(8): 839-850.

128. Kuberka M, von HD, Schoof H, Heschel I, Rau G. Magnification of the pore size in biodegradable collagen sponges. Intenational Journal of Artificial Organs 2002; 1: 67-73.

129. Claase MB, Grijpma DW, Mendes SC, De Bruijn JD, Feijen J. Porous PEOT/PBT scaffolds for bone tissue engineering: preparation, characterization, and in vitro bone marrow cell culturing. Journal of Biomedical Materials Research 2003; 64: 291-300.

130. Borden M, El-Amin SF, Attawia M, Laurencin CT. Structural and human cellular assessment of a novel microsphere-based tissue engineered scaffold for bone repair. Biomaterials 2003; 24: 597-609.

131. Doillon CJ, Whyne CF, Brandwein S, Silver FH. Collagen-based wound dressings: control of the pore structure and morphology. Journal of Biomedical Materials Research 1986; 20: 1219-1228.

132. Dow Corning Corporation, Midland, Michigan 48686-0994, Assignee; US Patent No 0438195. 1948.

133. Colas A. Silicones: preparation and performances. Dow Corning, technical document MMV0995-01 1995; 1-14.

134. M.J. Owen. Why silicones behave funny. Chemtech 1981; 11: 288-292.

135. Briquet F, Colas A, Thomas X. Silicones for medical use. Dow Corning France - European Healthcare Centre. Presented at the XIIIth "Technological Congress" "Polymers for Biomedical Use" Le Mans (France), March 1996.

136. Hara M. Various crosslinking methods for collagens: merit and demerit of methods by radiation. Journal of Oral Tissue Engineering 2006; 3(3): 118-124.

137. Weadock KS, Olson RM, Silver FH, Evaluation of collagen crosslinking techniques, Biomaterials, Medical Devices and Artificial Organs 1983-84; 11(4): 293-318.

138. Sabatini DD, Bensch K, Barnett RJ. Cytochemistry and electronmicroscopy. The preservation of cellular ultrastructure and enzymatic activity by aldehydes fixation. Journal of Cell Biology 1963; 17: 19-58.

139. Kiernan JA. Formaldehyde, formalin, paraformaldehyde and glutaraldehyde: What they are and what they do. Microscopy Today 2000; 1: 8-12.

140. Monsan P, Puzo G, Marzarguil H. Etude du mecanisme d'etablissement des iliasons glutaraldehyde-proteines. Biochinie 1975; 57: 1281-1292.

141. Nimni ME, Cheung D, Strates B, Kodama M, Sheikh K. Chemically modified collagen: a natural biomaterial for tissue replacement. Journal of Biomedical Materials Research 1987; 21: 741-771.

142. Chvapil M, Gibeault D, Wang TF. Use of chemically purified and cross-linked bovine pericardium as a ligament substitute Journal of Biomedical Materials Research 1987; 21(12): 1383-1393.

143. Mcpherson JM, Ledger PW, Sawamura S, Conti A, Wade S, Reihanian H, Wallace GD. The preparation and physicochemical characterization of an injectable form of reconstituted, glutaraldehyde cross-linked, bovine corium collagen. Journal of Biomedical Materials Research 1986; 20: 79-92.

144. Jayakrishnan A, Jameela SR, Glutaraldehyde as a fixative in bioprosthetic and drug delivery matrices, Biomaterials 1996; 17: 471-484.

145. Olde Damink LHH, Dijkstra PJ, Van Luyn MJA, Van Wachem PB, Niewenhuis P, Feijen J. Glutaraldehyde as a crosslinking agent for collagen-based biomaterials. Journal of Materials Science: Materials in Medicine 1995; 6: 460-472.

146. Okuda K, Urabe I, Yamada Y, Okada H. Reaction of glutaraldehyde with amino and thiol compounds. Journal of Fermentation and Bioengineering 1991; 71: 100-105.

147. Cheung DT, Nimni ME, Mechanism of crosslinking of proteins by glutaraldehyde II. Reaction with monomeric and polymeric collagen. Connective Tissue Research 1982; 10(2): 201-216.

148. Hardy PM, Nicholls AC, Rydon HN. The nature of the crosslinking of proteins by glutaraldehyde. Part 1. Interaction of glutaraldehyde with the amino-groups of 6-aminohexanoic acid and of alpha-N-acetyl-lysine. Journal of the Chemical Society, Perkin Transactions 1, 1976; 9: 958-962.

149. Woodroof EA. Use of glutaraldehyde and formaldehyde to process tissue heart values. Journal of Biological Engineering 1978; 2: 1-9.

150. Johnson TJA. Glutaraldehyde fixation chemistry: oxygenconsuming reactions. European. Journal of Cell Biology. 1987; 45: 160-169.

151. Hardy PM, Hughes GJ, Rydon HN. The nature of the crosslinking of proteins by glutaraldehyde. Part 2. The formation of quaternary pyridinium compounds by the action of glutaraldehyde on proteins and the identification of a 3-(2-piperidyl) pyridinium derivative, anabilysine, as a crosslinking entity. Journal of the Chemical Society, Perkin Transactions 9, 1979; 9: 2282–2288

152. Lubig R, Kusch P, Roper K, Zahn H. Zum Reaktionsmechanismus von Glutaraldehyd mit Proteinen. Monatshefte für Chemie 1981; 112(11): 1313-1323.

153. Cheung DT, Nimni ME, Mechanism of crosslinking of proteins by glutaraldehyde I: reaction with model compounds. Connective Tissue Research 1982; 10(2): 187-199.

154. Ruijgrok JM, Boon ME, De Wljn JR. Optimizing glutaraldehyde crosslinking of collagen: effects of time, temperature and concentration as measured by

shrinkage temperature. Journal of Materials Science: Materials in Medicine 1994; 5(2): 80-87.

155. Chen C, Sung H, Liang H, Chang W. Feasibility study using a natural compound (reuterin) produced by Lactobacillus reuteri in sterilizing and crosslinking biological tissues. Journal of biomedical materials research 2002; 61(3): 360-369.

156. Speer DP, Chvapil M, Eskelson CD, Ulreich J. Biological effects of residual glutaraldehyde in glutaraldehyde-tanned collagen biomaterials. Journal of Biomedical Material Research 1980; 14: 753-764.

157. Gough JE, Scotchford CA, Downes S. Cytotoxicity of glutaraldehyde crosslinked collagen/poly(vinyl alcohol) films is by the mechanism of apoptosis. Journal of Biomedical Material Research 2002; 61(1): 121-130.

158. Maizato MJS, Higa OZ, Mathor MB, Camillo AP, Spencer PJ, Pitombo RN, *et al.* Glutaraldehyde-treated bovine pericardium: Effects of lyophilization on cytotoxicity and residual aldehydes. Artificial Organs 2003; 27(8): 692-694.

159. Seifer E, Frater RWM, inventors; Albert Einstein College of Medicine of Yeshiva University (Bronx, NY), assignee. Anticalcification treatment for aldehyde-tanned biological tissue. US Patent Number 5476516; 1995.

160. Gough JE, Scotchford CA, Downes S. Cytotoxicity of glutaraldehyde crosslinked collagen/poly(vinyl alcohol) films is by the mechanism of apoptosis. Journal of Bomedical Material Research 2002; 61(1): 121-130.

161. Chvapil M, inventor; Firma Carl Freudenberg, assignee; Process for the production of collagen fiber fabrics in the form of felt-like membranes or sponge-like layer. US Patent Number 3823212; 1974.

162. Yannas IV. Tissue and organ regeneration in adults. New York: Springer; 2001.

163. Yannas IV. Studies on the biological activity of the dermal regeneration template. Wound Repair and Regeneration 1998; 6: 518-524.

164. Petite H, Frei V, Huc A, Herbage D. Use of diphenylphosphorylazide for crosslinking collagen-based biomaterials. Journal of Biomedical Materials Research 1994; 28: 159-165.

165. Weadock K, Olson RM, Silver FH. Evaluation of collagen crosslinking techniques. Biomaterials, medical devices, and artificial organs 1983; 11: 293-318.

166. Huang C, Yannas IV. Mechanochemical studies of enzymatic degradation of insoluble collagen fibers. Journal of Biomedical Materials Research 1977; 8: 137-154.

167. Grillo HC, Gross J. Thermal reconstitution of collagen from solution, and the response to its heterologous implantation. Journal of Surgical Research 1962; 2: 69-82.

168. Yannas IV, Burke JF, Huang C, Gordon PL. Correlation of in vivo collagen degradation rate with in vitro measurements. Journal of Biomedical Materials Research 1975; 9: 623–628.

169. Weadock KS, Miller EJ, Keuffel EL, Dunn MG. Effect of physical crosslinking methods on collagen-fiber durability in proteolytic solutions. Journal of Biomedical Materials Research 1996; 32: 221-226.

170. Sterilization of plastics. ZEUS® Technical Whitepaper [Online]. Available from: URL: http://www.zeusinc.com/pdf/Zeus_Sterilization.pdf

171. Friess W. Collagen-biomaterial for drug delivery. European Journal of Pharmaceutics and Biopharmaceutics 1998; 45: 113-136.

172. Olde Damink LH, Dijkstra PJ, Van Luyn MJ, Van Wachem PB, Nieuwenhuis P, Feijen J. Influence of ethylene oxide gas treatment on the in vitro degradation behavior of dermal sheep collagen. Journal of Biomedical Materials Research 1995; 29: 149-155.

173. Cheung DT, Perelman N, Tong D, Nimni ME. The effect of gamma-irradiation on collagen molecules, isolated alphachains, and crosslinked native fibers. Journal of Biomedical Materials Research 1990; 24: 581-589.

174. Liu BC, Harrell R, Davis RH, Dresden MH, Spira M. The effect of gamma irradiation on injectable human amnion collagen. Journal of Biomedical Materials Research 1989; 23: 833-844.

175. Ohan MP, Dunn MG. Glucose stabilizes collagen sterilized with gamma irradiation. Journal of Biomedical Materials Research 2003; 67A: 1188-1195

176. Cooper DR, Russell AE. The Decomposition of Soluble Collagen by y-Irradiation. Biochemical Journal 1969; 113: 263-269.

177. Miyata T, Sohde T, Rubin AL, Stenzel KH. Effects of Ultraviolet Irradiation on Native and Telopeptide-Poor Collagen. Biochimica et Biophysica Acta 1971; 229: 672-680.

178. Grant RA, Cox RW, Kent CM. The effects of gamma irradiation on the structure and reactivity of native and cross-linked collagen fibres. Journal of Anatomy 1973; 115(1): 29-43.

179. Noah EM, Chen J, Jiao X, Heschel I, Pallua N. Impact of sterilization on the porous design and cell behavior in collagen sponges prepared for tissue engineering. Biomaterials 2002; 23: 2855-2861.

180. Material Considerations: Irradiation processing [Online]. Available from: URL: http://www.sterigenics.com/download.php?file=13_2.pdf

181. Morgan JR (editor), Yarmush ML (editor). Tissue engineering methods and protocols. Totowa, New Jersey, USA: Humana Press; 1998: 3-17.

182. Paggiaro AO, Kamamoto F, Rodas ACD, Mathor MB, Herson MR, Ferreira MC. Scanning Electron Microscopy as a Tool for the Evaluation of Collagen Lattices. Acta Microscopica 2003; 21(1): 205-208.

183. Yannas IV. Synthesis of Tissues and Organs. ChemBioChem 2004; 5: 26-39.

184. Moore S, Stein WH. Photometric ninhydrin method for use in the chromatography of amino acids. Journal of Biological Chemistry. 1948; 176 (1): 367-388.

185. Mandl I, MacLennan JD, Howes EL, DeBellis RH, Sohler A. Isolation and characterization of proteinase and collagenase from CL. Histolyticum. Journal of Clinical Investigation 1953; 32 (12): 1323-1329.

186. Pek YS, Spector M, Yannas IV, Gibson LJ. Degradation of a collagen–chondroitin-6-sulfate matrix by collagenase and by chondroitinase. *Biomaterials* 2004; 25: 473-482.

187. Paddle-Ledinek JE, Nasa Z, Cleland HJ. Effect of different wound dressings on cell viability and proliferation. *Plastic and Reconstructive Surgery* 2006; 117(7S): 110-118.